The Role of State-Dependent Thalamocortical Communication in Visual System Plasticity

by

Jaclyn Durkin

A dissertation submitted in partial fulfillment
of the requirements for the degree of
Doctor of Philosophy
(Neuroscience)
in the University of Michigan
2019

Doctoral Committee:

Assistant Professor Sara J. Aton, Chair
Professor Anthony Hudetz
Professor Lori L. Isom
Professor Geoffrey G. Murphy
Professor Michal Zochowski

"*We are such stuff*
As dreams are made on, and our little life
Is rounded with a sleep."

-William Shakespeare, *The Tempest*

Jaclyn Durkin

djaclyn@umich.edu

ORCID iD: 0000-0002-0618-626X

Dedication

To my little family: Rob, Zed, and Bean.

Acknowledgements

Looking back, I can finally admit that 95% of the reason I came to Michigan for my PhD was the people. Now, as I write my PhD, I can say that this reasoning was wise, as I owe many thanks to the people at Michigan (and beyond) for helping me reach this point.

The Neuroscience Graduate Program has been endlessly supportive, both in regards to science and life outside the lab. Ed and Audrey, thank you for your advice and also for letting Brittany and I live in the Resting Potential for our first year. While I'm thanking the NGP, I need to mention that the faculty and students would completely stop functioning without the real heroes, the behind-the-scenes players. Rachel, Valerie, Carol: you are all astounding and I appreciate every question or email you answer.

To my cohort: I love you all, you brilliant, beautiful people. This definitely includes the 2012 cohort, as our years seemed to make one giant family. You are incredible. Thank you for the weekends, happy hours, football games, concerts, and movie nights. It would be remiss of me to not give special thanks to BK, the light of my grad school life. I can't believe I was so lucky to have you as a Bootcamp lab partner and that we embraced each other's tiredness/weirdness. I'm going to miss going to Ashley's with you and ordering the exact same thing every time (until they change the menu).

My family has provided a wealth of encouragement over the last 5+ years. Though I moved 10 hours away from them, they made themselves available any time of day or night to listen to me panic about my degree. Thank you Dad, Mom, and Bob for always supporting me. Thanks to Julia and Jimmy for helping me get closer to figuring out what

I want to do with my life. To the rest of my siblings and extended family, I appreciate every text, phone call, or email of support. Also Kevin, who is basically family and understands this process better than anyone else, thanks for being there for over 20 years. I look forward to being back on the east coast for our Wawa trips in your man van.

Even before I decided to come to Michigan, my Berg family gave me confidence and encouragement. Thank you for understanding that I am horrendous at answering text messages, and for the feelings of reuniting after a year and knowing we can just pick up where we left off. I am so excited to be closer to most of you during this next stage of my life. While thanking Berg people, I also need to thank my undergraduate mentor, who tried to warn me about graduate school, to no avail. Dr. Gretchen Gotthard, you are a gem and I am so happy to be able to approach you as a colleague (though still forever your mentee).

It would be ridiculous to think that I could have gotten to this point without the overwhelming support and kindness from my lab. Aditi, Emily, Varna, and all undergrads: you are the unsung heroes of our lab. Jessy, thank you for sharing desk space with me, and also sorry for having to sit near me as I write this dissertation. You're going to do great in graduate school and I'm sad I won't be here to see it happen. Carlos and James, thank you for the chats about how sleep and politics don't make sense. Please start the podcast I've always wanted you to have together.

Brittany, I owe you an incredible debt of gratitude, for being my co-author many times, and for being my friend. Your support, love of Twin Peaks, and coding abilities keep me sane. I'm so glad to see a woman in science who is so completely determined to be excited, feminine, and unapologetic. Nicolette, I miss you as my back-to-back, and

also my rock and confidence. I learned so much from just sitting near you and absorbing it, like some strange osmosis. Thank you for mysteriously relocating my desk next to yours while I was out of town. I'm so proud of you and hope that I can be one-tenth of the scientist you are.

I have been fortunate to have a lab mom in Sha. Every single day, regardless of how she is doing, she greets me with a "hi Jackie!" and a smile. She also cooks feasts of homemade Chinese food and gives incredible hugs. I would write more, but I might start crying because I adore Sha so much. Our lab instituted an annual Sha Appreciation Day because we know the lab would fall to pieces without her.

To my mentor Sara: Thank you for giving me the lab experience I've always dreamed of. You are an incredible mentor and it's been so exciting to watch the lab change and evolve over the last 5 years with you. You are smart and kind and ridiculously bad at saying "no," which I understand. Somehow you are able to handle all of your commitments and maintain a sense of humor. You are also one of the weirdest people I have ever met, which I'm sure you recognize is the highest compliment I can bestow on someone. I knew from the moment I started working with you that I wanted to stay in the lab, so thank you for giving me the opportunity to learn from you.

Finally, I want to thank my partner, Rob. Your love and patience have meant everything to me. I'm so thankful for you and our cat children. I love you oodles.

This work was supported by a Graduate Research Fellowship from the National Science Foundation, as well as a Predoctoral Research Fellowship from Rackham Graduate School.

Table of Contents

List of Figures

Figures

Supplemental Figures

List of Abbreviations

REM	Rapid Eye Movement
NREM	Non-Rapid Eye Movement
SWS	Slow Wave Sleep
EEG	Electroencephalogram
EMG	Electromyogram
LFP	Local Field Potential
LGN	Lateral Geniculate Nucleus
TRN	Thalamic Reticular Nucleus
V1	Primary Visual Cortex
TC	Thalamocortical
CT	Corticothalamic
SHY	Synaptic Homeostasis Hypothesis
OSRP	Orientation Specific Response Potentiation
VEP	Visually Evoked Potential
LTP	Long Term Potentiation
RI	Responsiveness Index
OSI	Orientation Specificity Index
ISI	Interspike Interval
DB	Davies-Bouldin
SD	Sleep Deprivation

ESD	Early Sleep Deprivation
LSD	Late Sleep Deprivation
CCG	Cross-correlogram
PCA	Principal Components Analysis
SFC	Spike Field Coherence
PSD	Power Spectral Density
FR	Firing Rate
CT0/CT12	Circadian Time 0 / Circadian Time 12
ChR2	Channelrhodopsin-2
Arch	Archaerhodopsin
GFP	Green Fluorescent Protein

Abstract

Sleep is a phylogenetically conserved state of unconsciousness that plays a critical role in cognitive processing and underlying synaptic plasticity. However, the mechanism through which sleep contributes to brain function remains a mystery. During non-Rapid Eye Movement (non-REM) sleep, coordinated firing of neurons in the thalamocortical circuit of the brain generate oscillations characteristic of this sleep stage. These oscillations have been correlated with increases in memory retention and learning in a number of animal models. My dissertation examines the role of this state-specific thalamocortical activity in mediating sleep-dependent synaptic plasticity within the mouse visual circuit – orientation specific response potentiation (OSRP).

Orientation-Specific Response Potentiation (OSRP) is a form of plasticity that takes place in adult mice after exposure to an oriented grating stimulus. OSRP occurs at thalamocortical synapses between the visual thalamus (LGN) and primary visual cortex (V1) and expresses as increased V1 firing to the presented stimulus. Our lab has demonstrated that OSRP is sleep-dependent. Furthermore, OSRP is positively correlated with the time spent in either rapid eye movement (REM) or non-REM (NREM) sleep.

To further characterize the cortical nuances of OSRP, I examined the changes in neural activity following OSRP induction. V1 firing rates increase specifically across both NREM and REM sleep states, but not across wakefulness. Additionally, sleep differentially affects firing rates of V1 neurons, re-distributing firing rates such that sparsely-firing neurons increase their firing over sleep, while faster-firing neurons

decrease their firing. Sparsely-firing neurons also fire more independently of the rest of the population, are more visually-responsive, and undergo the largest plastic changes in OSRP. Together, these data indicate re-distribution of firing may serve a functional role in sleep-dependent visual plasticity.

Since OSRP occurs through thalamocortical relay it is also critical to elucidate how stimulus information is communicated to V1 during post-stimulus sleep. Using dual site LGN/V1 recordings, I found that, in contrast to V1 neurons, LGN neurons show immediate, stimulus-specific changes. Furthermore, LGN firing coherence with V1 field potentials increases at during NREM sleep, at both delta (0.5-4 Hz) and spindle (7-14 Hz) frequencies. The largest coherence increases occur in LGN neurons are the highly stimulus responsive, indicating these neurons may provide stimulus specific information to V1 during NREM sleep. However, this evidence is correlational.

To characterize the necessity of NREM-specific oscillations in OSRP, a technician and I used optogenetics to state-specifically inhibit the circuitry that coordinates these oscillations. NREM-specific inhibition decreases the power and synchrony of NREM oscillations, subsequently preventing the consolidation of OSRP. Inhibition during REM and wake did not affect the oscillations or plasticity. Thus, I concluded that NREM oscillations promote the transfer of visually-specific information from LGN to V1.

Together, this work sheds light on sleep's role in brain plasticity in both an experience-specific and multi-regional manner. This thesis challenges major hypotheses in the field which argue that sleep uniformly downscales synaptic activity. V1 shows sleep-mediated, bidirectional alterations in firing – increasing the activity in experience-responsive neurons while decreasing the firing of others. Furthermore, it highlights a role

for the thalamus as an active participant in cortical plasticity, rather than a simple relay for waking sensory information. Elucidating these changes opens the door for future work to explore these mechanisms in a manner that does justice to both the structure-specific and memory-specific changes that occur during sleep.

Chapter 1 Introduction

This chapter includes the manuscript: **Durkin, J.,** & Aton, S.J. (2019). How sleep shapes thalamocortical function in the visual system. *Under review at the Annual Reviews in Vision Science*

1.1 Abstract

Recent data has shown that sleep plays a beneficial role for cognitive functions such as declarative memory consolidation and perceptual learning. Here we review recent findings on the role of sleep in promoting adaptive visual response changes in the lateral geniculate nucleus (LGN) and primary visual cortex (V1) following novel visual experiences. We discuss these findings in the context of what is currently known about how sleep affects the activity and function of thalamocortical circuits, and current hypotheses regarding how sleep facilitates synaptic plasticity.

1.2 Introduction

Sleep is a highly conserved and homeostatically regulated behavior, which is seen in nearly every animal species studied. One of the hallmarks of sleep is decreased responsiveness to sensory stimuli, leading to an increase in arousal threshold. It should come as no surprise that altered activity in the sensory processing circuits of the brain coincides with transitions from waking to sleep and vice versa. The thalamocortical

network connects thalamic sensory nuclei and cortical regions which process sensory information. Early hypotheses about neural activity during sleep suggested that sleep was simply a state of prolonged cortical inhibition,[1] allowing for disengagement from the world around us and relief from fatigue. However, over the last few decades, electrophysiological data have demonstrated that thalamocortical circuitry displays unique neural activity patterns in sleep states. This activity serves to reduce sensory input to cortex, but may also play a unique role in shaping the circuit's sensory functions during subsequent wake. This review will examine sleep-associated changes in neural activity within the visual thalamocortical network, focusing on recent work carried out in cats and rodent species. An understanding of these changes will provide insight into 1) how sleeping animals temporarily disengage from sensory input from their environment, and 2) how sleep promotes adaptive changes to visual system function initiated by changing visual experience during prior wakefulness.

1.3 The structure and function of visual thalamocortical circuits

Early processing of visual stimuli by the thalamocortical network can be considered as occurring in a circuit with three major components: relay thalamic nuclei, the thalamic reticular nucleus, and cortex, which are mutually interconnected (**Fig. 1.1A**).

1.3.1 The thalamus: dLGN and TRN

Form vision is mediated by retinal ganglion cells projecting to the dorsal lateral geniculate nucleus (dLGN) of the thalamus. This nucleus plays an important role in relaying information to cortex for visual perception. Quantitative analysis of dLGN receptive fields in the mouse confirmed the presence of classic center-surround

organization.[2] As is the case in most mammals, it was believed that the mouse LGN lacked visual response properties such as direction or orientation selectivity, and that these were generated at the level of visual.[3,4] However, recent work demonstrates that mouse LGN contains a significant proportion of cells that are orientation and/or direction selective, in contrast to the more traditionally studied cat LGN.[5-9] Interestingly, many of these cells are found in a region of the LGN that direction selective retinal ganglion cells synapse onto, providing a potential mechanism for the emergence of both direction and orientation selectivity.[7] Orientation selectivity in the LGN seems to be a direct result of retinogeniculate input, as opposed to cortical feedback, since inhibition of corticothalamic activity does not affect orientation selectivity in the LGN.[8]

In addition to relay thalamic nuclei, the thalamus also contains a cluster of GABAergic neurons called the thalamic reticular nucleus (TRN). TRN neurons form reciprocal connections with excitatory relay neurons in many thalamic nuclei. These connections act to modulate relay neurons' activity during wake and sleep alike. Because of these inhibitory connections with many sensory nuclei, the TRN is hypothesized to play an important role in controlling selection of sensory modalities. Francis Crick famously put forward the "searchlight" hypothesis of reticular thalamic function, which postulated that the TRN modulates thalamocortical circuits to select for specific sensory modalities over others.[10] More recently, Wimmer et al. tested this proposed function of the TRN using optogenetic and electrophysiological approaches in mice performing a divided attention task.[11] They demonstrated that by specifically manipulating the visual portion of the TRN, they could select for or against attending to a visual stimulus over an auditory stimulus. This bidirectional modulation suggests that the visual TRN is controlling LGN gain via

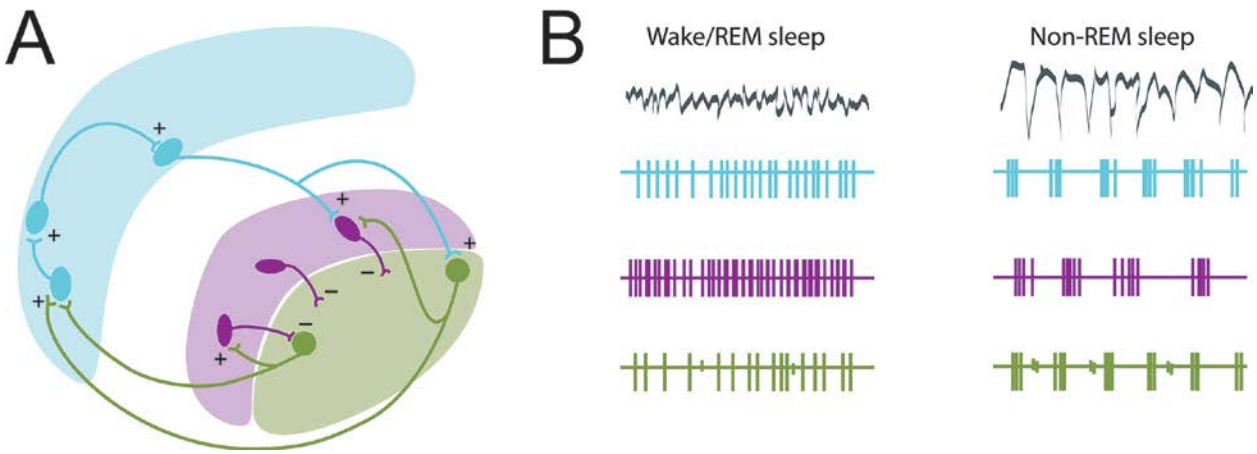

Figure 1.1 Structure and state-dependent activity of the thalamocortical circuit. (A) The thalamocortical circuit is comprised of the thalamus proper (green; LGN in the visual system), the thalamic reticular nucleus (purple), and the cortex (blue; V1 in the visual system). Reciprocal connections between these regions process sensory information, and also provide a mechanism for synchronization of activity during NREM sleep. (+) signifies excitatory connections, while (-) denotes inhibitory connections. **(B) Left:** During both waking and REM sleep, activity in the TC circuit is desynchronized, leading to a lower amplitude, faster EEG. Neurons in the TC circuit fire tonically. **Right:** During NREM sleep, neurons in the TC circuit fire in bursts, which synchronize across the circuit leading to a high amplitude, slow EEG.

feedforward inhibition, enabling the animal to select between multiple sensory inputs for a specific behavioral task.[11] Thus, the TRN plays a vital role in gating sensory information propagation from thalamocortical relay nuclei to sensory cortex.

1.3.2 Primary visual cortex (V1)

LGN thalamocortical relay neurons send excitatory projections to neurons of V1, primarily in layer 4.[12,13] Rodents generally have much lower visual acuity than predator species, and this is reflected in the responses of neurons in rodent V1.[14] Despite this, and cytoarchitectural differences in V1 (e.g., lack of orientation or ocular dominance columns), mouse V1 neurons do have similar basic response properties (e.g. orientation selectivity and eye preference) as V1 neurons in other mammals.[15,16] Orientation tuning among V1 neurons appears to be a function of both excitatory thalamic input, as the LGN has orientation tuning,[17] and inhibitory interneuron-mediated refinement.[15] For example, parvalbumin expressing interneurons show little orientation selectivity, and therefore could be important for gain control.[15,18] On the other hand, somatostatin expressing interneurons are relatively orientation-tuned, and could serve to gate excitatory inputs.[15,19] Recent work has shown that mouse V1 response properties vary as a function of the animal's behavior during wake. Locomotion, for example, appears to enhance visual responses in V1 neurons, without altering their response selectivity or spontaneous activity.[20] Further investigation determined enhancement of activity is caused by a disinhibitory circuit composed of vasoactive intestinal peptide (VIP) neurons, which act to inhibit somatostatin (SST) neurons, thus disinhibiting pyramidal neurons targeted by the SST neurons.[21] Optogenetic manipulation of VIP neurons demonstrated that this

disinhibitory circuit is necessary and sufficient for locomotion-induced enhancement of visual responsiveness.[21-23]

1.3.3 Corticothalamic feedback

V1 layer 6 neurons give rise to corticocortical and corticothalamic projections, which appear to play unique roles in sensory processing within V1. Recent work by the Scanziani lab has shown that layer 6 corticothalamic projections are particularly important for gain control of visual input.[24] This population of neurons project both to LGN (as the name implies) and also intracortically. The intracortical projections modulate visual activity indirectly through connections onto inhibitory interneurons, whose cells bodies reside in layer 6, but send axons to other layers of cortex.[25] Corticothalamic neurons are also uniquely positioned to influence thalamocortical activity in response to visual stimuli. For example, corticothalamic feedback can refine the borders of receptive fields, leading to sharper visual responses in the LGN.[26]

1.4 The thalamocortical circuit during sleep

Thalamocortical circuit dynamics are dramatically different between sleep and wake. Mammalian sleep consists of two very distinct states, rapid eye movement (REM) sleep and non-REM (NREM) sleep. These states can be identified and differentiated by thalamocortical electroencephalogram (EEG) features, as well as differences in neuronal firing patterns. REM, the phase of sleep associated with vivid dreaming, features low amplitude, desynchronized EEG activity in thalamocortical circuits (similar to wake), and pronounced theta (4-10 Hz) rhythms generated in the hippocampus. Like wake, REM is characterized by relatively tonic firing patterns among thalamic and cortical neurons (**Fig.**

1.1B). NREM, in contrast, is characterized by high amplitude, slow, synchronous EEG activity, which appears due to the transition to burst-pause firing patterns among cortical, thalamocortical, and TRN neurons during NREM sleep (**Fig. 1.1B**). NREM sleep shows features of homeostatic regulation, which are present at the EEG level, with higher-amplitude and more coherent oscillations present across the cortex after a period of sleep deprivation.[27,28]

Nearly a century of study has refined our understanding of the circuitry involved in promoting transitions between sleep and wake states, based in large part on regulation of thalamocortical circuit function. Early studies by Bremer demonstrated that disrupting ascending neuromodulatory pathways from the brainstem to the forebrain resulted in deficits in arousal.[29] More recent work has shown that release of norepinephrine, acetylcholine, dopamine, and serotonin in the thalamus and cortex promotes arousal, while reduction in levels of these neuromodulators contribute to the initiation of NREM sleep.[30-33] These neuromodulators act through IP3/DAG and cAMP messenger systems to reduce potassium leak currents, leading to a relative depolarization of neuronal membrane potential.[34] At the transition to NREM, neuromodulator release in thalamus decreases, leading to hyperpolarization in both thalamic reticular and relay thalamic neurons. This hyperpolarized membrane potential leads to selective de-inactivation of low-threshold T-type calcium channels[35] which are responsible for generating the bursting activity characteristic the thalamus in NREM sleep.

Both wake and REM show elevated levels of acetylcholine relative to NREM sleep. During either arousal from NREM sleep, or transitions to REM sleep, increases in acetylcholine (acting on nicotinic receptors) causes TRN neurons to undergo rapid

depolarization, followed by a slow muscarinic receptor-mediated hyperpolarization; this process terminates inhibition of thalamocortical relay neurons by the TRN.[35,36] Thalamocortical neurons are also depolarized by increases in acetylcholine and, with the lack of inhibition from TRN neurons, are unable to generate the oscillations associated with NREM sleep, marking the transition to either REM or.[37] Thus, acetylcholine release in the thalamus is believed to modulate the transition to “cortically-active” states (either REM or wake).[38] One difference between wake and REM transitions is that during transitions to wake, many additional neuromodulators, such as serotonin, dopamine, and norepinephrine are also released in thalamocortical circuits. In contrast serotonin, dopamine, and norepinephrine-producing neuronal nuclei are virtually silent during REM sleep, and stimulation of these regions appears to suppress REM and promote wake.[39] Thus NREM, REM, and wake are distinct from one another with regard to neuromodulator release profile.

1.5 Thalamocortical oscillations during NREM sleep

During NREM sleep, thalamocortical networks generate unique circuit-level oscillations, brought about through synchronous burst firing. In humans, NREM sleep is often subdivided into stages, based on characteristic prominent oscillatory features of the EEG. For example, stage 2 NREM sleep is characterized by the presence of sleep spindles (discrete occurrences of waxing-and-waning 7-15 Hz), while subsequent stage 3 NREM sleep is marked by the appearance of delta (1-4 Hz) and slow (< 1 Hz) oscillations. These thalamocortical oscillations are not only markers of NREM sleep, but also play an important role in the maintaining the sleep state.[40]

1.5.1 Sleep spindles

Sleep spindles are discrete, 7-15 Hz EEG events, each lasting approximately 0.5-3 seconds,[41] with a characteristic waxing-and-waning envelope (**Fig 1.2A**). The neurobiological mechanisms of spindle generation have been extensively reviewed previously.[41,42] Briefly, during the transition from wake to sleep, neuromodulatory input to the thalamus is reduced, causing a gradual drop in membrane potential. As the membrane potential of neurons in the thalamus falls to a range between -60 and -65 mV, spindling behavior begins to emerge.[43,44] At this hyperpolarized level, glutamatergic input to the TRN is able to activate low-threshold T-type calcium (Cav3.2, Cav3.3) channels in reticular thalamic neurons, generating a transient calcium spike. Subsequent bursting of TRN neurons leads to generation of IPSPs in thalamocortical neurons, and membrane hyperpolarization which activates low-threshold calcium (Cav3.1) channels. Calcium influx through these channels initiates bursting in thalamocortical relay neurons, which generates volleys of EPSPs in cortical and TRN neurons,[30,45] which initiate the next cycle of burst firing. Spiking of cortical neurons, and subsequent corticothalamic (CT) feedback, synchronize the firing of TRN neurons in successive cycles of bursting - a feature which appears to underlie the waxing phase of the spindle envelope.[46] Both TRN and thalamocortical relay neurons receive excitatory CT input. However the amplitude EPSPs produced by CT input are larger in the TRN than in relay neurons, due to the greater abundance of postsynaptic glutamate receptors in the TRN compared with relay nuclei.[40,47,48] During spindles, inhibition of thalamocortical neurons by IPSPs from TRN bursts tends to overwhelm excitatory input from CT neurons. This inhibitory input allows for the continuation of hyperpolarization-induced activation of T-type calcium channels

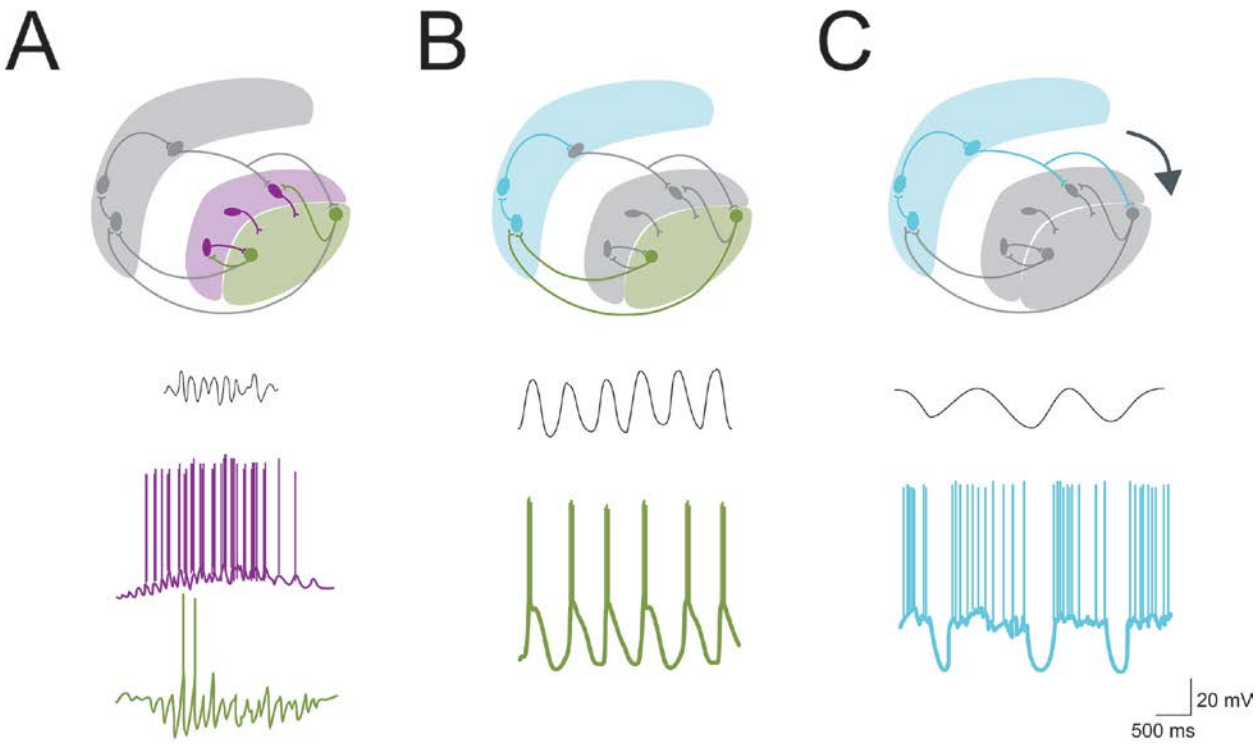

Figure 1.2 Generation of NREM oscillations within the TC circuit. (A) Sleep spindles (7-15 hz) are generated by the interaction between the TRN (purple) and thalamus proper (green). Sample intracellular recording adapted from Steriade & Deschênes[128] and Steriade[55]. **(B)** Delta is generated in both cortex (blue) and thalamus proper. The better-understood clock-like delta of the thalamus is shown as an intracellular trace modified from Amzica & Steriade[129] and Timofeev & Steriade[56]. **(C)** The slow oscillation is generated in cortex (blue) and through layer 6 connections to thalamus synchronizes the other TC oscillations (arrow). Intracellular activity of the cortical slow oscillation adapted from TImofeev & Chauvette[130].

during subsequent spindle volleys. Ultimately, spindles wane and terminate, due in part to the gradual desynchronization of thalamocortical relay, TRN and CT activity.[41,49]

Spindle generation is blocked outside of NREM sleep, due to increased neuromodulator levels. During wake, norepinephrine and serotonin block potassium leak conductance in TRN neurons, preventing the activation of low threshold T-type calcium channels.[50] High acetylcholine release, which occurs during both REM and wake, can lead to spindle blockade through a number of mechanisms.[51] Acetylcholine from the peribrachial region hyperpolarizes TRN neurons while simultaneously increasing conductance, preventing burst firing to set off the spindle initiation.[52] Acetylcholine can also act on TC relay neurons, depolarizing them through both fast nicotinic and slow muscarinic activity.[53] This depolarization blocks the low-threshold calcium spikes required for spindle activity in TC neurons.[51]

1.5.2 Delta

Delta (1-4 hz) oscillations are generated by mechanisms intrinsic to both the thalamus and cortex during NREM sleep. The best described of these is the clock-like mechanism for generating delta rhythms intrinsic to thalamocortical relay neurons (**Fig 1.2B**). Rhythms in membrane potential are generated via reciprocal interactions between a hyperpolarization-activated cation current (I_h) and a transient low-threshold calcium current (I_t).[54] As thalamocortical relay neurons hyperpolarize beyond the range where spindling occurs in thalamocortical circuits (between -65 and -90 mV),[43,44] I_h is activated, moving the membrane potential closer to depolarization, activating I_t and generating a low-threshold spike.[55] This mechanism appears to be intrinsic to thalamic relay neurons, as delta rhythms are generated within structures such as the LGN independent of input

from cortex.[56] Delta oscillations also appear to be generated via an independent mechanism in cortex, independent of thalamic input.[57] While the precise mechanism underlying generation of delta within the cortex is less understood, it appears to emerge initially among cortical pyramidal neurons within cortical layers 2/3 and 5.[58-60]

1.5.3 Slow oscillation

The slow oscillation (<1 hz) was first described in the context of intracellular recordings of cortical neurons.[61] The slow oscillation consists of “up states” (slow depolarizations with superimposed action potentials) and “down states” (long hyperpolarizations), occuring at less than 1 hz (**Fig 1.2C**). The up state of the slow oscillation is a prolonged depolarization caused by NMDA receptor- and non-NMDA receptor-mediated EPSPs and a persistent sodium current; during up states fast IPSPs from local GABAergic cortical cells are also present.[30,61] Subsequent down state hyperpolarization appears to be initiated by a combination of short-term synaptic depression of active synaptic connections (due to depletion of calcium), slow inactivation of sodium current, and activation of potassium current (gated by calcium and sodium).[62] This hyperpolarized state is due to disfacilitation, not inhibition, as GABAergic neurons fire in the same up/down phase as pyramidal neurons.[63,64]

The slow oscillation plays a key role in the thalamocortical network during NREM sleep because of its unique role in synchronizing the other NREM oscillations.[61] Via periodic activation of corticothalamic neurons, the slow oscillation causes synchronous, rhythmic activation of neurons in the thalamus. This mechanism promotes coherent spindle and delta rhythms across the extent of the thalamus during NREM sleep.[56,65] Corticothalamic input can initiate delta oscillations in thalamocortical neurons, and can

also reset the phase of the ongoing delta oscillations to synchronize periodic activity across the thalamocortical network.[66] Corticothalamic feedback to the thalamus synchronizes sleep spindles, but also plays important roles in initiating and terminating them.[67,68] Thus available data suggest that the coordination of these rhythms depends on the reciprocal loops between cortex and thalamus.

1.6 The function of thalamocortical oscillations during NREM sleep

The synchronous bursting patterns associated with thalamocortical activity during NREM is distinct from the relatively tonic firing pattern of thalamic and cortical neurons seen during wake or REM sleep. This change in activity pattern appears to be crucial for filtering out incoming sensory input, leading to a higher arousal threshold during sleep. One possibility is that the hyperpolarized membrane potential (combined with inhibition mediated by GABAergic TRN neurons) makes thalamic responses refractory to incoming excitatory input. In support of this idea, recent work has demonstrated that subnetworks of TRN neurons may be specialized for state-dependent filtering of sensory input at the level of the thalamus. While TRN neurons projecting to limbic structures show activity that coincides with arousal, TRN neurons projecting to sensory thalamic nuclei (such as those projecting to LGN) are more likely to be active during NREM sleep, with firing synchronized by NREM oscillations, and are more likely to participate in spindle-generation.[69] The activity of this population of sensory-projecting TRN neurons is suppressed by aroused attention during wake.[69] This suggests that sensory-projecting TRN neurons and the NREM oscillations they generate are important for blocking incoming sensory input, allowing for the maintenance of sleep. However, it is worth noting

that sensory gating during NREM is not monolithic, but rather, varies as a function of NREM stage and oscillatory phase. Recently, Schabus et al. demonstrated that if a sensory stimulus coincides with a spindle or the down state of the slow oscillation, it is unlikely to elicit a response in cortex; however, cortical responses can be elicited during the depolarizing up-state of the slow oscillation.[70]

Numerous studies have linked NREM oscillations to the cognitive benefits of sleep.[42,71-75] There is a wealth of correlational data from human subjects and animal models suggesting a link between specific oscillations and across-sleep improvements on specific tasks.[40] Intriguingly, the density and amplitude of NREM oscillations can increase in specific cortical regions after modality-specific training. For example, waking auditory stimulation leads to increased power of sleep spindles during subsequent NREM sleep and increased coherence between frontal and temporal (auditory) regions.[76] Similarly, following sensorimotor learning, slow wave (delta and slow oscillatory) activity increases during NREM in motor and proprioceptive cortical regions.[77]

More recently, experimental manipulation of NREM oscillations (through administration of hypnotic drugs, transcranial stimulation, auditory stimulation, or optogenetics) have aimed to demonstrate causal role of specific rhythms in cognitive processes. For example, boosting slow oscillations through transcranial magnetic stimulation in human subjects increases retention of hippocampus dependent declarative memory.[78] Optogenetically-driven, synchronized rhythms generated simultaneously in secondary motor area and primary sensory cortices (mimicking synchronized delta activity during NREM) were sufficient to promote perceptual memory retention in mice. Using this same paradigm, optogenetic disruption of cortical activity during NREM sleep

blocked memory retention.[79] Such manipulations have been used to demonstrate a crucial role of specific phase relationships between NREM oscillations (e.g., between spindles and slow waves) for cognitive performance enhancement. For example, administration of the hypnotic drug zolpidem increases the temporal coupling of NREM slow oscillations and spindles, which predicts across-sleep improvements in verbal memory.[80] Auditory closed-loop stimulation has also been used as a noninvasive strategy to alter the temporal coupling between NREM oscillations following learning. Using this technique, increasing the phase coupling between spindles and slow waves (by stimulating in phase with slow oscillation up states) following training on a declarative memory task improves memory consolidation.[81] Together, these data suggest that both thalamocortical oscillations themselves, and the temporal relationships between these oscillations during NREM sleep, are essential for at least some of the cognitive benefits of sleep.

1.7 Thalamocortical activity in REM sleep

During both wake and REM sleep, input from the brainstem nuclei cause depolarization of thalamocortical and cortical neurons. During REM, brainstem mesopontine nuclei release acetylcholine in thalamic structures, while nucleus basalis projections release acetylcholine in the cortex.[55,82] In thalamocortical relay neurons, cholinergic input from the pons causes prolonged depolarization, with an increase in input resistance, leading to increased responsiveness of thalamocortical relay neurons during wake and REM.[37,83] Depolarization of thalamocortical relays and cortical neurons inhibit slower oscillatory activities associated with NREM sleep, and promote faster oscillations,

including beta (20-30 Hz) and gamma (30-60 Hz).[84-86] These fast oscillations can be generated in thalamocortical systems by activation of the mesopontine cholinergic nuclei, and require muscarinic receptor activation.[86] Both intracortical and corticothalamic connections appear to be required to synchronize these fast oscillations across thalamocortical networks during REM and wake states.[85]

Ponto-geniculo-occipital (PGO) waves are discrete propagating waves, characteristically appearing during REM sleep in cats, rats, and primates.[87] These waves are caused by bursts of action potentials initiating in the pontine region, which propagate through the LGN to the occipital cortex in species with highly developed visual systems.[88] PGO waves emerge in synchrony with saccadic eye movements occuring during REM sleep, thus one possibility is that they reflect a corollary discharge from eye movements.[87] Another is that they have additional functions in thalamocortical circuits mediating visual perception, for example in facilitating visual imagery during the vivid dreams associated with REM sleep in humans.

The function of PGO waves with regard to cognition is largely unstudied. However, in rodents, similar events, referred to simply as P waves (it is unclear whether they propagate through thalamocortical visual circuits in the same manner) have been implicated in promoting hippocampus- and amygdala-dependent memory consolidation.[87] P waves appear to facilitate synaptic plasticity in these structures during REM sleep - a process that is augmented by prior learning.[89-91]

1.8 Sleep-dependent thalamocortical activity patterns and visual system plasticity

In recent years, sleep has been shown to play a critical role in promoting synaptic plasticity throughout the brain.[73,92] Sleep-dependent plasticity has been shown to have a functional role in promoting adaptive visual response changes in thalamocortical circuits following novel visual experiences.

1.8.1 Ocular dominance plasticity

Ocular dominance plasticity (ODP) is one of the best studied examples of *in vivo* brain circuit plasticity initiated by changes in sensory input. ODP occurs in V1 during a period of early postnatal development, in which V1 neurons are highly sensitive to the relative strength of inputs representing the two eyes. If during this timeframe, one of the two eyes is occluded (a process known as monocular deprivation), the relative weights of these synaptic inputs and their morphology can be dramatically altered.[93] Monocular deprivation first causes V1 neurons' responses to stimulation of the deprived eye to be significantly reduced; subsequently responses to stimulation of the spared eye become enhanced (**Fig. 1.3A**).[94-97] Critically, ODP induced in developing cat visual system by just a few hours of monocular visual experience is significantly enhanced by a period of subsequent sleep.[98] While brief monocular visual experience alone causes a relatively modest ocular dominance shift in V1 (and initial depression of deprived-eye responses), subsequent sleep increases the overall shift by increasing the magnitude of firing rate responses to spared-eye stimulation.[99] This selective potentiation of responses during sleep is mediated by increased cortical firing and activation of cellular pathways involved in long-term potentiation (LTP) of glutamatergic synapses[99] as well as by transcription and translation of genes and proteins required for synaptic plasticity.[100,101] Some of these

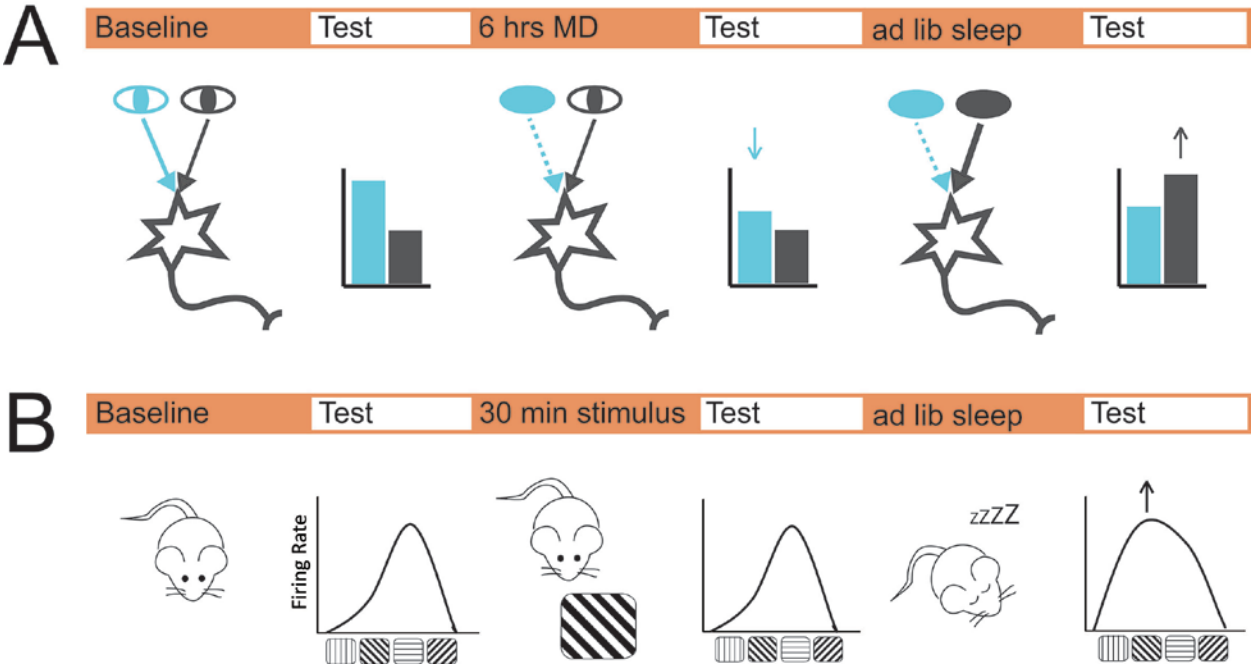

Figure 1.3 ODP and OSRP are sleep-dependent forms of visual system plasticity. (A) In cats, ODP is initiated following 6 h of monocular deprivation and manifests as a decrease in TC input to V1 from the deprived eye (blue) and an increase in TC input to V1 from the open eye (dark gray; see arrows). Sleep is required for this enhancement of input for the open eye. These changes in neuronal activity at baseline, after 6-h monocular deprivation, and after 6-h ad lib sleep periods are schematized below. Under test periods, relative firing rates responses to stimulation of each eye are provided. Adapted from Aton et al.[103] and Frank[107]. **(B)** OSRP is initiated by prolonged (i.e., 30-min) exposure to a grating stimulus and manifests as an enhancement in response (e.g., firing rate) to the presented orientation (see arrow). This enhancement is not seen immediately following stimulus presentation, but instead requires sleep for consolidation, as sleep deprivation prevents OSRP.

pathways appear to be activated selectively during post-MD REM sleep, and REM deprivation disrupts their activation.[102] However, there is also evidence that firing patterns associated with NREM oscillations (including delta and sleep spindles) mediate sleep-dependent augmentation of spared-eye responses in V1.[103]

In contrast to studies in cat binocular visual cortex, rodent studies have assessed sleep dependent changes in monocular V1 following monocular deprivation. In this system, loss of (all) visual input to contralateral V1 caused by monocular deprivation leads to an immediate decrease in firing, followed by a gradual recovery over the next 2 days. This recovery process seems to rely not on Hebbian plasticity mechanisms, but rather on homeostatic scaling.[104] Recent data suggest that this homeostatic upscaling occurs specifically during wake, and that sleep may actually inhibit this process.[105] Taken together, these data suggest that sleep associated activity in the visual system may play a role in regulating both Hebbian and homeostatic plasticity mechanisms, to modulate visual responses to changing inputs.[106,107]

1.8.2 Orientation-specific response potentiation

Orientation-specific response potentiation (OSRP) is another form of experience-dependent plasticity which occurs in the adult mouse visual system in response to presentation of a flickering grating of a single orientation over several minutes.[108,109] OSRP is characterized by an increase in the amplitude of V1 visually evoked potential (VEP) responses[108,110] or in V1 neurons' firing rate responses[109,111] to stimuli of the same orientation (**Fig. 1.3B**). OSRP appears to be initiated at thalamocortical synapses, relies on NMDA receptor activation and AMPA receptor trafficking,[108] and occludes thalamocortical LTP (induced by theta burst stimulation) in vivo.[110] Taken together, a

parsimonious interpretation of available data is that visual experience induces potentiation of thalamocortical synapses, which leads to stimulus-specific response changes in V1.

Early studies on OSRP indicated that V1 response changes were not detectable immediately following stimulus presentation, but required a period of several hours to be "consolidated".[108] Work from our lab has shown that changes in V1 neurons' firing rate responses are not seen after presentation of oriented gratings for as long as 1 h, but can be detected after as little as 6 h of subsequent sleep.[109] The mechanism driving consolidation of OSRP is not simply time-dependent, as sleep deprivation of similar duration (in the absence of additional visual input) disrupts OSRP (**Fig. 1.3B**).[109,111,112] Based on prior data that changes in the strength of thalamocortical synapses mediate OSRP, we hypothesized changes in V1 responses are preceded by changes in the LGN.

1.9 Thalamocortical circuit activity and synaptic plasticity

Work carried out in the visual system to date suggests that sleep promotes response changes in visual system neurons by promoting changes in the strength of specific synapses. Multiple hypotheses have been put forward to explain how sleep contributes to brain plasticity and cognitive function.[73,88,113] Here we will examine two of the major hypotheses regarding the role of sleep-dependent thalamocortical activity in promoting synaptic plasticity.

1.9.1 *Slow wave activity and synaptic downscaling*

Why has sleep (and sleep-specific neural activity) proved so crucial for cognition and brain plasticity? Arguably the most prominent hypothesis in the sleep field, the

synaptic homeostasis hypothesis (SHY), posits that due to the multitude of learning experiences occurring during wake, net synaptic strength is increased, and that sleep plays a critical role in offsetting this net potentiation through global synaptic downscaling.[113,114] As originally described, the mechanism for SHY is a non-Hebbian form of plasticity, in that it does not selectively alter synapses based on inputs, but rather does so globally to combat oversaturation of synapses.[113,115] Thus increases in network activity should cause downscaling of synapses, or vice versa, to maintain neuronal activity within a specific range.[116] Synaptic downscaling would potentially also enhance the signal-to-noise ratio, by reducing synapse strength equally across synapses, so that "important" synapses are stronger relative to "less important" synapses.[113] Because there are some data available to suggest that firing rates among cortical neurons decrease across NREM sleep,[117] and because some features of NREM sleep (e.g., the coherence of neuronal firing during slow wave activity, and the amplitude of slow waves themselves), proponents of SHY have linked downscaling to slow wave oscillations during NREM. This aspect of the hypothesis is particularly elegant, because it relates a potential homeostatic feature of synapse regulation to the homeostatic regulation of sleep itself.

Since its proposal, there has been a wealth of biochemical, electrophysiological, and anatomical evidence emerging in support of SHY. Biochemical analysis of immediate early genes and phosphoproteins involved in synaptic potentiation appear to be elevated during both wake and sleep deprivation relative to sleep.[118] Electrophysiological recordings of cortical neurons show increased firing across sleep deprivation and decreased firing across sleep.[117] More recent work assessing dendritic spine structure has shown a modest but still significant relative decline in spine size after a period of

sleep relative to after a similar period of sleep deprivation.[119] Despite this, there are a number of caveats related to SHY.[73] First, most of the data in support of the hypothesis come from juvenile animals at a developmental stage (around the time of weaning) when synapse elimination is naturally at its peak, and from somatosensory and motor cortices, which are necessarily highly active during experimental sleep deprivation. Second, there are no data linking sleep-dependent synaptic downscaling to any sleep-dependent cognitive process (e.g., to memory consolidation or functional plasticity in sensory cortex). Third and most importantly, a definitive mechanism for SHY is lacking. One appealing possibility is that the cortical slow oscillation and delta oscillations are mediators of downscaling.[73] Because lower frequency stimulation has been hypothesized to drive synaptic depression, the synchronized slow activity of these oscillations could be regulating downscaling of synapses through slow, sustained calcium activity. However, to date, there are no experiments linking slow wave activity in thalamocortical circuits to synaptic downscaling.

1.9.2 Sleep facilitation of synapse-specific potentiation

Recent data have suggested that synaptic potentiation can occur during sleep under certain conditions (e.g., following learning).[73] Biochemical analyses of cortical tissue have shown that following behavioral manipulations leading to synaptic remodeling (e.g. monocular deprivation to induce ODP), cellular pathways involved in mediating synaptic potentiation are activated in a sleep dependent manner.[101-103] Following training on a novel motor task, spine formation occurs preferentially during sleep among neurons in motor cortex.[120] Finally, our lab's work on OSRP has demonstrated that visual cortical neurons require sleep in order to consolidate this LTP-like form of plasticity.[109]

Given the hypothesis that NREM oscillations drive synaptic downscaling, one would assume that slow wave activity of NREM could not support synaptic strengthening. However, work by Chauvette et al. challenges this assumption, by pointing to the up state of the cortical slow oscillation.[121] Though the slow oscillation up and down states cycle at approximately 1 hz, the up state features high-frequency spike trains, with increases in calcium levels at the transition from down to up state.[121,122] This alternating depolarized and hyperpolarized activity could support LTP. In cats, stimulation of the ascending somatosensory pathway elicited evoked potentials in somatosensory cortex, which were potentiated across a bout of NREM sleep.[121] Furthermore, this enhancement was dependent upon calcium and required both AMPA and NMDA receptors, indicating a LTP mechanism. Recent data also suggest a role for sleep spindles in synaptic potentiation. Presynaptic bursts of activity at ~10 Hz are used to model the effects of sleep spindles on a circuit. This frequency of stimulation overlaps with theta burst stimulation, which is commonly used to elicit LTP. Rosanova and Ulrich recorded patterns of cortical activity associated with a spindle *in vivo*, and then repeated this pattern as an *in vitro* stimulus to mimic grouping of spindles by the slow oscillation.[123] When this grouped spindle stimulation pattern was applied to cortical pyramidal cells *in vitro*, it elicited both short term and long term synaptic potentiation.[123] Consistent with a role of spindles in synaptic potentiation, rhythmic spike-bursts in thalamocortical relay neurons during spindles depolarize dendrites, but not cell bodies, of cortical neurons, leading to large calcium influx.[124] Spindle-locked calcium activity appears limited to the dendritic arbors, and does not appear to correlate with neuronal firing.[124] This indicates that calcium influx during spindles might provide an optimal scenario for non-Hebbian forms of synaptic plasticity.

1.9.3 Sleep's effects on firing rates and information content in the visual system

Recent work has begun to assess the heterogeneous effects of sleep and wake across populations of neurons that have a wide spectrum of baseline firing rates and other properties. For example, Watson et al. recently demonstrated that sleep-associated changes in firing rates of frontal cortical neurons varied depending on the neurons baseline firing rates, with higher firing neurons showing a net decreases in firing rate and more sparsely firing neurons showing a net increases.[125] A related study recently showed similarly heterogeneous effects of sleep on the firing rates of hippocampal neurons, with the extent of change dependent on baseline firing rates.[126] Thus, it appears as though sleep may support re-distribution of neuronal firing rates in these systems.

1.10 Conclusions and outline

In addition to its other benefits for cognitive function, sleep plays an essential role in promoting changes in visual system function following novel visual experience. These changes include alterations in the response properties of neurons in V1, which occur within just a few hours of experience in a sleep-dependent manner. Like other thalamocortical circuits, LGN and V1 undergo dramatic changes in neuronal and network activity as animals transition from wake to NREM sleep, and from NREM to REM sleep. Thus it is tempting to speculate that during sleep, these changes in network dynamics promote the synaptic plasticity that underlies V1 response changes that emerge following a period of post-experience sleep. Indeed, recent work suggests that disruption of NREM-associated thalamocortical oscillations interferes with sleep-dependent brain plasticity, while augmentation of these oscillations (through invasive or non-invasive means)

promotes it. Future work is needed to understand exactly how these oscillations promote intracellular processes that could lead to synapse-specific strengthening or weakening, and whether similar mechanisms underlie thalamocortical plasticity in other systems of the brain (e.g., the somatosensory and auditory systems).

The aim of this dissertation is to understand the role that state-specific thalamocortical communication plays in the consolidation of visual system plasticity. We know that sleep is required for consolidation of OSRP; however, we want to better understand the sleep-specific changes in physiology that may be driving plasticity in thalamocortical circuits. Using a combination of electrophysiology, optogenetics, and computational tools, I have investigated the experience-dependent changes in thalamocortical network activity that accompany, and promote, plasticity.

In **Chapter 2**, I investigate the state-dependence of the changes in visual cortical firing rates following plasticity induction in an attempt to contextualize OSRP in relation to the most prominent hypothesis in the sleep field, the Synaptic Homeostasis Hypothesis (SHY). I show that experience-dependent changes in visual cortical responses do not occur across visual experience, but are instead sleep-dependent. Importantly, increases in firing rate appear to occur specifically across sleep, in contrast with the predictions put forth by SHY. This work was published in *SLEEP* in 2016.[111]

In **Chapter 3**, Brittany Clawson and I (co-first authors) add to a growing body of literature studying the differential regulation of cortical neuron firing rates across sleep and wake states. For the first time, we demonstrate that sleep redistributes cortical firing rates, regardless of waking visual experience, and that sleep deprivation prevents this redistribution. Furthermore, we show that sparsely firing neurons tend to carry more

visually-relevant information, are weakly coupled to V1 population activity, and show the highest levels of OSRP. Thus, we argue that sleep selectively augments firing of these more selective, sparsely firing neurons. This work was published in *Frontiers in Systems Neuroscience* in 2018.[127]

In **Chapter 4**, I demonstrate that although V1 neurons do not change their response properties over visual stimulus presentation, LGN neurons show selective enhancements in firing rate across stimulus presentation. Furthermore, if tested immediately following stimulus presentation, an OSRP-like enhancement for the presented stimulus is detectable in LGN neurons. The level of enhancement is correlated with spike-field coherence of LGN spikes to the V1 field potential during post-stimulus NREM sleep at relevant NREM oscillation frequencies. Thus, we hypothesized that NREM oscillation are a possible mechanism for relaying this visual information from LGN to V1 during the consolidation period. Aneesha Suresh and I (co-first authors) next test the hypothesis that NREM oscillations play a crucial role in OSRP consolidation by optogenetically disrupting NREM delta and spindle oscillations through the inhibition of corticothalamic (CT) feedback. When we inhibit CT feedback during NREM, but not wake or REM, we significantly reduce NREM oscillations and block consolidation of OSRP. This work was published in *PNAS* in 2017.[112]

1.11 References

1. Pavlov, P.I., 2010. Conditioned reflexes: an investigation of the physiological activity of the cerebral cortex. *Annals of neurosciences*, *17*(3), p.136.

2. Grubb, M.S. and Thompson, I.D., 2003. Quantitative characterization of visual response properties in the mouse dorsal lateral geniculate nucleus. *Journal of neurophysiology*, *90*(6), pp.3594-3607.

3. Hubel, D.H. and Wiesel, T.N., 1962. Receptive fields, binocular interaction and functional architecture in the cat's visual cortex. *The Journal of physiology*, *160*(1), pp.106-154.

4. Wiesel, T.N. and Hubel, D.H., 1963. Single-cell responses in striate cortex of kittens deprived of vision in one eye. *Journal of neurophysiology*, *26*(6), pp.1003-1017.

5. Marshel, J.H., Kaye, A.P., Nauhaus, I. and Callaway, E.M., 2012. Anterior-posterior direction opponency in the superficial mouse lateral geniculate nucleus. *Neuron*, *76*(4), pp.713-720.

6. Niell, C.M., 2013. Vision: more than expected in the early visual system. *Current biology*, *23*(16), pp.R681-R684.

7. Piscopo, D.M., El-Danaf, R.N., Huberman, A.D. and Niell, C.M., 2013. Diverse visual features encoded in mouse lateral geniculate nucleus. *Journal of Neuroscience*, *33*(11), pp.4642-4656.

8. Scholl, B., Tan, A.Y., Corey, J. and Priebe, N.J., 2013. Emergence of orientation selectivity in the mammalian visual pathway. *Journal of Neuroscience*, *33*(26), pp.10616-10624.

9. Zhao, X., Chen, H., Liu, X. and Cang, J., 2013. Orientation-selective responses in the mouse lateral geniculate nucleus. *Journal of Neuroscience*, *33*(31), pp.12751-12763.

10. Crick, F., 1984. Function of the thalamic reticular complex: the searchlight hypothesis. *Proceedings of the National Academy of Sciences*, *81*(14), pp.4586-4590.

11. Wimmer, R.D., Schmitt, L.I., Davidson, T.J., Nakajima, M., Deisseroth, K. and Halassa, M.M., 2015. Thalamic control of sensory selection in divided attention. *Nature*, *526*(7575), p.705.

12. Antonini, A., Fagiolini, M. and Stryker, M.P., 1999. Anatomical correlates of functional plasticity in mouse visual cortex. *Journal of Neuroscience*, *19*(11), pp.4388-4406.

13. Dräger, U.C., 1974. Autoradiography of tritiated proline and fucose transported transneuronally from the eye to the visual cortex in pigmented and albino mice. *Brain research*, *82*(2), pp.284-292.

14. Van Hooser, S.D., 2007. Similarity and diversity in visual cortex: is there a unifying theory of cortical computation?. *The Neuroscientist*, *13*(6), pp.639-656.

15. Huberman, A.D. and Niell, C.M., 2011. What can mice tell us about how vision works?. *Trends in neurosciences*, *34*(9), pp.464-473.

16. Niell, C.M., 2015. Cell types, circuits, and receptive fields in the mouse visual cortex. *Annual review of neuroscience*, *38*, pp.413-431.

17. Sun, W., Tan, Z., Mensh, B.D. and Ji, N., 2016. Thalamus provides layer 4 of primary visual cortex with orientation-and direction-tuned inputs. *Nature neuroscience*, *19*(2), p.308.

18. Cardin, J.A., Palmer, L.A. and Contreras, D., 2007. Stimulus feature selectivity in excitatory and inhibitory neurons in primary visual cortex. *Journal of Neuroscience*, *27*(39), pp.10333-10344.

19. Ma, W.P., Liu, B.H., Li, Y.T., Huang, Z.J., Zhang, L.I. and Tao, H.W., 2010. Visual representations by cortical somatostatin inhibitory neurons—selective but with weak and delayed responses. *Journal of Neuroscience*, *30*(43), pp.14371-14379.

20. Niell, C.M. and Stryker, M.P., 2010. Modulation of visual responses by behavioral state in mouse visual cortex. *Neuron*, *65*(4), pp.472-479.

21. Fu, Y., Tucciarone, J.M., Espinosa, J.S., Sheng, N., Darcy, D.P., Nicoll, R.A., Huang, Z.J. and Stryker, M.P., 2014. A cortical circuit for gain control by behavioral state. *Cell*, *156*(6), pp.1139-1152.

22. Fu, Y., Kaneko, M., Tang, Y., Alvarez-Buylla, A. and Stryker, M.P., 2015. A cortical disinhibitory circuit for enhancing adult plasticity. *Elife*, *4*, p.e05558.

23. Stryker, M.P. and Zahs, K.R., 1983. On and off sublaminae in the lateral geniculate nucleus of the ferret. *Journal of Neuroscience*, *3*(10), pp.1943-1951.

24. Olsen, S.R., Bortone, D.S., Adesnik, H. and Scanziani, M., 2012. Gain control by layer six in cortical circuits of vision. *Nature*, *483*(7387), p.47.

25. Bortone, D.S., Olsen, S.R. and Scanziani, M., 2014. Translaminar inhibitory cells recruited by layer 6 corticothalamic neurons suppress visual cortex. *Neuron*, *82*(2), pp.474-485.

26. Briggs, F. and Usrey, W.M., 2008. Emerging views of corticothalamic function. *Current opinion in neurobiology*, *18*(4), pp.403-407.

27. Berger, R.J. and Oswald, I., 1962. Effects of sleep deprivation on behaviour, subsequent sleep, and dreaming. *Journal of Mental Science*, *108*(455), pp.457-465.

28. Borbély, A.A., Baumann, F., Brandeis, D., Strauch, I. and Lehmann, D., 1981. Sleep deprivation: effect on sleep stages and EEG power density in man. *Electroencephalography and clinical neurophysiology*, *51*(5), pp.483-493.

29. Bremer, F., 1935. Cerveau" isole" et physiologie du sommeil. *CR Soc Biol (Paris)*, *118*, pp.1235-1241.

30. Brown, R.E., Basheer, R., McKenna, J.T., Strecker, R.E. and McCarley, R.W., 2012. Control of sleep and wakefulness. *Physiological reviews*, *92*(3), pp.1087-1187.

31. Eban-Rothschild, A., Appelbaum, L. and de Lecea, L., 2017. Neuronal mechanisms for sleep/wake regulation and modulatory drive. *Neuropsychopharmacology*.

32. Saper, C.B. and Fuller, P.M., 2017. Wake–sleep circuitry: an overview. *Current opinion in neurobiology*, *44*, pp.186-192.

33. Weber, F. and Dan, Y., 2016. Circuit-based interrogation of sleep control. *Nature*, *538*(7623), p.51.

34. Hirsch, J.C., Fourment, A. and Marc, M.E., 1983. Sleep-related variations of membrane potential in the lateral geniculate body relay neurons of the cat. *Brain research*, *259*(2), pp.308-312.

35. McCormick, D.A. and Bal, T., 1997. Sleep and arousal: thalamocortical mechanisms. *Annual review of neuroscience*, *20*(1), pp.185-215.

36. Pinault, D. and Deschênes, M., 1992. Muscarinic inhibition of reticular thalamic cells by basal forebrain neurones. *Neuroreport*, *3*(12), pp.1101-1104.

37. Curro Dossi, R., Pare, D. and Steriade, M., 1991. Short-lasting nicotinic and long-lasting muscarinic depolarizing responses of thalamocortical neurons to stimulation of mesopontine cholinergic nuclei. *Journal of neurophysiology*, *65*(3), pp.393-406.

38. Watson, C.J., Baghdoyan, H.A. and Lydic, R., 2010. Neuropharmacology of sleep and wakefulness. *Sleep medicine clinics*, *5*(4), pp.513-528.

39. Steriade, M. and McCarley, R.W., 2005. Brain control of wakefulness and sleeping.

40. Steriade, M., 2006. Grouping of brain rhythms in corticothalamic systems. *Neuroscience*, *137*(4), pp.1087-1106.

41. Lüthi, A., 2014. Sleep spindles: where they come from, what they do. *The Neuroscientist*, *20*(3), pp.243-256.

42. Clawson, B.C., Durkin, J. and Aton, S.J., 2016. Form and function of sleep spindles across the lifespan. *Neural plasticity*, *2016*.

43. Nun, A., CurróDossi, R., Contreras, D. and Steriade, M., 1992. Intracellular evidence for incompatibility between spindle and delta oscillations in thalamocortical neurons of cat. *Neuroscience*, *48*(1), pp.75-85.

44. Steriade, M., Dossi, R.C. and Nunez, A., 1991a. Network modulation of a slow intrinsic oscillation of cat thalamocortical neurons implicated in sleep delta waves: cortically induced synchronization and brainstem cholinergic suppression. *Journal of Neuroscience*, *11*(10), pp.3200-3217.

45. Talley, E.M., Cribbs, L.L., Lee, J.H., Daud, A., Perez-Reyes, E. and Bayliss, D.A., 1999. Differential distribution of three members of a gene family encoding low voltage-activated (T-type) calcium channels. *Journal of Neuroscience*, *19*(6), pp.1895-1911.

46. Kandel, A. and Buzsáki, G., 1997. Cellular–synaptic generation of sleep spindles, spike-and-wave discharges, and evoked thalamocortical responses in the neocortex of the rat. *Journal of Neuroscience*, *17*(17), pp.6783-6797.

47. Golshani, P., Liu, X.B. and Jones, E.G., 2001. Differences in quantal amplitude reflect GluR4-subunit number at corticothalamic synapses on two populations of thalamic neurons. *Proceedings of the National Academy of Sciences*, *98*(7), pp.4172-4177.

48. Jones, E.G., 2002. Thalamic circuitry and thalamocortical synchrony. *Philosophical Transactions of the Royal Society of London B: Biological Sciences*, *357*(1428), pp.1659-1673.

49. Bonjean, M., Baker, T., Lemieux, M., Timofeev, I., Sejnowski, T. and Bazhenov, M., 2011. Corticothalamic feedback controls sleep spindle duration in vivo. *Journal of Neuroscience*, *31*(25), pp.9124-9134.

50. McCormick, D.A. and Wang, Z., 1991. Serotonin and noradrenaline excite GABAergic neurones of the guinea-pig and cat nucleus reticularis thalami. *The Journal of physiology*, *442*(1), pp.235-255.

51. Steriade, M., 2004. Acetylcholine systems and rhythmic activities during the waking–sleep cycle. *Progress in brain research*, *145*, pp.179-196.

52. Hu, B., Steriade, M. and Deschênes, M., 1989. The effects of brainstem peribrachial stimulation on perigeniculate neurons: the blockage of spindle waves. *Neuroscience*, *31*(1), pp.1-12.

53. McCormick, D.A., 1992. Neurotransmitter actions in the thalamus and cerebral cortex and their role in neuromodulation of thalamocortical activity. *Progress in neurobiology*, *39*(4), pp.337-388.

54. McCormick, D.A. and Pape, H.C., 1990. Properties of a hyperpolarization-activated cation current and its role in rhythmic oscillation in thalamic relay neurones. *The Journal of physiology*, *431*(1), pp.291-318.

55. Steriade, M., 2003. The corticothalamic system in sleep. *Frontiers in bioscience*, *8*, pp.d878-899.

56. Timofeev, I. and Steriade, M., 1996. Low-frequency rhythms in the thalamus of intact-cortex and decorticated cats. *Journal of neurophysiology*, *76*(6), pp.4152-4168.

57. Villablanca, J. and Salinas-Zeballos, M.E., 1972. Sleep-wakefulness, EEG and behavioral studies of chronic cats without the thalamus: The" athalamic" cat. *Archives italiennes de biologie*.

58. Steriade, M., McCormick, D.A. and Sejnowski, T.J., 1993a. Thalamocortical oscillations in the sleeping and aroused brain. *Science*, *262*(5134), pp.679-685.

59. Ball, G.J., Gloor, P. and Schaul, N., 1977. The cortical electromicrophysiology of pathological delta waves in the electroencephalogram of cats. *Electroencephalography and clinical neurophysiology*, *43*(3), pp.346-361.

60. Petsche, H., Pockberger, H. and Rappelsberger, P., 1984. On the search for the sources of the electroencephalogram. *Neuroscience*, *11*(1), pp.1-27.

61. Steriade, M., Nunez, A. and Amzica, F., 1993b. A novel slow (< 1 Hz) oscillation of neocortical neurons in vivo: depolarizing and hyperpolarizing components. *Journal of neuroscience*, *13*(8), pp.3252-3265.

62. Massimini, M. and Amzica, F., 2001. Extracellular calcium fluctuations and intracellular potentials in the cortex during the slow sleep oscillation. *Journal of Neurophysiology*, *85*(3), pp.1346-1350.

63. Contreras, D., Timofeev, I. and Steriade, M., 1996b. Mechanisms of long-lasting hyperpolarizations underlying slow sleep oscillations in cat corticothalamic networks. *The Journal of physiology*, *494*(1), pp.251-264.

64. Timofeev, I., Grenier, F. and Steriade, M., 2001. Disfacilitation and active inhibition in the neocortex during the natural sleep-wake cycle: an intracellular study. *Proceedings of the National Academy of Sciences*, *98*(4), pp.1924-1929.

65. Contreras, D., Destexhe, A., Sejnowski, T.J. and Steriade, M., 1996a. Control of spatiotemporal coherence of a thalamic oscillation by corticothalamic feedback. *Science*, *274*(5288), pp.771-774.

66. Lytton, W.W., Destexhe, A. and Sejnowski, T.J., 1996. Control of slow oscillations in the thalamocortical neuron: a computer model. *Neuroscience*, *70*(3), pp.673-684.

67. Fuentealba, P. and Steriade, M., 2005. The reticular nucleus revisited: intrinsic and network properties of a thalamic pacemaker. *Progress in neurobiology*, *75*(2), pp.125-141.

68. Fuentealba, P., Timofeev, I., Bazhenov, M., Sejnowski, T.J. and Steriade, M., 2005. Membrane bistability in thalamic reticular neurons during spindle oscillations. *Journal of Neurophysiology*, *93*(1), pp.294-304.

69. Halassa, M.M., Chen, Z., Wimmer, R.D., Brunetti, P.M., Zhao, S., Zikopoulos, B., Wang, F., Brown, E.N. and Wilson, M.A., 2014. State-dependent architecture of thalamic reticular subnetworks. *Cell*, *158*(4), pp.808-821.

70. Schabus, M.D., Dang-Vu, T.T., Heib, D.P.J., Boly, M., Desseilles, M., Vandewalle, G., Schmidt, C., Albouy, G., Darsaud, A., Gais, S. and Degueldre, C., 2012. The fate of incoming stimuli during NREM sleep is determined by spindles and the phase of the slow oscillation. *Frontiers in neurology*, *3*, p.40.

71. Diekelmann, S. and Born, J., 2010. The memory function of sleep. *Nature Reviews Neuroscience*, *11*(2), p.114.

72. Maquet, P., 2001. The role of sleep in learning and memory. *science*, *294*(5544), pp.1048-1052.

73. Puentes-Mestril, C. and Aton, S.J., 2017. Linking network activity to synaptic plasticity during sleep: Hypotheses and recent data. *Frontiers in neural circuits*, *11*, p.61.

74. Stickgold, R., 2005. Sleep-dependent memory consolidation. *Nature*, *437*(7063), p.1272.

75. Walker, M.P. and Stickgold, R., 2006. Sleep, memory, and plasticity. *Annu. Rev. Psychol.*, *57*, pp.139-166.

76. Cantero, J.L., Atienza, M., Salas, R.M. and Dominguez-Marin, E., 2002. Effects of prolonged waking-auditory stimulation on electroencephalogram synchronization and cortical coherence during subsequent slow-wave sleep. *Journal of Neuroscience*, *22*(11), pp.4702-4708.

77. Huber, R., Ghilardi, M.F., Massimini, M. and Tononi, G., 2004. Local sleep and learning. *Nature*, *430*(6995), p.78.

78. Marshall, L., Helgadóttir, H., Mölle, M. and Born, J., 2006. Boosting slow oscillations during sleep potentiates memory. *Nature*, *444*(7119), p.610.

79. Miyamoto, D., Hirai, D., Fung, C.C.A., Inutsuka, A., Odagawa, M., Suzuki, T., Boehringer, R., Adaikkan, C., Matsubara, C., Matsuki, N. and Fukai, T., 2016. Top-down cortical input during NREM sleep consolidates perceptual memory. *Science*, *352*(6291), pp.1315-1318.

80. Niknazar, M., Krishnan, G.P., Bazhenov, M. and Mednick, S.C., 2015. Coupling of thalamocortical sleep oscillations are important for memory consolidation in humans. *PloS one*, *10*(12), p.e0144720.

81. Ngo, H.V.V., Martinetz, T., Born, J. and Mölle, M., 2013. Auditory closed-loop stimulation of the sleep slow oscillation enhances memory. *Neuron*, *78*(3), pp.545-553.

82. Rasmusson, D.D., Szerb, J.C. and Jordan, J.L., 1996. Differential effects of α-amino-3-hydroxy-5-methyl-4-isoxazole propionic acid and N-methyl-d-aspartate receptor antagonists applied to the basal forebrain on cortical acetylcholine release and electroencephalogram desynchronization. *Neuroscience*, *72*(2), pp.419-427.

83. Glenn, L.L. and Steriade, M., 1982. Discharge rate and excitability of cortically projecting intralaminar thalamic neurons during waking and sleep states. *Journal of Neuroscience*, *2*(10), pp.1387-1404.

84. Llinas, R.R., Grace, A.A. and Yarom, Y., 1991. In vitro neurons in mammalian cortical layer 4 exhibit intrinsic oscillatory activity in the 10-to 50-Hz frequency range. *Proceedings of the National Academy of Sciences*, *88*(3), pp.897-901.

85. Nunez, A., Amzica, F. and Steriade, M., 1992. Voltage-dependent fast (20–40 Hz) oscillations in long-axoned neocortical neurons. *Neuroscience*, *51*(1), pp.7-10.

86. Steriade, M., Dossi, R.C., Pare, D. and Oakson, G., 1991b. Fast oscillations (20-40 Hz) in thalamocortical systems and their potentiation by mesopontine cholinergic nuclei in the cat. *Proceedings of the National Academy of Sciences*, *88*(10), pp.4396-4400.

87. Gott, J.A., Liley, D.T. and Hobson, J.A., 2017. Towards a functional understanding of PGO waves. *Frontiers in Human Neuroscience*, *11*, p.89.

88. Benington, J.H. and Frank, M.G., 2003. Cellular and molecular connections between sleep and synaptic plasticity. *Progress in neurobiology*, *69*(2), pp.71-101.

89. Datta, S., 2000. Avoidance task training potentiates phasic pontine-wave density in the rat: a mechanism for sleep-dependent plasticity. *Journal of Neuroscience*, *20*(22), pp.8607-8613.

90. Datta, S., Li, G. and Auerbach, S., 2008. Activation of phasic pontine-wave generator in the rat: a mechanism for expression of plasticity-related genes and proteins in the dorsal hippocampus and amygdala. *European Journal of Neuroscience*, *27*(7), pp.1876-1892.

91. Datta, S. and O'Malley, M.W., 2013. Fear extinction memory consolidation requires potentiation of pontine-wave activity during REM sleep. *Journal of Neuroscience*, *33*(10), pp.4561-4569.

92. Aton, S.J., 2013. Set and setting: how behavioral state regulates sensory function and plasticity. *Neurobiology of learning and memory*, *106*, pp.1-10.

93. Hubel, D.H. and Wiesel, T.N., 1970. The period of susceptibility to the physiological effects of unilateral eye closure in kittens. *The Journal of physiology*, *206*(2), pp.419-436.

94. Crair, M.C., Ruthazer, E.S., Gillespie, D.C. and Stryker, M.P., 1997. Relationship between the ocular dominance and orientation maps in visual cortex of monocularly deprived cats. *Neuron*, *19*(2), pp.307-318.

95. Freeman, R.D. and Olson, C.R., 1979. Is there a ‘consolidation’effect for monocular deprivation?. *Nature*, *282*(5737), p.404.

96. Frenkel, M.Y. and Bear, M.F., 2004. How monocular deprivation shifts ocular dominance in visual cortex of young mice. *Neuron*, *44*(6), pp.917-923.

97. Olson, C.R. and Freeman, R.D., 1980. Profile of the sensitive period for monocular deprivation in kittens. *Experimental Brain Research*, *39*(1), pp.17-21.

98. Frank, M.G., Issa, N.P. and Stryker, M.P., 2001. Sleep enhances plasticity in the developing visual cortex. *Neuron*, *30*(1), pp.275-287.

99. Aton, S.J., Seibt, J., Dumoulin, M., Jha, S.K., Steinmetz, N., Coleman, T., Naidoo, N. and Frank, M.G., 2009. Mechanisms of sleep-dependent consolidation of cortical plasticity. *Neuron*, *61*(3), pp.454-466.

100. Dumoulin, M.C., Aton, S.J., Watson, A.J., Renouard, L., Coleman, T. and Frank, M.G., 2013. Extracellular signal-regulated kinase (ERK) activity during sleep consolidates cortical plasticity in vivo. *Cerebral cortex*, *25*(2), pp.507-515.

101. Seibt, J., Dumoulin, M.C., Aton, S.J., Coleman, T., Watson, A., Naidoo, N. and Frank, M.G., 2012. Protein synthesis during sleep consolidates cortical plasticity in vivo. *Current Biology*, *22*(8), pp.676-682.

102. Bridi, M.C.D., Aton, S.J., Seibt, J., Renouard, L., Coleman, T. and Frank, M.G., 2015. Rapid eye movement sleep promotes cortical plasticity in the developing brain. *Science advances*, *1*(6), p.e1500105.

103. Aton, S.J., Broussard, C., Dumoulin, M., Seibt, J., Watson, A., Coleman, T. and Frank, M.G., 2013. Visual experience and subsequent sleep induce sequential plastic changes in putative inhibitory and excitatory cortical neurons. *Proceedings of the National Academy of Sciences*, *110*(8), pp.3101-3106.

104. Hengen, K.B., Lambo, M.E., Van Hooser, S.D., Katz, D.B. and Turrigiano, G.G., 2013. Firing rate homeostasis in visual cortex of freely behaving rodents. *Neuron*, *80*(2), pp.335-342.

105. Hengen, K.B., Pacheco, A.T., McGregor, J.N., Van Hooser, S.D. and Turrigiano, G.G., 2016. Neuronal firing rate homeostasis is inhibited by sleep and promoted by wake. *Cell*, *165*(1), pp.180-191.

106. Mrsic-Flogel, T.D., Hofer, S.B., Ohki, K., Reid, R.C., Bonhoeffer, T. and Hübener, M., 2007. Homeostatic regulation of eye-specific responses in visual cortex during ocular dominance plasticity. *Neuron*, *54*(6), pp.961-972.

107. Frank, M.G., 2017. Sleep and plasticity in the visual cortex: more than meets the eye. *Current opinion in neurobiology*, *44*, pp.8-12.

108. Frenkel, M.Y., Sawtell, N.B., Diogo, A.C.M., Yoon, B., Neve, R.L. and Bear, M.F., 2006. Instructive effect of visual experience in mouse visual cortex. *Neuron*, *51*(3), pp.339-349.

109. Aton, S.J., Suresh, A., Broussard, C. and Frank, M.G., 2014. Sleep promotes cortical response potentiation following visual experience. *Sleep*, *37*(7), pp.1163-1170.

110. Cooke, S.F. and Bear, M.F., 2010. Visual experience induces long-term potentiation in the primary visual cortex. *Journal of Neuroscience*, *30*(48), pp.16304-16313.

111. Durkin, J. and Aton, S.J., 2016. Sleep-dependent potentiation in the visual system is at odds with the synaptic homeostasis hypothesis. *Sleep*, *39*(1), pp.155-159.

112. Durkin, J., Suresh, A.K., Colbath, J., Broussard, C., Wu, J., Zochowski, M. and Aton, S.J., 2017. Cortically coordinated NREM thalamocortical oscillations play an essential, instructive role in visual system plasticity. *Proceedings of the National Academy of Sciences*, *114*(39), pp.10485-10490.

113. Tononi, G. and Cirelli, C., 2003. Sleep and synaptic homeostasis: a hypothesis. *Brain research bulletin*, *62*(2), pp.143-150.

114. Tononi, G. and Cirelli, C., 2006. Sleep function and synaptic homeostasis. *Sleep medicine reviews*, *10*(1), pp.49-62.

115. Frank, M.G., 2012. Erasing synapses in sleep: is it time to be SHY?. *Neural plasticity*, *2012*.

116. Turrigiano, G.G., 1999. Homeostatic plasticity in neuronal networks: the more things change, the more they stay the same. *Trends in neurosciences*, *22*(5), pp.221-227.

117. Vyazovskiy, V.V., Olcese, U., Lazimy, Y.M., Faraguna, U., Esser, S.K., Williams, J.C., Cirelli, C. and Tononi, G., 2009. Cortical firing and sleep homeostasis. *Neuron*, *63*(6), pp.865-878.

118. Vyazovskiy, V.V., Cirelli, C., Pfister-Genskow, M., Faraguna, U. and Tononi, G., 2008. Molecular and electrophysiological evidence for net synaptic potentiation in wake and depression in sleep. *Nature neuroscience*, *11*(2), p.200.

119. De Vivo, L., Bellesi, M., Marshall, W., Bushong, E.A., Ellisman, M.H., Tononi, G. and Cirelli, C., 2017. Ultrastructural evidence for synaptic scaling across the wake/sleep cycle. *Science*, *355*(6324), pp.507-510.

120. Yang, G., Lai, C.S.W., Cichon, J., Ma, L., Li, W. and Gan, W.B., 2014. Sleep promotes branch-specific formation of dendritic spines after learning. *Science*, *344*(6188), pp.1173-1178.

121. Chauvette, S., Seigneur, J. and Timofeev, I., 2012. Sleep oscillations in the thalamocortical system induce long-term neuronal plasticity. *Neuron*, *75*(6), pp.1105-1113.

122. Timofeev, I. and Chauvette, S., 2017. Sleep slow oscillation and plasticity. *Current opinion in neurobiology*, *44*, pp.116-126.

123. Rosanova, M. and Ulrich, D., 2005. Pattern-specific associative long-term potentiation induced by a sleep spindle-related spike train. *Journal of Neuroscience*, *25*(41), pp.9398-9405.

124. Seibt, J., Richard, C.J., Sigl-Glöckner, J., Takahashi, N., Kaplan, D.I., Doron, G., Limoges, D., Bocklisch, C. and Larkum, M.E., 2017. Cortical dendritic activity correlates with spindle-rich oscillations during sleep in rodents. *Nature communications*, *8*(1), p.684.

125. Watson, B.O., Levenstein, D., Greene, J.P., Gelinas, J.N. and Buzsáki, G., 2016. Network homeostasis and state dynamics of neocortical sleep. *Neuron*, *90*(4), pp.839-852.

126. Miyawaki, H. and Diba, K., 2016. Regulation of hippocampal firing by network oscillations during sleep. *Current biology*, *26*(7), pp.893-902.

127. Clawson, B.C., Durkin, J., Suresh, A.K., Pickup, E.J., Broussard, C.G. and Aton, S.J., 2018. Sleep Promotes, and Sleep Loss Inhibits, Selective Changes in Firing Rate, Response Properties and Functional Connectivity of Primary Visual Cortex Neurons. *Frontiers in systems neuroscience*, *12*.

128. Steriade, M. and Deschênes, M., 1988. Intrathalamic and brainstem-thalamic networks involved in resting and alert states. In: *Cellular Thalamic Mechanisms*. Eds: Bentivoglio M, Spreafico R, Elsevier, Amsterdam, 37-62.

129. Amzica, F. and Steriade, M., 1998. Electrophysiological correlates of sleep delta waves1. *Electroencephalography and clinical neurophysiology*, *107*(2), pp.69-83.

130. Timofeev, I. and Chauvette, S., 2011. Thalamocortical oscillations: local control of EEG slow waves. *Current topics in medicinal chemistry*, *11*(19), pp.2457-2471.

Chapter 2 Sleep-dependent plasticity in the visual system is at odds with the Synaptic Homeostasis Hypothesis

This chapter includes the manuscript: **Durkin, J**., & Aton, S. J. (2016). Sleep-dependent potentiation in the visual system is at odds with the synaptic homeostasis hypothesis. *Sleep*, *39*(1), 155-159.

2.1 Abstract

Two commentaries recently published in SLEEP[1,2] came to very different conclusions regarding how data from a mouse model of sleep-dependent neural plasticity[3] (orientation-specific response potentiation; OSRP) fit with the synaptic homeostasis hypothesis (SHY). To assess whether SHY offers an explanatory mechanism for OSRP, we present new data on how cortical neuron firing rates are modulated as a function of novel sensory experience and subsequent sleep in this model system.

We carried out longitudinal extracellular recordings of single-neuron activity in the primary visual cortex across a period of novel visual experience and subsequent sleep or sleep deprivation. Spontaneous neuronal firing rates and visual responses were recorded from the same population of visual cortex neurons before control (blank screen) or novel (oriented grating) stimulus presentation, immediately after stimulus presentation, and after a period of subsequent ad lib sleep. Firing rate responses to visual stimuli were unchanged across waking experience, regardless of whether a blank screen or an

oriented grating stimulus was presented. Firing rate responses to stimuli of the presented stimulus orientation were selectively enhanced across post-stimulus sleep, but these changes were blocked by sleep deprivation. Neuronal firing increased significantly across bouts of post-stimulus rapid eye movement (REM) sleep and non-rapid eye movement (NREM) sleep, but not across bouts of wake. The current data suggest that following novel visual experience, potentiation of a subset of V1 synapses occurs across periods of sleep. This finding cannot be explained parsimoniously by SHY.

2.2 Introduction

We have recently demonstrated that a form of visual system plasticity, marked by specific enhancements in firing rate to a visual stimulus, is dependent on sleep for consolidation[3]. Following the publication of this work, Heller[1] and Cirelli and Tononi[2] presenting opposing interpretations of our data as evidence against or evidence for the synaptic homeostasis hypothesis (SHY). In an attempt to address these two editorials, we performed a careful analysis of firing rate changes during and following stimulus presentation to induce OSRP, detailed in the following experiment. Here, we would like to present additional data to clarify why this form of plasticity cannot be explained parsimoniously by SHY.

Simply stated, the underlying assumption for SHY is that during waking experiences, synapses are strengthened, and during sleep, synapses are weakened. Aimed at explaining the cognitive benefits of sleep, SHY proposes that synapses throughout the brain undergo a global (if not necessarily uniform) decrease in strength as a function of sleep. Such a process could improve the function of neural circuits by

reducing synaptic “noise” caused by strengthening of connections in wake. Proponents of the hypothesis have posited that “sleep is the price the brain pays for plasticity.”[4] In other words, reduction in the neuronal signal-to-noise ratio through homeostatic synaptic downscaling is the *sine qua non* of *why* the brain has evolved to sleep. Such an incredibly far-reaching assertion requires a proportional amount of supportive evidence; Occam’s razor must be applied, no matter how elegant the hypothesis seems. In support of SHY, converging electrophysiological, anatomical, and molecular data have shown subtle decreases in synaptic strength across the brain after a period of sleep when compared with a period of wake.[5-8] Critically, however, such changes have been described primarily for rodents in their home cage in the absence of novel experience or learning.[7,8] Thus, one fair criticism of SHY is that there is a paucity of data implicating downscaling as a mechanism for adaptive brain plasticity (e.g., during sleep-dependent memory consolidation). And while data *simulations* may indicate that SHY *could* improve neural circuit function[9,10] (as described by Drs. Cirelli and Tononi in their commentary[2]), no experimental studies have conclusively demonstrated that sleep-dependent downscaling *actually occurs* in the context of sleep-dependent cognitive processes. Second, no studies have selectively interfered with downscaling during sleep (indeed, the cellular mechanism for sleep-dependent downscaling has not been clearly defined[11])—so its function is unknown. Third, a strict interpretation of SHY is that sleep promotes cognitive functions *exclusively* through synaptic weakening—which is not supported by data from several labs indicative of sleep-dependent synaptic strengthening.[3,12-18]

Nonetheless, if further evidence was needed that SHY is highly influential in the field, one might cite the fact that discussion of our data has been centered on how it

relates to SHY. As Dr. Heller correctly stated in his commentary,[1] our previous findings do not disprove SHY. However, they do suggest that SHY does not account for some forms of sleep-dependent brain plasticity.[3,17] The plasticity we recently described (orientation-specific response potentiation; OSRP) is initiated in primary visual cortex (V1) by presenting a novel visual stimulus (a flickering oriented grating). OSRP is expressed as a relative increase in V1 responses to the presented stimulus orientation over subsequent hours.[3,19] This process relies on the same *in vivo* mechanisms as thalamocortical long-term potentiation (LTP),[20] and critically, post-stimulus sleep deprivation interferes with OSRP.[3] A parsimonious explanation is that in this case, synapses are potentiated during sleep. However, this simple interpretation runs counter to SHY, which does not allow for large-scale (i.e., circuit-wide) synaptic strengthening outside of wake.

Drs. Cirelli and Tononi commented that two factors suggest a mechanism consistent with SHY for sleep-dependent OSRP. First, they state that "visual responses were not recorded immediately after training," conjecturing that enhancement of orientation-specific responses occurs across waking visual experience. This statement is simply not true; we showed that preference for the presented stimulus orientation is unchanged immediately after stimulus presentation, but only shifts in favor of the presented stimulus 6-12 hours later[3]—a finding consistent with what others have reported.[19] Their second concern is that by comparing neuronal firing responses to stimuli of different orientations, rather than the absolute amplitude of visually evoked potentials (VEPs), we have obscured any absolute changes in V1 visual responses. The distinction between single neuron firing rate responses and VEPs is not germane; VEPs and V1

neuronal firing are correlated across stimulus conditions,[21-23] and changes in VEP amplitudes are predicted by changes in V1 neuronal firing during visually induced response plasticity.[24,25] The relative change in firing for various stimulus orientations was the salient feature of OSRP in our study, just as it was for prior studies using VEPs.[19,20] Nonetheless, absolute changes in spontaneous[26,27] or stimulus evoked[28] neuronal firing rates have recently been found during homeostatic plasticity in the cortex (e.g., increases in firing rates following visual deprivation). Here, we present a meta-analysis of raw firing rate changes from a large number of *in vivo* stereotrode recordings (comprising the 23 mouse experiments previously reported[3] and an additional 46 experiments subsequently carried out using identical methods), to address whether overall synaptic strength appears to go up or down in V1 with sleep. For all experiments, mice were implanted with 2 bundles of stereotrode wires (7 per bundle, spaced 1-2 mm apart in right-hemisphere V1) for single-neuron and local field potential recordings (reference and ground wires placed over left-hemisphere V1 and cerebellum, respectively) and nuchal EMGs as described previously.[3] Spike trains from individual neurons were discriminated offline; only stably recorded and reliably discriminated V1 neurons (with single-unit spiking continuously recorded throughout the experiment) were included in subsequent analyses. All animal procedures were approved by the University of Michigan Committee on Use and Care of Animals.

2.3 Results

2.3.1 Cortical firing rates do not change across waking visual experience which induces OSRP

To test whether synaptic downscaling is a likely mediator of OSRP, we first assessed whether V1 neuronal firing rates increased in non-anesthetized, head-fixed mice across waking visual experience (**Fig. 2.1A-B**). We found that firing rates for individual V1 neurons were virtually identical at the beginning and end of a 1-h waking visual stimulus period (3.4±0.4 Hz and 3.4±0.4 Hz for the first and last 5 min of stimulus presentation). Presentation of a blank screen over the same 1-h time window resulted in similar firing rate changes (mean changes of 0.01±0.05 Hz and -0.11±0.09 Hz across oriented grating stimulus presentation and blank screen presentation, respectively; **Fig. 2.1C**). Immediately following stimulus presentation, firing rate responses to the presented stimulus orientation were only slightly (and not significantly) enhanced (*N.S.*, RM ANOVA). Responses to stimuli of the orthogonal orientation, and spontaneous activity, showed a similar degree of change (increases of 0.15±0.09 Hz and 0.17±0.09 Hz, respectively, vs. 0.16±0.08 Hz for presented stimulus responses; all *N.S.*, RM ANOVA vs. baseline). Moreover, firing rate changes were similar in mice presented with a blank screen over the same time period (an increase of in spontaneous activity of 0.16±0.17 Hz, also *N.S.*, RM ANOVA; **Fig. 2.2A**). Thus no significant spontaneous or stimulus evoked firing rate changes are present immediately following waking visual experience.

2.3.2 Sleep following waking visual experience enhances firing rates to the presented stimulus

We next asked whether evidence for sleep-dependent downscaling was present in our recordings. We compared visually evoked firing rate responses (and spontaneous firing) 12 h after baseline visual response assessment, in freely-behaving animals which either were allowed *ad lib* sleep or were sleep deprived (**Fig. 2.2A**). Neuronal firing was recorded continuously from mice across the post-stimulus interval to assess response changes associated with behavioral state, as previously described[3]. Following uninterrupted post-stimulus sleep, neuronal firing rate responses to the presented stimulus orientation were selectively enhanced, increasing on average by 0.54±0.24 Hz ($p < 0.05$, RM ANOVA vs. baseline), vs. 0.31±0.20 Hz and 0.39±0.25 Hz, respectively, for blank screen and the orthogonal stimulus orientation ($P < 0.05$ for both comparisons, RM ANOVA). These orientation-specific firing rate response increases were eliminated by post-stimulus sleep deprivation. When mice were deprived of sleep by gentle handling during either the first or last half of the day (early sleep dep. and late sleep dep., **Fig. 2.2A**), V1 neurons' spontaneous activity and responses to stimuli were virtually unchanged from baseline.

2.3.3 Cortical firing rates increase across sleep following waking visual experience

Taken together, our data suggest that OSRP is dependent on selective, orientation-specific potentiation of V1 circuitry during post-stimulus sleep, resulting in enhanced firing rate responses to stimuli of the presented stimulus orientation. If these increases in firing rate are a function of sleep, one would predict that: (1) firing rate changes could be detected across individual bouts of either NREM or REM sleep, and (2)

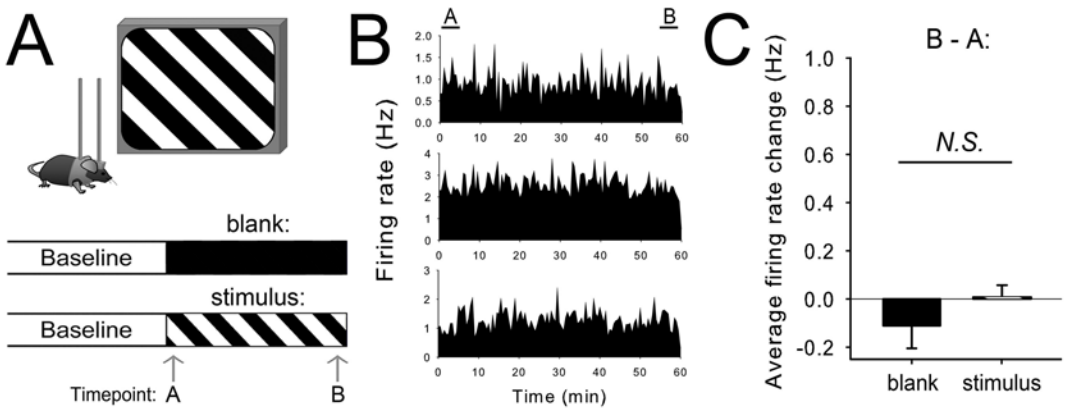

Figure 2.1 Cortical neurons' firing rates do not change across waking visual experience which induces OSRP. **(A)** To assess firing rate changes over waking experience, firing rates were compared during the first (Timepoint A) and last (Timepoint B) 5-min windows of oriented grating (stimulus) presentation or blank screen (blank) presentation, beginning at lights-on. **(B)** Firing rate histograms for three representative V1 neurons during 1-h stimulus presentation. (C) Firing rate changes for individual neurons (in Hz) were not significantly changed across stimulus presentation, and were not different between stimulus (*n* = 20 experiments [8 from a previous study[3]], 268 neurons) and blank screen (*n* = 3 experiments, 44 neurons) conditions.

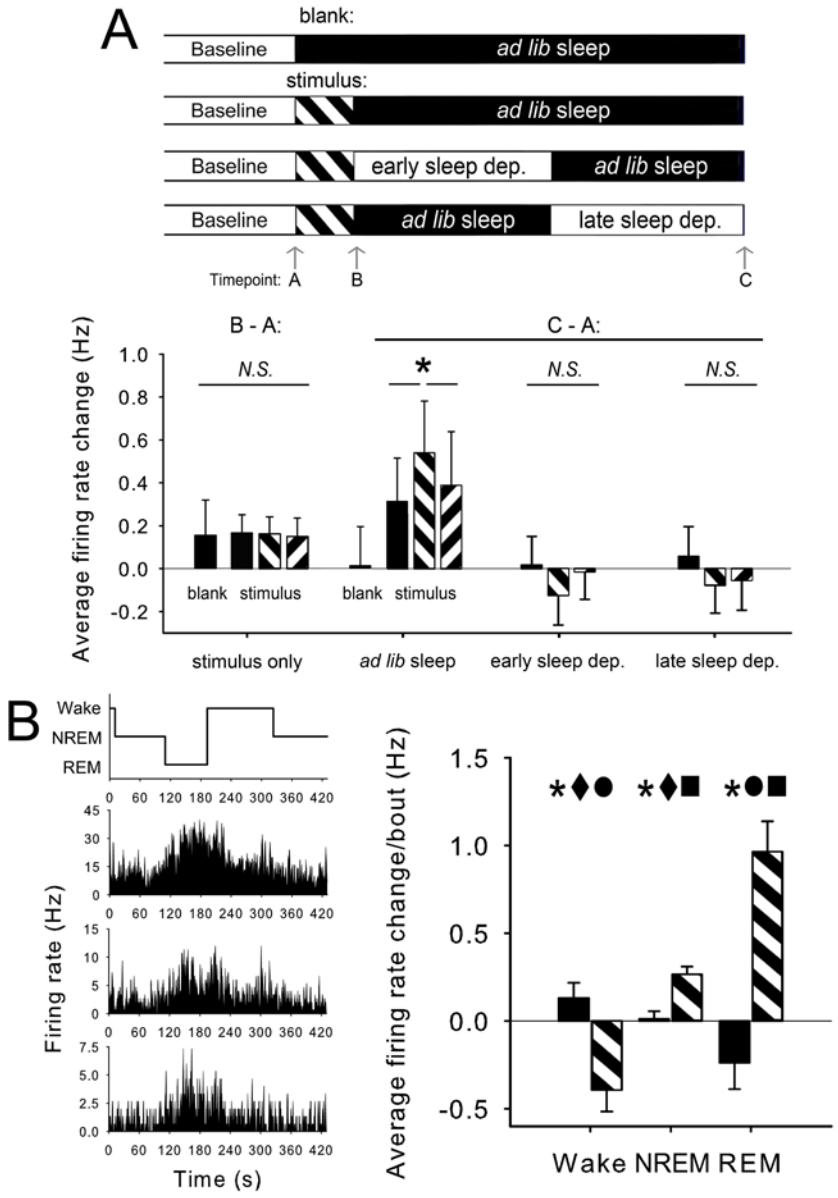

Figure 2.2 Cortical neurons' firing rates increase across subsequent sleep. (A) No differences in either spontaneous firing rate or orientation-specific responses (presented and orthogonal orientations are shown) were seen immediately after blank screen or stimulus presentation (Timepoint B). After subsequent *ad lib* sleep (Timepoint C; *n* = 11 experiments [4 from a previous study[3]], 137 neurons), firing rate responses were selectively enhanced for the presented stimulus. * indicates P < 0.05 for presented vs. orthogonal, presented vs. blank, Holm-Sidak post hoc test, P < 0.05, RM ANOVA. Post-sleep firing rate changes following blank screen presentation (n = 8 experiments [4 from a previous study[3]], 105 neurons) were negligible. Subsets of mice underwent behavioral sleep deprivation in the first (early sleep dep., *n* = 14 experiments [4 from a previous study[3]], 176 neurons) or second (late sleep dep., *n* = 13 experiments [3 from a previous study[3]], 166 neurons) half of the post stimulus sleep period. In both sleep deprivation conditions, response rate changes across the day were negligible, and stimulus-specific potentiation of responses was lost. **(B)** To determine how neuronal firing changed during sleep and wake bouts, firing rates were averaged over the first and last 30 seconds of individual bouts of wake, NREM, or REM. Changes in firing were calculated for each bout ≥1 min over the first 4 h following presentation of oriented gratings (striped bars; *n* = 509, 1152, and 287 measurements from 4 mice for wake, NREM, and REM, respectively) or blank screen (black bars; *n* = 630, 1625, and 236 measurements from 4 mice). Bouts with zero firing were excluded from analysis. * indicates P < 0.005 for stimulus vs. blank screen; ■, ●, and ♦ indicate P < 0.001 vs. wake, NREM, and REM, respectively in the stimulus condition, 2-way RM ANOVA with Holm-Sidak post hoc test.

following stimulus presentation, firing rate increases would occur preferentially during sleep (vs. wake). To test these predictions, we quantified firing rates for individual neurons at the beginning and end of each bout of wake, NREM, and REM ≥1 min duration. Changes in firing rate across bouts were averaged for the 3 states over the first 4 h following presentation of oriented gratings or (for comparison) following presentation of blank screen (**Fig. 2.2B**). Similar to what we found in our previous study,[3] presentation of gratings led to significant increases in firing rate overall (main effect of stimulus presentation, $F = 16.4$, $P < 0.001$, two-way RM ANOVA). However, these increases were not uniform across states (stimulus × state interaction, $F = 33.3$, $P < 0.001$, two-way RM ANOVA). Relatively large increases in firing rate (0.96±0.17 Hz) occurred across bouts of REM, with smaller increases (0.27±0.04 Hz) occurring across bouts of NREM, and decreases in firing (-0.39±0.12 Hz) occurring across bouts of wake (main effect of state, $F = 12.0$, $P < 0.001$; wake vs. REM, wake vs. NREM, and REM vs. NREM, $P < 0.001$, Holm-Sidak post hoc test). State-specific firing rate changes were in the opposite direction in the hours following blank screen presentation, with mean per-bout changes of -0.24±0.15 Hz, 0.01± 0.04 Hz, and 0.13±0.09 Hz, respectively, in REM, NREM, and wake.

2.4 Discussion

Three of our current findings are inconsistent with SHY. First, firing rates do not increase significantly across a novel waking experience that induces OSRP. Second, after this experience, stimulus-specific visual responses increase in a sleep-dependent manner. Third, firing rates in V1 increase significantly across individual bouts of post-stimulus NREM, and increase even more across bouts of post-stimulus REM. One caveat

is that in these studies, we directly measured neuronal activity, but not synaptic strength. In response to changing sensory input, *in vivo* firing rate change increases (as measured here) may result from Hebbian plasticity mechanisms,[20,29] homeostatic mechanisms,[26] or alterations in membrane excitability.[30] Nonetheless, our data present a case where there is no evidence for homeostatic downscaling of synapses during sleep, and where downscaling is not a parsimonious mechanistic explanation for sleep-dependent plasticity. Rather, in light of what is already known about OSRP,[20] the most parsimonious explanation of our current and past[3,17,29] findings is that cortical synapses are strengthened during sleep.

Hypotheses are useful for advancing our understanding only when they can be amended or falsified. Because SHY has been so influential, two questions neuroscientists must ask are: (1) whether synaptic potentiation associated with novel learning *can* occur during sleep and, (2) whether synaptic potentiation, downscaling, or both are present in the context of naturally occurring sleep-dependent plasticity. The answer to the first question is “yes” - our lab and others[3,12-17] have already provided substantial evidence that synaptic potentiation *can occur* during sleep instead of wake. The second question can only be answered with data from the brain in the context of experience-dependent plasticity, not with rigid adherence to one hypothesis about the function of sleep.

2.5 References

1. Heller C. The ups and downs of synapses during sleep and learning. Sleep 2014;37:1157-8.

2. Cirelli C, Tononi G. Sleep and synaptic homeostasis. Sleep 2014;38:161-2.

3. Aton SJ, Suresh A, Broussard C, Frank MG. Sleep promotes cortical response potentiation following visual experience. Sleep 2014;37:1163-70.

4. Tononi G, Cirelli C. Sleep and the price of plasticity: From synaptic and cellular homeostasis to memory consolidation and integration. Neuron 2014;81:12-34.

5. Cirelli C, Gutierrez CM, Tononi G. Extensive and divergent effects of sleep and wakefulness on brain gene expression. Neuron 2004;41:35-43.

6. Maret S, Faraguna U, Nelson AB, Cirelli C, Tononi G. Sleep and waking modulate spine turnover in the adolescent mouse cortex. Nat Neurosci 2011;14:1418-20.

7. Vyazovskiy VV, Cirelli C, Pfister-Genskow M, Faraguna U, Tononi G. Molecular and electrophysiological evidence for net synaptic potentiation in wake and depression in sleep. Nat Neurosci 2008;11:200-8.

8. Vyazovskiy VV, Olscese U, Lazimy YM, et al. Cortical firing and sleep homeostasis. Neuron 2009;63:865-78.

9. Nere A, Hashmi A, Cirelli C, Tononi G. Sleep-dependent synaptic down-selection (I): modeling the benefits of sleep on memory consolidation and integration. Front Neurol 2013;4.

10. Hashmi A, Nere A, Tononi G. Sleep-dependent synaptic down-selection (ii): single-neuron level benefits for matching, selectivity, and specificity. Front Neurol 2013;4.

11. Tononi G, Cirelli C. Time to be SHY? Some comments on sleep and synaptic homeostasis. Neural Plast 2012;2012:415250.

12. Yang G, Lai CS, Cichon J, Ma L, Li W, Gan WB. Sleep promotes branch-specific formation of dendritic spines after learning. Science 2014;344:1173-8.

13. Vecsey CG, Baillie GS, Jaganath D, et al. Sleep deprivation impairs cAMP signalling in the hippocampus. Nature 2009;461:1122-5.

14. Heller H, Ruby N, Rolls A, Makam M, Colas D. Adaptive and pathological inhibition of neuroplasticity associated with circadian rhythms and sleep. Behav Neurosci 2014;128:273-82.

15. Chauvette S, Seigneur J, Timofeev I. Sleep oscillations in the thalamocortical system induce long-term plasticity. Neuron 2012;75:1105-13.

16. Mascetti L, Foret A, Schrouff J, et al. Concurrent synaptic and systems memory consolidation during sleep. J Neurosci 2013;33:10182-90.

17. Aton SJ, Seibt J, Dumoulin M, et al. Mechanisms of sleep-dependent consolidation of cortical plasticity. Neuron 2009;61:454-66.

18. Ulloor J, Datta S. Spatio-temporal activation of cyclic AMP response element-binding protein, activity-regulated cytoskeletal-associated protein and brain-derived nerve growth factor: a mechanism for pontine-wave generator activation-dependent two-way active-avoidance memory processing in the rat. J Neurochem 2005;95:418-28.

19. Frenkel MY, Sawtell NB, Diogo AC, Yoon B, Neve RL, Bear MF. Instructive effect of visual experience in mouse visual cortex. Neuron 2006;51:339-49.

20. Cooke SF, Bear MF. Visual experience induces long-term potentiation in the primary visual cortex. J Neurosci 2010;30:16304-13.

21. Creutzfeldt O, Rosina A, Ito M, Probst W. Visually evoked response of single cells and of the EEG in primary visual area of the cat. J Neurophysiol 1969;32:127-39.

22. Schroeder CE, Tenke CE, Givre SJ, Arezzo JC, Vaughan HCJ. Striate cortical contribution to the surface-recorded pattern-reversal VEP in the alert monkey. Vision Research 1991;31:1143-57.

23. Schroeder CE, Mehta AD, Givre SJ. A spatiotemporal profile of visual system activation revealed by current source density analysis in the awake macaque. Cereb Cortex 1998;8:575-92.

24. Sawtell NB, Frenkel MY, Philpot BD, Nakazawa K, Tonegawa S, Bear MF. NMDA receptor-dependent ocular dominance plasticity in adult visual cortex. Neuron 2003;38:977-85.

25. Fischer QS, Graves A, Evans S, Lickey ME, Pham TA. Monocular deprivation in adult mice alters visual acuity and single-unit activity. Learn Mem 2007;14:277-86.

26. Hengen K, Lambo M, SD VH, DB K, Turrigiano G. Firing rate homeostasis in visual cortex of freely behaving rodents. Neuron 2013;80:335-42.

27. Keck T, Keller G, Jacobson R, Eysel U, Bonhoeffer T, Hubener M. Synaptic scaling and homeostatic plasticity in the mouse visual cortex in vivo. Neuron 2013;80:327-34.

28. Mrsic-Flogel TD, Hofer SB, Ohki K, Reid RC, Bonhoeffer T, Hubener M. Homeostatic regulation of eye-specific responses in visual cortex during ocular dominance plasticity. Neuron 2007;54:961-72.

29. Aton SJ, Broussard C, Dumoulin M, et al. Visual experience and subsequent sleep induce sequential plastic changes in putative inhibitory and excitatory cortical neurons. Proc Natl Acad Sci U S A 2013;110:3101-6.

30. Mahon S, Charpier S. Bidirectional plasticity of intrinsic excitability controls sensory inputs efficiency in layer 5 barrel cortex neurons in vivo. J Neurosci 2012;32:11377-89.

Chapter 3 Sleep promotes, and sleep loss inhibits, selective changes in firing rate, response properties, and functional connectivity of primary visual cortex neurons.

This chapter includes the manuscript: Clawson, B. C., **Durkin, J.**, Suresh, A. K., Pickup, E. J., Broussard, C., Aton, S. J. (2018). Sleep Promotes, and Sleep Loss Inhibits, Selective Changes in Firing Rate, Response Properties and Functional Connectivity of Primary Visual Cortex Neurons. Frontiers in Systems Neuroscience, 12: 40.

3.1 Abstract

Recent studies suggest that sleep differentially alters the activity of cortical neurons based on firing rates during preceding wake - increasing the firing rates of sparsely firing neurons and decreasing those of faster firing neurons. Because sparsely firing cortical neurons may play a specialized role in sensory processing, sleep could facilitate sensory function via selective actions on sparsely firing neurons. To test this hypothesis, we analyzed longitudinal electrophysiological recordings of primary visual cortex (V1) neurons across a novel visual experience which induces V1 plasticity (or a control experience which does not), and a period of subsequent *ad lib* sleep or partial sleep deprivation. We find that across a day of *ad lib* sleep, spontaneous and visually-evoked firing rates are selectively augmented in sparsely firing V1 neurons. These sparsely firing neurons are more highly visually responsive, and show greater orientation selectivity than their high firing rate neighbors. They also tend to be “soloists” instead of “choristers” - showing relatively weak coupling of firing to V1 population activity. These

population-specific changes in firing rate are blocked by sleep disruption either early or late in the day, and appear to be brought about by increases in neuronal firing rates across bouts of REM sleep. Following a patterned visual experience that induces orientation-selective response potentiation (OSRP) in V1, sparsely firing and weakly population-coupled neurons show the highest level of sleep-dependent response plasticity. Across a day of *ad lib* sleep, population coupling strength increases selectively for sparsely firing neurons - this effect is also disrupted by sleep deprivation. Together, these data suggest that sleep may optimize sensory function by augmenting the functional connectivity and firing rate of highly responsive and stimulus-selective cortical neurons, while simultaneously reducing noise in the network by decreasing the activity of less selective, faster-firing neurons.

3.2 Introduction

Sleep is hypothesized to play a critical role in learning and memory, by facilitating long-lasting plastic changes in the strength of synapses and across networks.[4,5,9,15,29,42] Among the mechanisms by which sleep may promote information storage in the brain, general synaptic downscaling has been proposed as a possible mediator. In theory, widespread synaptic downscaling is proposed as a homeostatic response by which network excitability could be constrained and signal-to-noise ratios for neuronal firing could be improved following widespread synaptic potentiation associated with waking experience.[36,37] This idea is supported by biochemical and transcriptomic studies in rodents, demonstrating that cellular markers of neuronal activity and synaptic strengthening are increased in the forebrain after a period of wake, and decreased after

a period of sleep.[10,24,39] However, recent studies suggest that these effects may vary between brain areas[14,35] and as a function of experience.[4,30,31,34,38] Thus it is unclear whether downscaling is a phenomenon associated with experience-dependent plasticity in neuronal circuits, such as are initiated by learning. In addition, it is unclear whether downscaling occurs during rapid eye movement (REM) or non-REM (NREM) sleep. For example, studies of cortical neurons have attributed decreases in firing to slow wave activity in NREM,[40] while studies of hippocampal neurons have shown firing increases across bouts of NREM, and rapid decreases across REM sleep.[20] Moreover, it is unclear whether, or how, sleep-dependent downscaling would affect the response properties and information-processing capabilities of individual neurons. Recent data suggest that sleep-associated decreases in synaptic strength and neuronal excitability are heterogeneous, even within a given brain region. For example, only a subset of synaptic structures appear to be reduced in size in the cortex across sleep,[13] and only a subset of cortical neurons show significant decreases in firing rate after sleep.[40] The idea that these changes are not uniform, but may preferentially affect a specific subpopulation of network neurons, is supported by recent studies of firing rate changes in rodent frontal cortex and hippocampus across bouts of sleep and wake behavior. For example, Watson et al found that while most rat cortical neurons show firing decreases across bouts of REM sleep, only those neurons that have the fastest baseline firing rates show firing decreases in NREM sleep. Overall changes in firing across sleep periods (containing REM, NREM, and microarousals) are opposite between higher firing neurons (which show net firing decreases) and sparsely firing neurons (which show net firing increases). Thus instead of uniformly decreasing firing rates, sleep seems to narrow the distribution of firing rates

among cortical neurons.[41] In contrast to what is seen in frontal cortex, firing rates among both interneurons and principal neurons in hippocampal area CA1 generally increase across bouts of NREM, and dramatically decrease across bouts of REM.[20] Available data suggests that as is true for cortical neurons, these changes in firing across sleep differentially affect higher-firing and lower-firing neurons.[25]

Recent studies have also characterized neurons in sensory cortical areas based on how coupled their firing is to that of the population.[7,28] So-called “choristers” fire in a manner which is tightly linked to spontaneous population-level activity, while “soloists” tend to fire independently from the population. In sensory areas, fast-spiking interneurons, and bursting pyramidal neurons, tend to fire as choristers, while non-bursting pyramidal neurons fire as soloists.[28] Bachatene et al. also demonstrated that population-coupling strength of neurons in sensory cortex varies as a function of firing rate.[7] Thus, the neurons on the lower end of the firing rate distribution appear to be comprised of soloists, while high-firing neurons are likely choristers.[7] Critically, the relationship between neurons’ population coupling strength, their sensory response characteristics, and their information-carrying capacity remains a matter of speculation.[7,28] While soloists may be able to respond very selectively and precisely to sensory stimuli, choristers’ firing appears to carry additional information regarding an animal’s behavioral state and other non-sensory factors.[28] Thus two important unanswered questions are how sleep and wake states affect soloist and chorister populations, and how this might be relate to sleep-dependent plasticity in neural circuits.

Recent work from our lab has shown that mean firing rates are differentially affected by sleep in mouse primary visual cortex (V1), depending on prior visual

experience. For example, we have shown that when mice are presented with a single oriented grating over a prolonged period (several minutes to an hour), neurons in V1, show an enhanced firing rate response to grating stimuli of the same orientation, but only after a period of sleep.[6,16,17] After a visual experience that induces OSRP, firing rates for V1 neurons increase across bouts of sleep, particularly across REM sleep.[17] Thus state-dependent changes in V1 neurons' firing rates are functionally linked to sensory plasticity and may vary as a function of prior sensory experience.

Here we aim to address how brain state-dependent changes in different neuronal populations may affect the basic function and information-processing capabilities of sensory cortex.[2] We first assess how both spontaneous and visually-evoked firing rates of sparse- or fast-firing V1 neurons are affected by visual experience, across a period of subsequent *ad lib* sleep, or across a similar period with partial sleep deprivation. We then assess how these parameters are affected in neurons which fire in a manner that is either weakly or strongly coupled to V1 population activity. We also determine which neurons' orientation preferences are most altered in the context of OSRP.

3.3 Materials and Methods

3.3.1 In vivo neurophysiology.

All mouse procedures were approved by the University of Michigan Institutional Animal Care and Use Committee. For chronic recordings, male and female C57BL/6J mice (Jackson) aged 1-3 months (an age range where OSRP is induced robustly by visual experience)[6,16,19] were implanted with custom-built drivable headstages (EIB-36 Neuralynx) under isoflurane anesthesia, using previously described techniques.[6] For

each mouse, two 200 µm-diameter bundles of seven stereotrodes each (25 µm nichrome wire, California Fine Wire; Grover Beach, CA) were placed in right hemisphere V1 (0.5-1 mm apart), reference and ground electrodes were placed in left hemisphere V1 and cerebellum, respectively, and three electromyography (EMG) electrodes were placed in nuchal muscle.

Following surgical procedures, mice were individually housed in standard caging with beneficial environmental enrichment (nesting material, toys, and treats) throughout all subsequent experiments. With the exception of OSRP or blank screen experimental days, during which room lights were kept off, lights were maintained on a 12-h:12-h light:dark cycle (lights on at 8 AM, lights off at 8 PM). Food and water were provided *ad lib* throughout all procedures. After 1-2 weeks of post-operative recovery, mice were prepared for chronic stereotrode recording in their home cage, which was placed inside a sound-attenuated recording chamber (Med Associates). Mice were tethered using a lightweight cable for neural recording, and were habituated to daily handling, restraint, and head fixation over a period of 5 days. During this time, electrodes were gradually lowered into V1 until stable neuronal recordings were obtained. Recording stability was defined by the continuous presence of spike waveforms on individual electrodes for at least 24 h prior to the onset of baseline recording. Signals from each electrode were split and differentially filtered to obtain spike data (200 Hz-8 kHz) and local field potential (LFP)/EMG activity (0.5-200 Hz). Data were amplified at 20 ×, digitized, further digitally amplified at 20-100 ×, and recorded using Plexon Omniplex software and hardware (Plexon Inc.; Dallas, TX). For all chronic recordings, single-unit data was referenced locally to a recording channel without single-unit activity, to eliminate low-frequency noise.

3.3.2 Visual stimuli, OSRP induction, and assessment of visual response properties.

A continuous 24-h baseline recording was carried out for each mouse, starting at lights-on (8 AM; CT0 – Circadian Time 0). The following day at CT0, mice were head-fixed. To assess baseline (AM) visual response properties in V1 neurons, phase-reversing oriented gratings (spatial frequency 0.05 cycles/degree, 100% contrast, reversal frequency 1.0 Hz) of 4 orientations (0, 45, 90, and 135 degrees from horizontal) and a blank (dark) screen (to assess spontaneous activity) were presented to the left (contralateral) visual field. Each of these stimuli was presented 8 times (10 s for each presentation) in a random, interleaved fashion. Neuronal firing rate responses were quantified and averaged for each stimulus orientation (and blank [dark] screen) across total presentation time (i.e., 10 s × 8 repetitions). Immediately following this baseline (8 AM; CT 0) test, either a single grating stimulus (of a randomly-selected orientation) or a blank [dark] screen was continuously presented over a 30-min period to induce OSRP. Mice were then returned to their home cage and recordings continued until CT12 in complete darkness (with far-infrared illumination only, to prevent additional visual experience), at which time mice were again head-fixed for a second (PM) test of visual response properties. Between 30-min grating (or blank screen) presentation and PM testing, mice were either allowed to sleep *ad lib* (Vis Stim + Sleep: n = 14 mice, Blank Screen + Sleep: n = 7 mice), or were kept awake over the first 6 h (Vis Stim + early sleep deprivation [ESD]: n = 11 mice) or last 6 h (Vis Stim + late sleep deprivation [LSD]: n = 13 mice), using gentle handling procedures.[6] Briefly, when mice were observed (under far-infrared illumination) taking stereotyped sleep postures and LFP data indicated transitioning from wake to NREM sleep, cages were tapped gently to awaken the mice.

Later in the procedure (typically within the last 1-2 hours), disturbance of the nest or lightly brushing the mouse with a cotton-tipped applicator was used to prevent sleep.

For each stably-recorded neuron (i.e., those with consistent spike waveforms on the two stereotrode channels across 24-h baseline recording, and across the 12-h experiment; see below for details of single-unit identification), a number of visual response properties were assessed during CT0 (i.e., the time of expected lights-on; “AM”) and CT12 (i.e., the time of expected lights-off; “PM”) tests (at 8 AM and 8 PM, respectively), using previously-described metrics.[3,4,6] Mean firing rates (in Hz) were averaged across all repetitions of the same visual stimulus (or blank [i.e., dark] screen). Mean blank screen firing (in Hz) was used as a metric of each neuron’s spontaneous activity. Mean firing at each neuron’s preferred stimulus orientation (i.e., that which evoked maximal firing rate response) was used as a metric of maximal visually-evoked firing rate. An orientation selectivity index (OSI45; used to indicate the strength of orientation tuning, regardless of orientation preference) was calculated for each neuron, as 1 - [(average firing rate at ± 45° from preferred orientation)/(average firing rate at the preferred stimulus orientation)]. Thus OSI45 values for individual neurons range from 0 (minimal selectivity for the preferred stimulus orientation) to 1 (maximal selectivity for the preferred stimulus orientation). Neuronal visual responsiveness (to any visual stimulus) was assessed as a responsiveness index (RI), calculated as 1 - [(average firing rate at blank screen presentation)/(average firing rate at the preferred stimulus orientation)]. RI values for individual V1 neurons typically range from 0 (not visually responsive) to 1 (maximally responsive), although negative values are possible for non-responsive neurons). Changes in these values between AM and PM tests (i.e., during the inactive

phase of the rest-activity cycle; from CT 0 to CT12) were assessed in non-sleep deprived and sleep deprived mice. For mice presented with a visual stimulus to induce OSRP, initial preference for the presented stimulus orientation was quantified as the ratio of mean firing rate responses for the presented orientation (X°) to that of the orthogonal to presented stimulus (X+90°) as described previously. Changes in this measure (and in other visual response properties) were quantified by subtracting CT0 baseline (AM) (X°/X+90°) ratio from CT12 (PM) (X°/X+90°) ratio; this difference was then expressed as a percent change from the baseline value.

3.3.3 Histology.

At the conclusion of each recording, mice were deeply anesthetized with barbiturate injection, and an electrolytic lesion was made at each electrode site (2 mA, 3 s per electrode). Mice were then perfused with formalin and euthanized. Brains were post-fixed, cryosectioned at 50 µm, and stained with DAPI (Fluoromount-G; Southern Biotech) to verify electrode placement in V1.

3.3.4 Single unit identification and data analysis.

Single-neuron data were discriminated offline using standard principle component-based procedures as described previously.[3,6,16,17,26,27] To ensure stable tracking of single-neuron activity across time, all data analyses were carried out on spike data that was continuously acquired throughout the experiment. Example data are shown for pair of neurons stably recorded on the same V1 stereotrode, from a freely-behaving mouse, in **Fig. 3.1**. As shown in **Fig. 3.1**, spikes from individual neurons were discriminated based

on consistent spike waveform shape and width, relative spike amplitude on the two stereotrode wires, and relative positioning of waveform clusters in three-dimensional principal component space. Single-neuron isolation was verified quantitatively using standard techniques.[21] Clusters with interspike interval (ISI)-based absolute refractory period violations were eliminated from analysis. Waveform cluster separation (for channels with more than one discriminated single unit) was validated using MANOVA on the first 3 principal components ($p < 0.05$ for all sorted clusters), and the Davies-Bouldin (DB) validity index,[33] as described previously.[16,27]

Only neurons that 1) met the criteria described above and 2) were reliably discriminated and continuously recorded throughout each experiment (*i.e.*, across both 24-h baseline and 12-h experimental condition) were included in firing rate analyses. For analysis of firing rate changes across the population of recorded V1 neurons (e.g., in **Figs. 3.3-3.8**), spontaneous and maximal visually-evoked firing rates (calculated as described above) were $\log_{(10)}$-transformed. For ANOVA analyses of visual response properties and firing rate changes, all recorded neurons in a given experimental group were grouped into sextiles, based on either their spontaneous firing rate, maximal visually-evoked firing rate, or population coupling strength (see below) at baseline. Sextiling of data allowed statistical comparisons between changes seen in the highest and lowest firing neurons, and direct comparisons of our results with those of other labs.[41] Changes in firing rate across the day were expressed as a fold change.

Intracortical LFP and nuchal EMG signals were used to categorize recorded data into REM, NREM, and wake states over 10-s intervals of recording using custom software. Firing rates were calculated separately within REM, NREM, and wake using

NeuroExplorer software (Plexon). To assess neuronal firing rate changes across individual bouts of these states, we used a calculation similar to that described previously.[17] Briefly, firing rates across time were $\log_{(10)}$-transformed, and mean firing rates across the first and last 30 s of each state bout were calculated. Changes in firing rate were calculated using custom software, by subtracting the mean firing rate in the first 30 from the mean firing rate in the last 30 s. Bouts with less than 60 s duration, and neurons with a firing rate of 0 Hz in either the first or last 30 s of a particular bout, were excluded from the analysis. Mean rate changes were averaged for all the bouts of a given state (i.e., REM, NREM, or wake) occurring across the entire *ad lib* sleep portion of the experiment for each animal. Thus for Vis Stim + Sleep and Blank Screen + Sleep mice, data were averaged over the CT0 to CT12 *ad lib* sleep recording period; for Vis Stim + ESD mice, data were averaged over the last 6 h of recording; for Vis Stim + LSD mice, data were averaged over the first 6 h of recording.

To assess population coupling, neurons were cross-correlated with the population rate activity during the AM test using a cross-correlogram (CCG) algorithm. Population rate time series were first constructed from the firing of all single units and multi-unit activity across the AM test, with the neuron of interest's spike times removed; this was done separately for each neuron. Each neuron's spike train was then cross-correlated with the population rate in 1 ms bins, with counts per bin normalized to the number of reference events as probabilities to account for differences in firing rate. A 95% confidence interval was applied to each CCG. CCGs were corrected using a shift-predictor procedure during the AM and PM tests to correct for coincident firing due to common visually-driven input (similar to methods described in (Bachatene et al., 2015))

and CCGs were smoothed with a Gaussian filter with a 3 bin width. Peaks in the corrected CCGs were used as measures of population coupling; these peaks were compared between AM and PM tests to assess changes in population coupling across the day.

3.4 Results

3.4.1 Visual response plasticity among V1 neurons relies on both visual experience and sleep.

To characterize effects of visual experience and brain states on visual response properties and firing rates, we first quantified V1 neuronal firing in recordings from C57BL/6J mice. An example showing the stability of our V1 neuronal recordings (from a representative mouse) is shown in **Fig. 3.1**. Mice underwent continuous recording across a 24-h baseline period (to verify stability of neuronal recordings), a baseline (AM) visual response assessment (at lights-on; CT0), a 30-min presentation of a single oriented flickering grating (or, as a negative control, a blank screen), and a 12-h post-stimulus period in complete darkness (to prevent additional visual experience). During this post-stimulus period, mice were either allowed *ad lib* sleep, or were sleep deprived by gentle handling over the first or last 6 h (early sleep deprivation [ESD] or late sleep deprivation [LSD]). At CT12, response properties were reassessed to quantify OSRP and other changes in visual responses (**Fig. 3.2A**). As we have shown previously (Aton et al., 2014; Durkin et al., 2017; Durkin and Aton, 2016), oriented grating presentation resulted in an increase among V1 neurons' firing rate responses to the presented stimulus orientation. Consistent with our prior findings, both ESD and LSD disrupted OSRP. This was true for

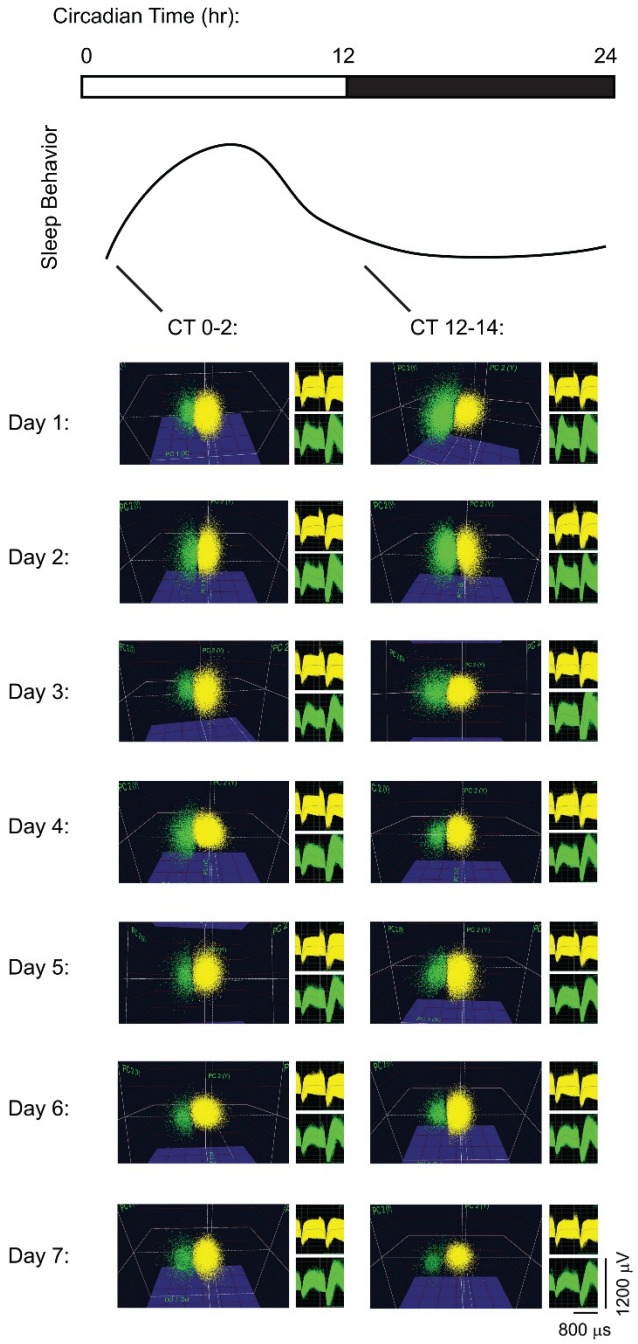

Figure 3.1. Long-term recordings of V1 neurons. Spike data are shown from two representative neurons on a V1 stereotrode across 7 days of continuous recording. For display purposes (i.e., to show stability of spike waveforms over time) neuronal spike data are shown over 2-h intervals of recording time at lights-on (CT0-2) and at lights-off (CT12-14) each day, clustered in three-dimensional principal component (PCA) space. Waveforms for the spikes in the two clusters are shown to the right of PCA plots.

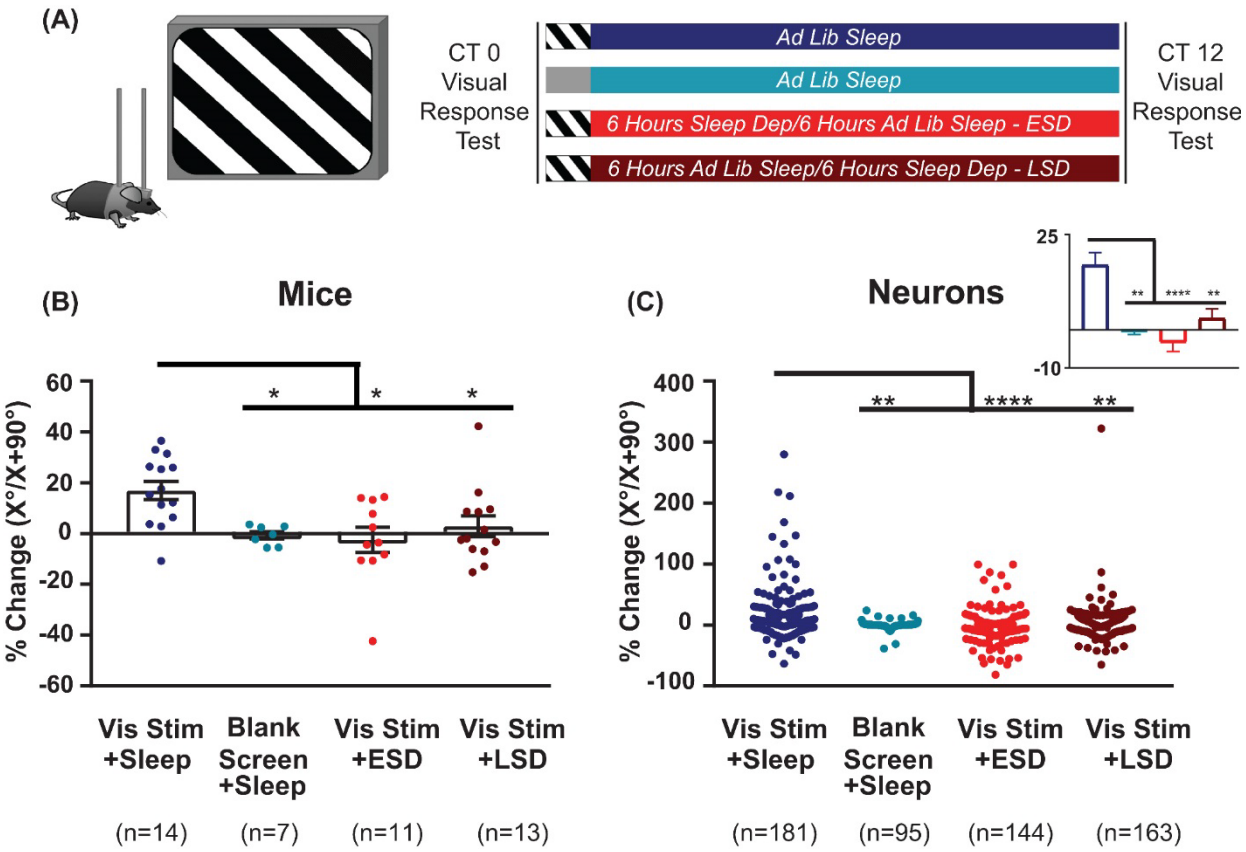

Figure 3.2. OSRP is induced in V1 by visual experience and dependent on subsequent sleep. (A) Experimental design. Mice were implanted with stereotrodes to record V1 neurons' firing across baseline (AM) visual response testing (at lights-on; CT0), 30-minute oriented grating stimulus presentation (to induce OSRP) or blank screen presentation, 12 h of subsequent ad lib sleep, early sleep deprivation (ESD) or late sleep deprivation (LSD), and a final (PM) visual response test at CT12. Mice were kept in complete darkness (under far-infrared illumination) across CT0-12, to avoid additional visual experience after stimulus presentation. **(B)** OSRP data, showing per-mouse average % changes in neurons' responses to the presented visual stimulus orientation (X°) vs. the orthogonal orientation (X + 90°) ($p = 0.007$, Kruskal-Wallis one-way ANOVA on ranks). Bar graphs show mean ±SEM. Numbers of mice are indicated for each group. **(C)** Neuron by neuron data, as in B ($p < 0.0001$, Kruskal-Wallis one-way ANOVA on ranks). For all panels, * indicates $p < 0.05$, ** indicates $p < 0.01$, *** indicates $p < 0.001$, and **** indicates $p < 0.0001$, Dunn's post hoc test.

both the average OSRP of each mouse (i.e., measured across all neurons recorded from each mouse; **Fig. 3.2B**) and for all neurons recorded in a given condition (**Fig. 3.2C**). As we have shown previously, there were no significant differences between OSRP measurements for male vs. female mice,[16] different neuronal subclasses (i.e., principal neurons vs. fast-spiking interneurons),[6] or differential timing of sleep deprivation.[6]

3.4.2 Spontaneous and visually-evoked firing among V1 neurons approximates a lognormal distribution

Watson et al. recently demonstrated that mean firing rates of frontal cortical neurons show a roughly lognormal distribution.[41] For our V1 recordings, we calculated the baseline (AM) spontaneous firing rate during blank screen presentation. We found that, as is true in frontal cortex, the distribution of spontaneous firing rates shows a clearly non-normal distribution ($p < 0.0001$ for all experimental groups, D'Agostino-Pearson normality test – **Fig. 3.3A**). As shown in **Fig. 3.3B**, when neuronal firing rates are $\log_{(10)}$-transformed, although most groups' distributions remain statistically non-normal, each is a closer approximation of normality (Vis Stim + Sleep: $p = 0.002$, Blank Screen + Sleep: $p = 0.004$, Vis Stim + ESD: $p = 0.15$, Vis Stim + LSD: $p = 0.017$, D'Agostino-Pearson normality test). A similar pattern was seen for distributions of maximal visually-evoked firing rates (i.e., for responses to each neuron's preferred stimulus orientation; **Fig. 3.3C-D**). Thus spontaneous and visually-evoked firing rate data were $\log_{(10)}$-transformed for all subsequent analyses.

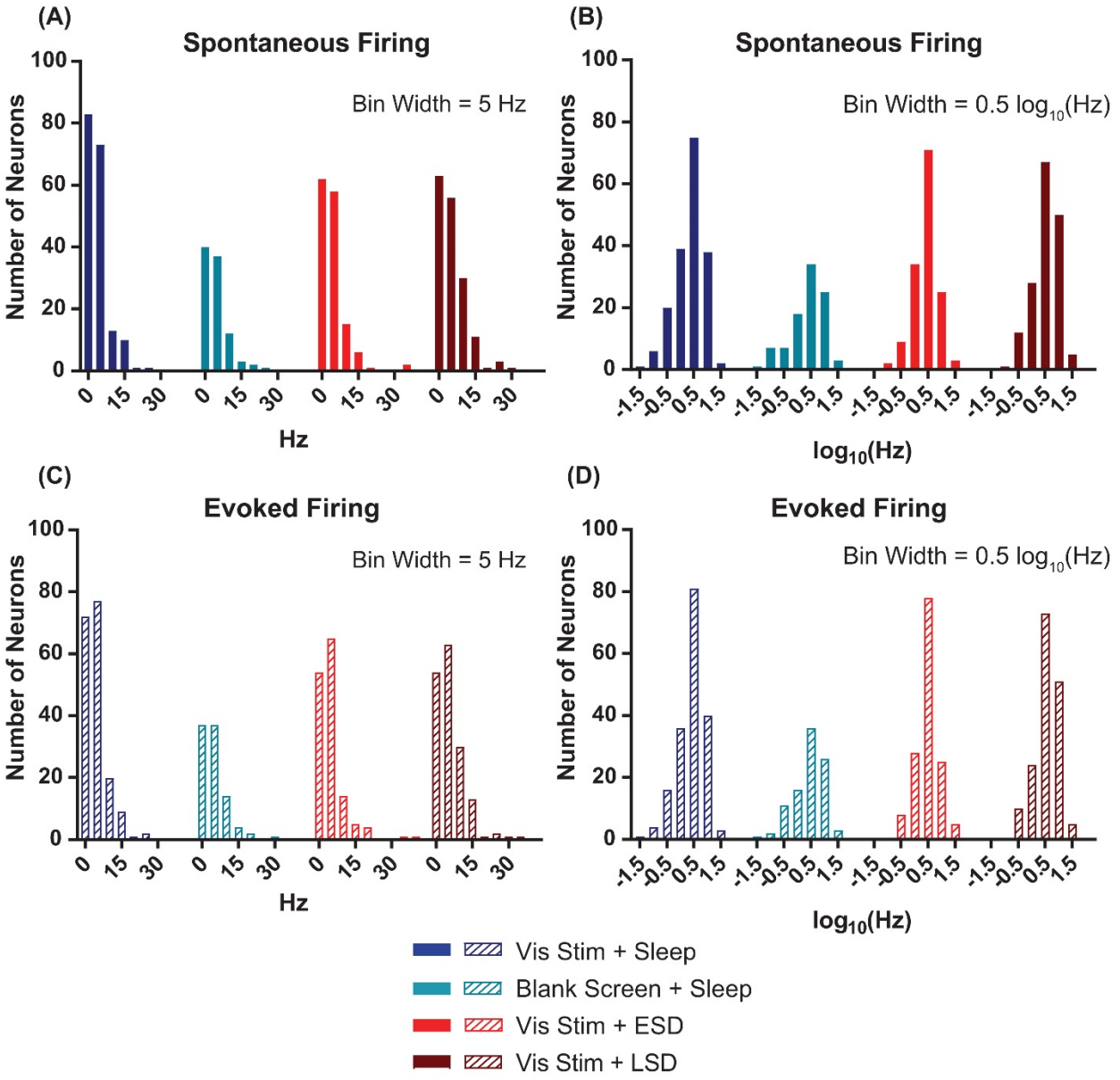

Figure 3.3. V1 neurons' spontaneous and evoked firing rates follow a log-normal distribution. (A) Distributions of baseline (AM) spontaneous firing rates of the neurons recorded from each of the treatment groups were non-normal ($p < 0.0001$, D'Agostino-Pearson normality test). **(B)** $\log_{(10)}$-transformed spontaneous firing rates' distributions approximated normality ($p = 0.002$, 0.004, 0.15, and 0.02, respectively, for Vis Stim + Sleep, Blank Screen + Sleep, Vis Stim + ESD, and Vis Stim + LSD, D'Agostino-Pearson normality test). **(C)** Distributions of baseline (AM) maximal evoked firing rates (i.e., for each neuron's preferred-orientation stimulus) of the neurons recorded from each of the treatment groups were non-normal ($p < 0.0001$, D'Agostino-Pearson normality test). **(D)** $\log_{(10)}$-transformed evoked firing rate data approximated normality ($p = 0.001$, 0.02, 0.55, and 0.05, respectively, for Vis Stim + Sleep, Blank Screen + Sleep, Vis Stim + ESD, and Vis Stim + LSD, D'Agostino-Pearson normality test).

3.4.3 Sleep promotes, and sleep deprivation impairs, re-distributions of firing rates among V1 neurons

We next assessed how sleep changes firing rates across the V1 neuronal population. As shown in **Fig. 3.4**, neurons recorded in both *ad lib* sleep conditions (following either visual stimulus or blank screen presentation) showed a re-distribution of both spontaneous (**Fig. 3.4A**) and maximal visually-evoked (**Fig. 3.4B**) firing rates across the day. This re-distribution was systematic, in that (as is true for firing changes across sleep in frontal cortex)[41], the lowest firing neurons showed increases in firing rate, and the highest firing neurons showed decreases in firing rate. This is illustrated by taking the regression of ($\log_{(10)}$-transformed) baseline (AM) spontaneous firing compared with the fold change in firing across the day. In the absence of systematic firing changes across the baseline V1 firing rate distribution, one would expect the slope of this regression to be zero. We find that firing rate changes among neurons in both *ad lib* sleep conditions (i.e., regardless of the type of visual experience) show negative relationships to baseline spontaneous firing, which are significantly different from zero (Vis Stim + Sleep: $p = 0.003$, Blank Screen + Sleep: $p < 0.001$ Spearman rank order, F-test $p < 0.001$). In contrast to what is seen in V1 of non-sleep deprived mice, V1 neurons recorded across both early and late sleep deprivation (ESD and LSD) conditions showed no systematic firing rate changes (for either spontaneous or visually-evoked firing rates). This is shown in **Fig. 3.4A-B**, where for ESD and LSD, the regressions of neurons' firing rate changes vs. their baseline firing rates do not differ from zero (*N.S.*, F-test).

Recent work[41] assessed sleep-dependent firing rate changes among neurons that had been grouped into sextiles based on their mean firing rates. We carried out a similar

analysis on V1 neurons' firing rate changes. As shown in **Fig. 3.4C-J,** in mice from both sleeping conditions, across-the-day firing rate changes varied in V1 depending on baseline firing rate sextile. For both spontaneous (**Fig. 3.4C-D**) and maximal visually-evoked (**Fig. 3.4G-H**) firing, the lowest-firing sextile of V1 neurons from the two sleeping conditions (regardless of visual experience) showed firing rate increases relative to the highest-firing sextile, where neurons tended to have firing rate reductions across the day. This effect was not present in either of the two sleep deprived groups (ESD and LSD), where both spontaneous (**Fig. 3.4E-F**) and visually-evoked (**Fig. 3.4I-J**) firing rate changes across the day did not vary as a function of baseline firing rate. Together, these analyses suggest that firing rates in V1 neurons are altered across a day of *ad lib* sleep, as a function of their baseline firing rate, and that sleep deprivation (at any time of day) disrupts this process.

3.4.4 V1 neurons' visual response properties vary as a function of baseline firing rate

Our analyses of firing rates suggest that specific subpopulations of V1 neurons (those with the lowest and highest baseline firing rates) undergo the largest sleep-dependent alterations in firing (increases and decreases in firing rate respectively). One question, in light of the well-described effects of sleep on visual response plasticity,[3,4,6,16,17,18] is how visual response properties vary between sparsely firing and higher firing neurons. We assessed how visual responses varied at baseline (i.e., during the AM visual response test at CT0) as a function of firing rate. As shown in **Fig. 3.5** (where baseline [AM] data from the four experimental groups are aggregated), we found that both visual responsiveness (**Fig. 3.5A**) and orientation selectivity (**Fig. 3.5B**) are

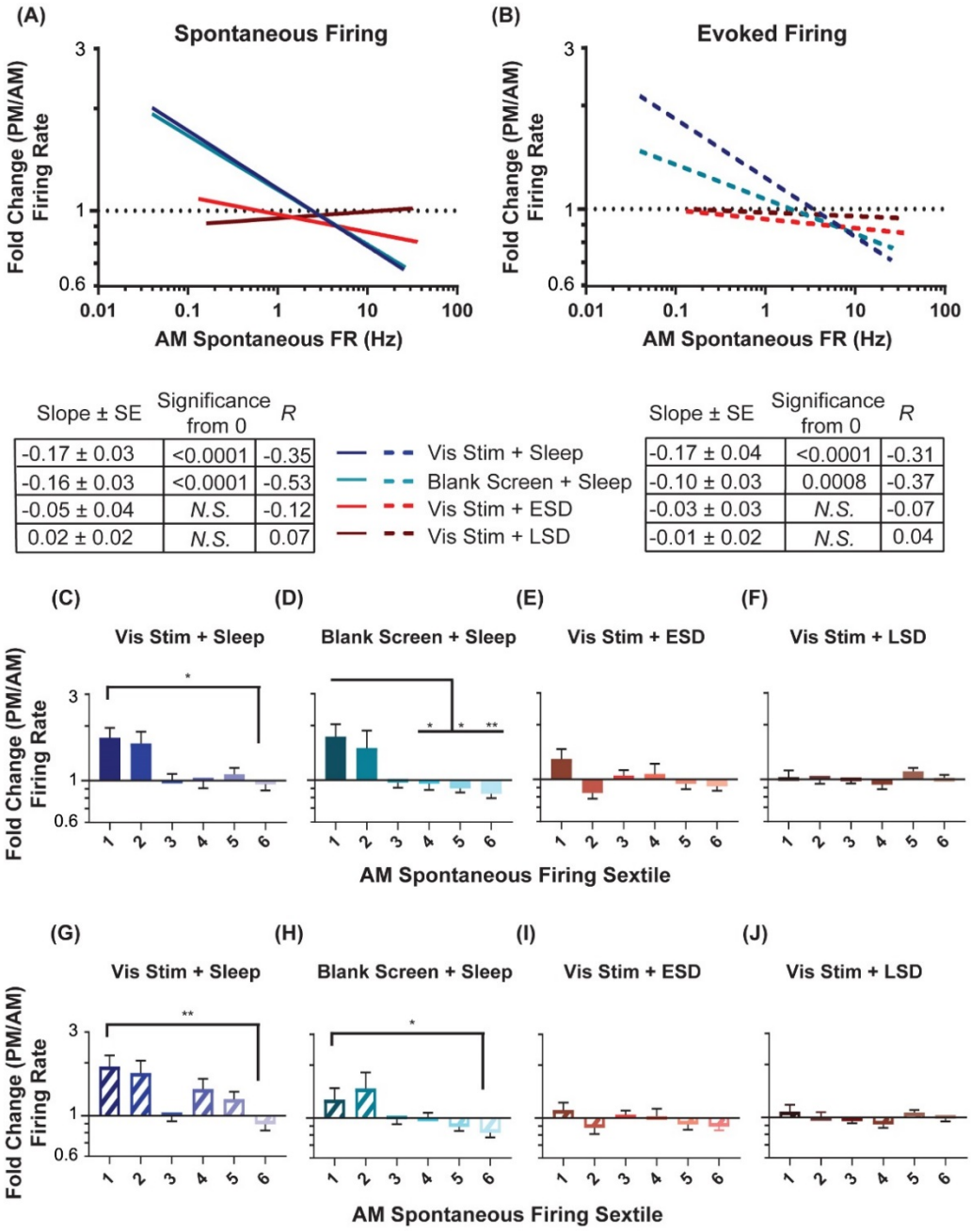

Figure 3.4. Sleep deprivation impairs neuronal firing rate homeostasis. (A-B). Linear fits of data for the change in spontaneous firing rate (A) and maximal visually-evoked firing rate (i.e., at each neuron's preferred stimulus orientation; B) across the day (expressed as a fold change and plotted on a $\log_{(10)}$ scale) vs the AM spontaneous firing rate of the cell (plotted on a $\log_{(10)}$ scale). In both groups with ad lib sleep, sparsely-firing neurons' firing rates increased (i.e., showed a fold change > 1) while highly active neurons' firing decreased (i.e., showed a fold change < 1). In (A) the lines for the visual stimulus and blank screen regressions closely overlap. The table below shows, for each experimental group, the regression slope and SE, Spearman R-value, and Bonferroni-corrected F test p-value. **(C-F)** Sextiles of the change in spontaneous firing rate, based on AM spontaneous firing rate, which is shown in (A) (p = 0.0015 for panel D, respectively, all others N.S., Kruskal-Wallis one-way ANOVA on ranks). **(G-J)** Sextiles of the change in evoked firing rate, based on AM spontaneous firing rate, which is shown in (B) (p = 0.0356, 0.0087 for panels G-H respectively, all others N.S., Kruskal-Wallis one-way ANOVA on ranks). Error bars indicate mean ± SEM for log changes in firing rate; * indicates p < 0.05, ** indicates p < 0.01, *** indicates p < 0.001, and **** indicates p < 0.0001, Dunn's post hoc test.

highest for sparsely firing neurons, and show a significant negative relationship with spontaneous firing rate. This relationship was statistically significant ($p < 0.0001$, Spearman rank order) and regressions were significantly different from 0 ($p < 0.0001$, F-test) across all four experimental groups (when examined separately). A similar relationship between spontaneous firing rate and visual response properties was seen during the CT12 (PM) test ($p < 0.0001$, Spearman rank order; $p < 0.0001$ for slope significance from 0, F Test). **Fig. 3.5C** and **D**, show that these properties vary significantly by firing rate sextile. Together, this suggests that those V1 neurons that show sleep-associated increases in firing (*i.e*., the lowest-firing neurons) are highly visually responsive and sharply orientation-tuned, and thus encode highly specific visual information. Conversely, V1 neurons that show sleep-associated firing decreases (*i.e.*, the highest-firing neurons) are less visually responsive and less orientation selective.

3.4.5 V1 neurons' visual response properties vary with population-coupling strength

Recent studies have categorized populations of neurons in sensory cortex, not based on firing rate, but rather on how strongly coupled their firing is to population activity.[7,28] Okun et al. and Bachetene et al. classified cortical neurons into 'choristers' (i.e., strongly coupled) and 'soloists' (i.e., weakly coupled) based on how correlated their firing was with population activity during both visual stimulation and spontaneous activity.[7,28] We similarly calculated coupling values for each neuron as the peak of the cross-correlogram (CCG) between each spike train and the population rate summed from all other neurons recorded simultaneously (**Fig. 3.6A-B**). Similar to results seen by Bachetene et al., there was a significant relationship between spontaneous firing rate and

population coupling (**Fig. 3.6C**), where highly-coupled neurons ("choristers") exhibited higher spontaneous firing rates ($p < 0.0001$, Spearman rank order).[7] We next examined how baseline visual response properties varied as a function of how strongly coupled neuronal firing is to V1 population activity. We found that across all groups, coupling strength showed a significant negative relationship to both visual responsiveness and orientation selectivity at baseline (**Fig. 3.6D-E**). These findings are consistent with previous literature demonstrating that weakly coupled neurons tend to encode more specific visual information, while strongly coupled neurons do not.[7,28] However, we also found that this relationship was likely mediated by differences in baseline spontaneous firing rates among neurons (p = 1e-8 and p = 3e-5, respectively, Sobel tests for mediation of the relationships between population coupling and visual responsiveness and between population coupling and orientation selectivity).

3.4.6 OSRP varies across the V1 population, as a function of both baseline firing rate and population coupling

To characterize how experience- and sleep-dependent plasticity varies across the population of V1 neurons, we next characterized changes in orientation preference across the day based on neurons' initial firing rate and population coupling. As shown in **Fig. 3.7**, we found that among neurons recorded from non-sleep deprived mice, OSRP was greatest among neurons with the lowest baseline firing rates. The magnitude of OSRP was negatively correlated with baseline firing rate in mice allowed *ad lib* post-stimulus sleep (Vis Stim + Sleep; p = 0.0375, Spearman rank order), but critically, showed no relationship to baseline firing rate in Blank Screen + Sleep, Vis Stim + ESD, or Vis Stim

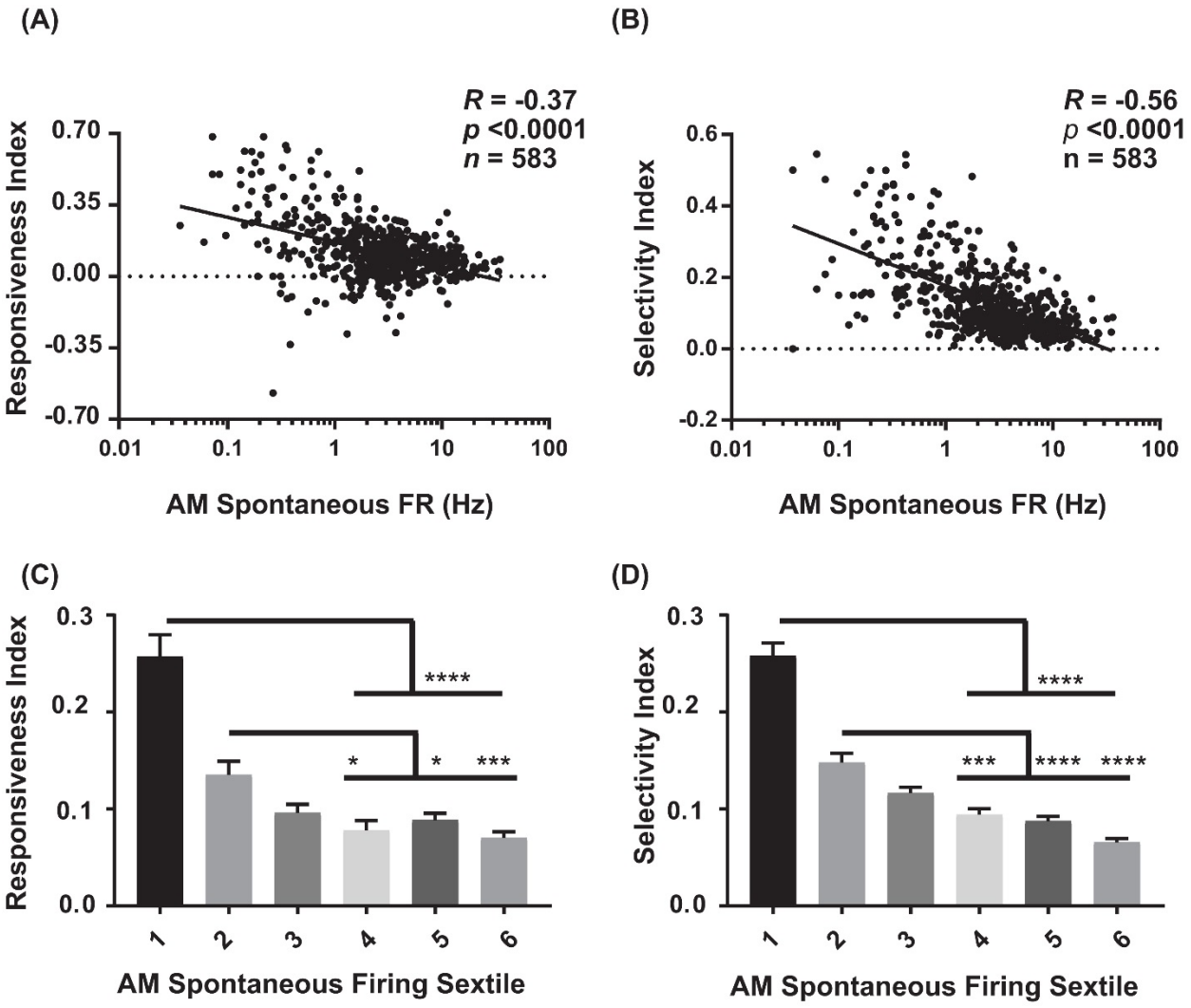

Figure 3.5. Visual response properties vary across the V1 population as a function of firing rate. (A) For baseline (AM) data aggregated across the four experimental groups, there is a significant negative relationship between neurons' spontaneous firing rate and the responsiveness index (RI) (Spearman rank order R- and p-values shown). **(B)** A similar negative relationship was seen between AM spontaneous firing rate and neurons' selectivity index (OSI45; Spearman rank order). **(C) and (D)** The aggregated data was sextiled based on AM spontaneous firing rate. Responsiveness index (RI; C) and selectivity index (OSI45; D) varied significantly across sextiles ($p < 0.0001$, Kruskal-Wallis one-way ANOVA on ranks), with sparsely firing neurons showing higher RI and OSI45 values than faster firing neurons. For panels C-D, * indicates $p < 0.05$, ** indicates $p < 0.01$, *** indicates $p < 0.001$, and **** indicates $p < 0.0001$, Dunn's post hoc test.

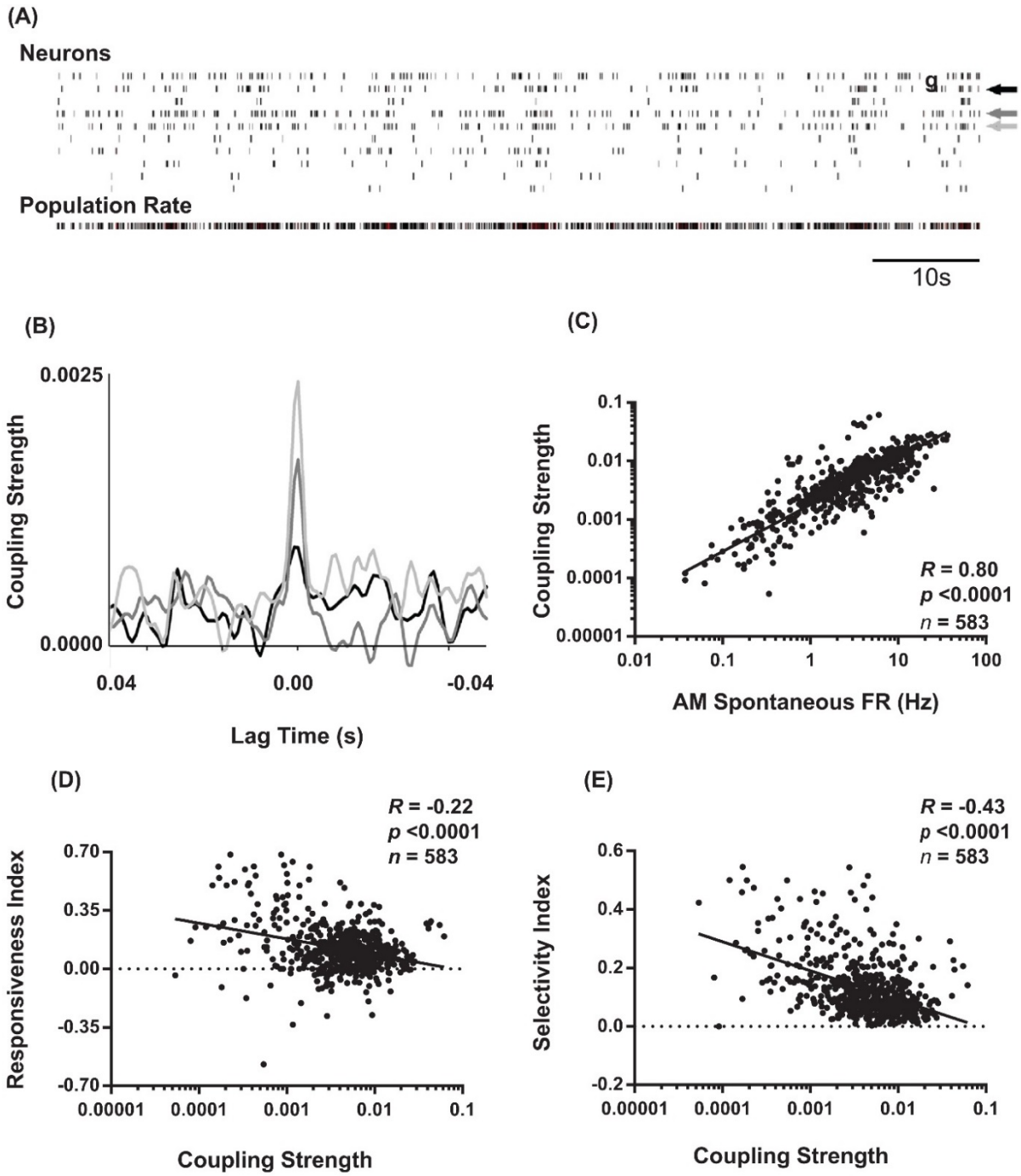

Figure 3.6. Coupling of V1 neurons' firing to population activity is negatively correlated with visual responsiveness and orientation selectivity. (A) Schematic representation of coupling strength calculation. Across AM visual response testing, spike times for individual neurons (indicated by arrows) were cross-correlated with population activity from all other simultaneously recorded neurons (i.e., with the reference neuron's activity subtracted from total firing; shown in bottom raster). **(B)** Superimposed cross-correlograms of spiking from the neurons indicated with arrows in the raster plot are shown, following subtraction of the shift-predictor described in Materials and Methods. Coupling strength for each neuron was calculated as the value of the cross-correlation at 0 lag time. **(C)** For baseline (AM) data aggregated from the four experimental groups, coupling strength and spontaneous firing rate show a strong positive correlation. In contrast, at baseline, coupling strength is negatively correlated with both RI **(D)** and OSI45 **(E)**. Spearman rank order R- and p-values shown.

+ LSD mice (*N.S.*, Spearman rank order; **Fig. 3.7A**). When neurons' spontaneous AM firing rates were grouped into sextiles (**Fig. 3.7C-F**), the lowest-firing sextile showed significantly greater OSRP than neurons in the highest-firing sextiles for mice allowed *ad lib* sleep. However, OSRP was similar in magnitude across baseline firing sextiles in both sleep deprived groups. Similarly, the baseline coupling of firing to population activity tended to be a good predictor of the magnitude of OSRP across the day in neurons recorded from Vis Stim + Sleep mice and Vis Stim + ESD mice (where weakly-coupled neurons showed significantly greater OSRP than strongly-coupled neurons), but not from Blank Screen + Sleep and Vis Stim + LSD mice (**Fig. 3.7B, Fig. 3.7G-J**). The relationship between population coupling and OSRP appeared to be mediated in part by baseline firing rate among neurons recorded from the Vis Stim + Sleep group (p = 1e-6, Sobel test).. However, the same was not true for neurons recorded from Vis Stim + ESD mice, where firing rates did not predict OSRP. These data show that experience-dependent plasticity is not expressed uniformly across the V1 population, but is greatest among sparsely firing and weakly population-coupled neurons after a period of subsequent sleep.

3.4.7 V1 neurons' population-coupling strength is altered by visual experience and sleep

Because population coupling could itself be altered as a function of circuit plasticity, we next assessed how the strength of population coupling changes across the day for different neuronal populations. AM and PM population coupling were highly correlated across all groups (R = 0.82, 0.94, 0.85, 0.64 for Vis Stim + Sleep, Blank Screen + Sleep, Vis Stim + ESD, and Vis Stim + LSD, respectively; all $p < 0.000001$, Spearman rank order). However, there was a significant increase in coupling from AM to PM time

points in the Vis Stim + Sleep condition (p = 0.014; Wilcoxon signed rank test) and significant decrease in coupling from AM to PM in the Vis Stim + ESD condition (p = 0.001; Wilcoxon signed rank test). These changes were not uniform, but instead varied across the distribution of both V1 neurons' baseline (AM) spontaneous firing rates (**Fig. 3.8A**) and their baseline (AM) population coupling strength (**Fig. 3.8B**). Spontaneous firing rates were predictive of across-the-day coupling strength changes for neurons recorded from both sleeping groups (p < 0.003 and p < 0.005 for Vis Stim + Sleep and Blank Screen + Sleep respectively, Spearman rank order, **Fig. 3.8A**), with lower-firing neurons showing the greatest increase in coupling strength across the day (**Fig. 3.8C-D**). There was no relationship between baseline firing rate and coupling strength changes for neurons recorded from Vis Stim + ESD and Vis Stim + LSD mice (**Fig. 3.8A, E-F**). Baseline population-coupling strength was predictive of coupling strength changes in three of the four experimental groups following visual stimulus presentation (Vis Stim + Sleep, Blank Screen + Sleep, and Vis Stim + ESD; all p < 0.005; Vis Stim + LSD *N.S.*, Spearman rank order, F-test), with neurons with the lowest coupling strength at baseline showing the largest increases in coupling strength across the day (**Fig. 3.8B**). In spite of the maintained correlation in the Vis Stim + ESD group, the net change in coupling is negative, in contrast to the range of changes in the sleep conditions (**Fig. 3.8G-J**).

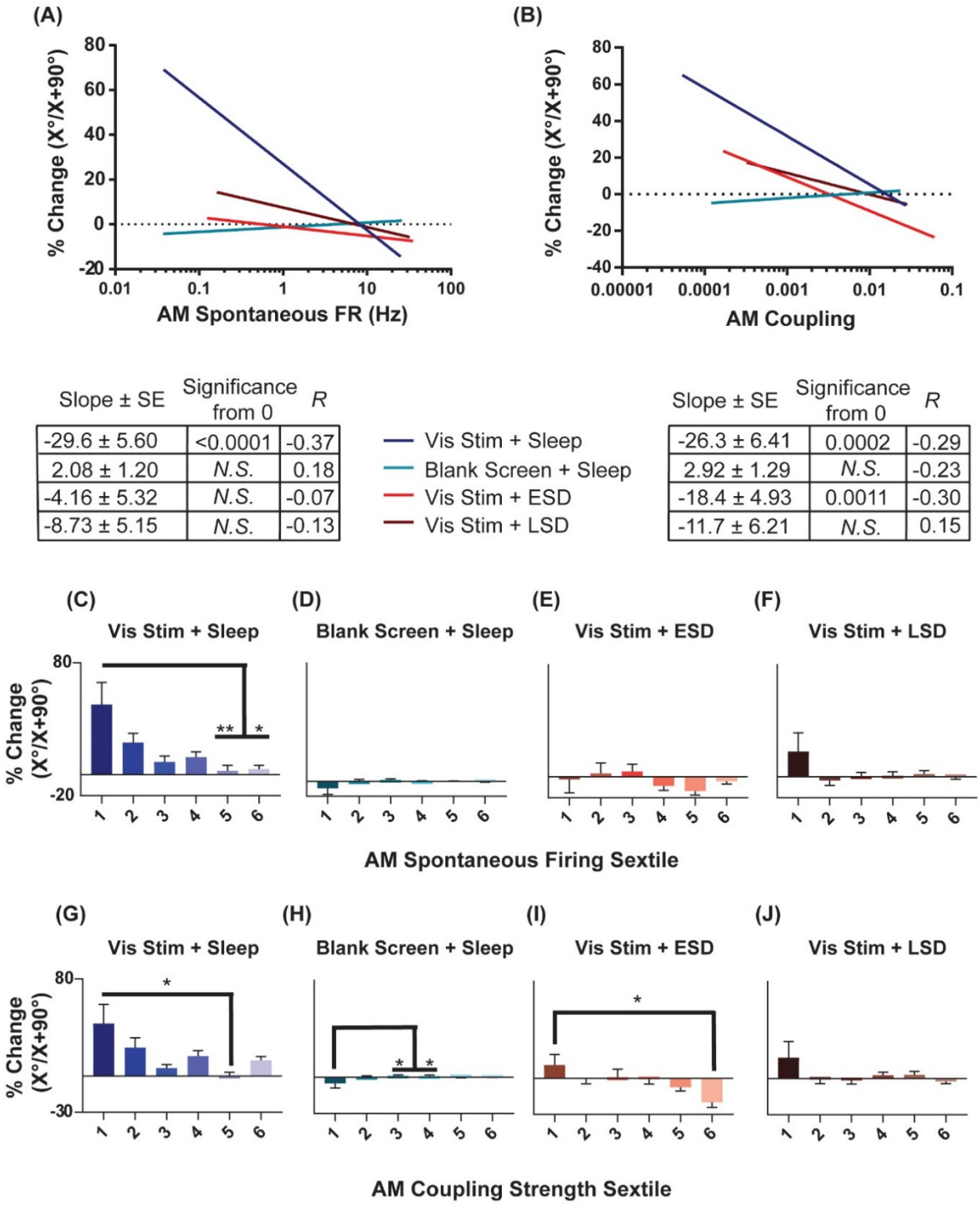

Slope ± SE	Significance from 0	*R*
-29.6 ± 5.60	<0.0001	-0.37
2.08 ± 1.20	*N.S.*	0.18
-4.16 ± 5.32	*N.S.*	-0.07
-8.73 ± 5.15	*N.S.*	-0.13

Slope ± SE	Significance from 0	*R*
-26.3 ± 6.41	0.0002	-0.29
2.92 ± 1.29	*N.S.*	-0.23
-18.4 ± 4.93	0.0011	-0.30
-11.7 ± 6.21	*N.S.*	0.15

Figure 3.7. OSRP is greatest in sparsely firing V1 neurons with weak population coupling. (A) and (B) Linear regressions of the relationship between OSRP (expressed as % changes in neurons' responses to the presented visual stimulus orientation [X°] vs. the orthogonal orientation [X + 90°] across the day, as in Figure 2) and AM spontaneous firing rate. The table below shows, for each experimental group, the regression slope and SE, Spearman R-value, and Bonferroni-corrected F test p-value. **(C-F)** Sextiles of the data, based on AM spontaneous firing rate, which is shown in (A) ($p = 0.0179$ for panel C, all others N.S., Kruskal-Wallis one-way ANOVA on ranks). **(G-J)** Sextiles of the data, based on AM coupling strength, which is shown in (B) ($p = 0.0011$, 0.0203 for panels H-I respectively, all others N.S., Kruskal-Wallis one-way ANOVA on ranks). Error bars indicate mean ± SEM for % changes in orientation preference; * indicates $p < 0.05$, and ** indicates $p < 0.01$, Dunn's post hoc test.

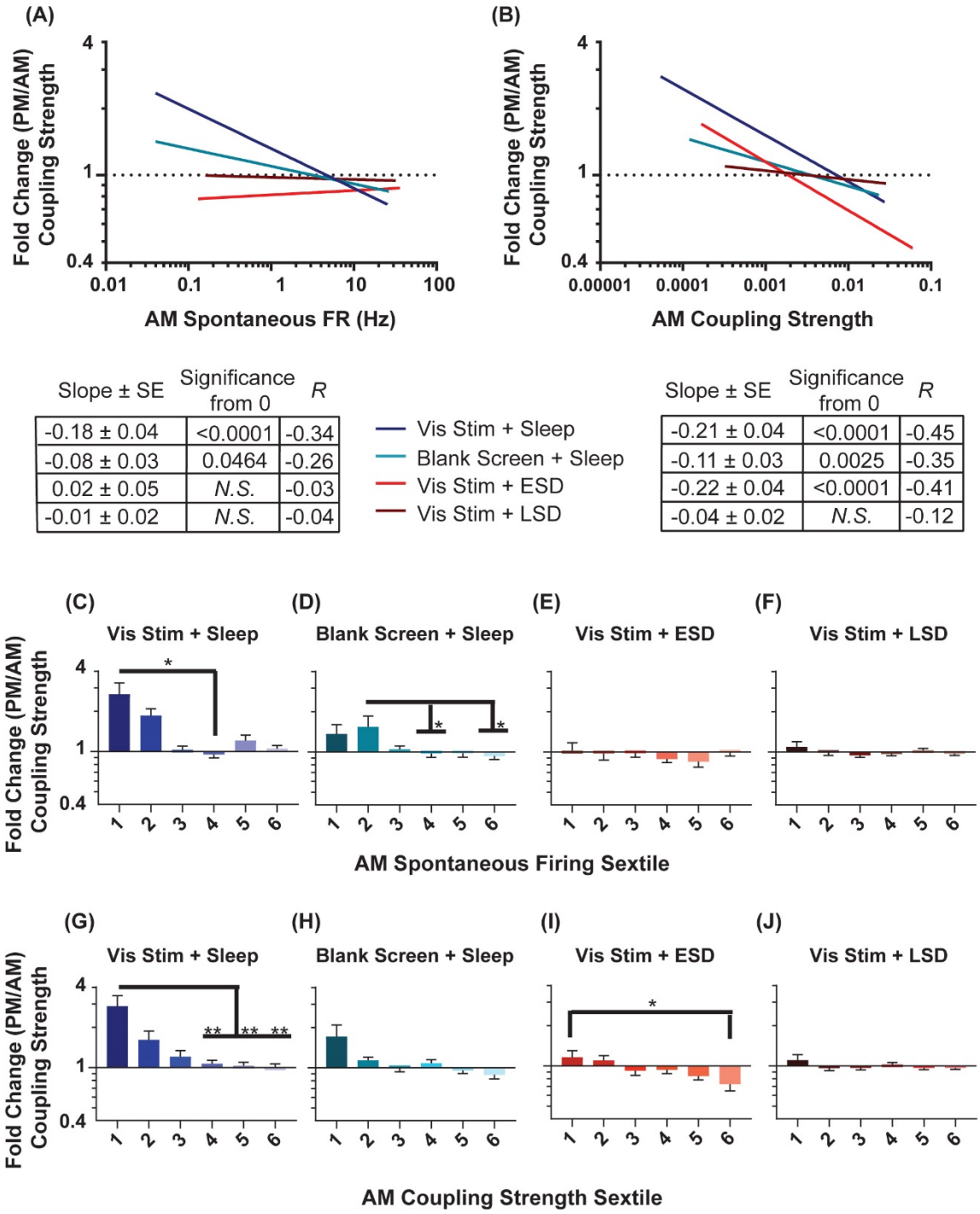

Slope ± SE	Significance from 0	*R*
-0.18 ± 0.04	<0.0001	-0.34
-0.08 ± 0.03	0.0464	-0.26
0.02 ± 0.05	*N.S.*	-0.03
-0.01 ± 0.02	*N.S.*	-0.04

Slope ± SE	Significance from 0	*R*
-0.21 ± 0.04	<0.0001	-0.45
-0.11 ± 0.03	0.0025	-0.35
-0.22 ± 0.04	<0.0001	-0.41
-0.04 ± 0.02	*N.S.*	-0.12

Figure 3.8. Changes in population coupling strength across the day vary as a function of neurons' baseline coupling and firing rate, visual experience, and sleep. (A-B). Linear fits of data for the fold change in coupling strength across the day as a function of AM spontaneous firing rate (A) and AM coupling strength (B). The table below shows, for each experimental group, the regression slope and SE, Spearman R-value, and Bonferroni-corrected F test p-value. **(C-F)** Sextiles of the data, based on AM spontaneous firing rate, which is shown in (A) (p = 0.0043, 0.0391 for panels C-D respectively, all others N.S., Kruskal-Wallis one-way ANOVA on ranks). **(G-J)** Sextiles of the data, based on AM coupling strength, which is shown in (B) (p = 0.0052, 0.0304 for panels G and I respectively, all others N.S., Kruskal-Wallis one-way ANOVA on ranks). Error bars indicate mean ± SEM for log changes in firing rate. * indicates p < 0.05, ** indicates p < 0.01, *** indicates p < 0.001, and **** indicates p < 0.0001, Dunn's post hoc test.

3.4.8 Firing rates of V1 neurons are differentially altered across bouts of NREM, REM, and wake

We next examined how firing rates among V1 neurons are altered across individual bouts of NREM, REM, and wake. Across groups, we found V1 firing changed little across NREM or wake bouts. In contrast, in both Vis Stim + Sleep and Blank Screen + Sleep mice, neurons showed an apparent increase in firing across bouts of REM (**Fig. 3.9**).

In Vis Stim + Sleep mice, as was true for firing increases across the day in these mice, this effect of REM was not uniform, but preferentially affected neurons with lower baseline firing rates (**Fig. 3.9A**). There was a similar trend across REM for neurons in Blank Screen + Sleep mice, although this did not reach statistical significance (**Fig. 3.9B**). There were no significant differences between sextiles in either sleep deprivation condition (**Fig. 3.9C-D**). When overall changes in firing rates across REM sleep were compared between groups, Vis Stim + Sleep and Blank Screen + Sleep showed larger total changes in firing rates than either sleep deprivation group ($p < 0.0001$, Kruskal-Wallis one-way ANOVA on ranks; Vis Stim + Sleep or Blank Screen + Sleep vs. Vis Stim + ESD, $p \leq 0.001$; Vis Stim + Sleep or Blank Screen + Sleep vs. Vis Stim + LSD, $p < 0.0001$, Dunn's post hoc test). A regression of sextile averages across two hour time blocks between CT0 and CT12 showed no significant modulation of firing changes during REM bouts by time of day in the Vis Stim + Sleep group. This suggests that REM bout-associated firing increases may be similar in magnitude across the entire rest phase following visual experience.

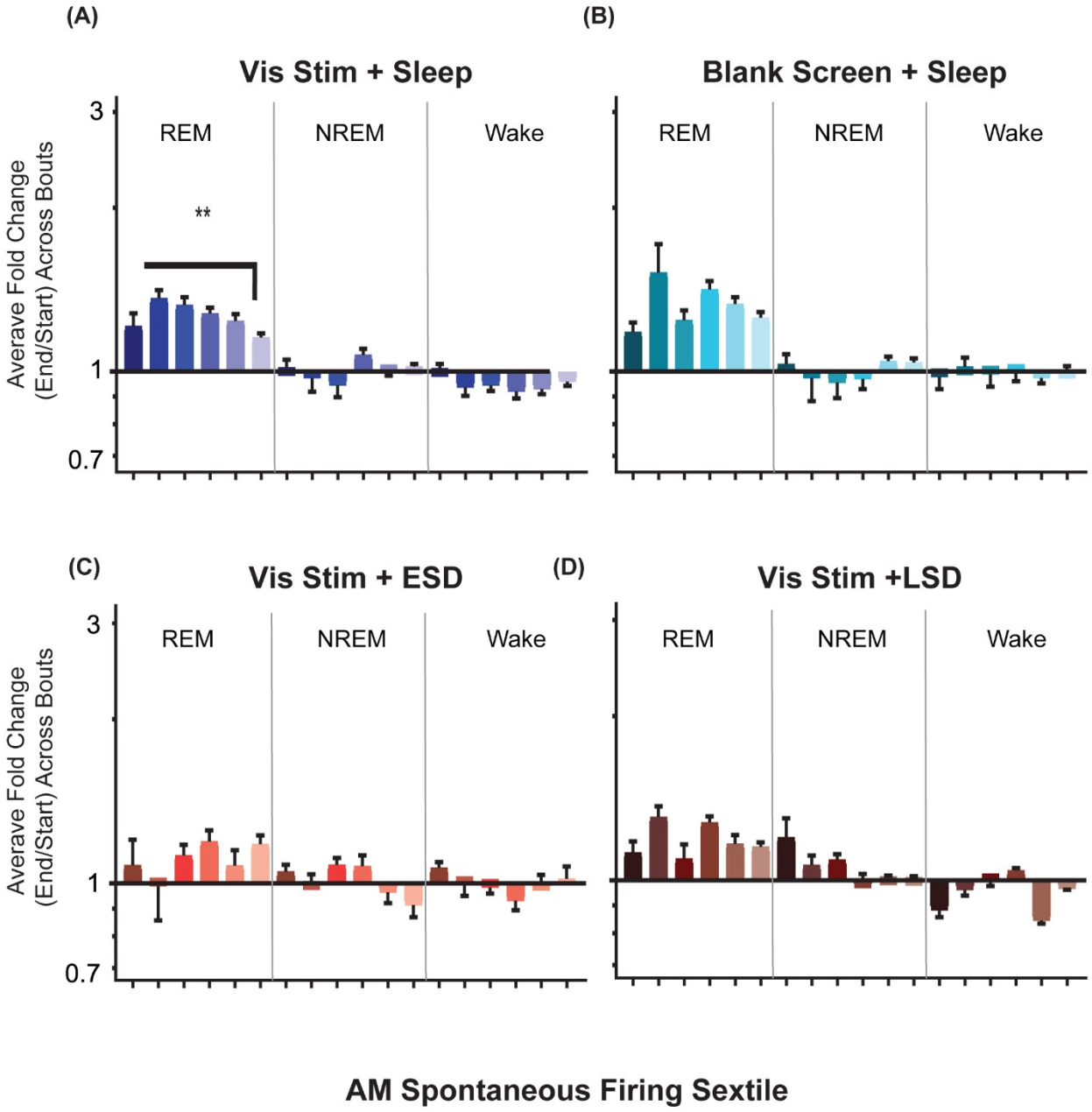

Figure 3.9. Firing rates of V1 neurons increase across bouts of REM sleep. (A-D) Neuronal firing rates were averaged over the first and last 30 s of each REM sleep, NREM sleep, or wake bout, and average firing rate changes across the portion of the day corresponding to ad lib sleep were calculated for each neuron (see Materials and Methods). Values indicate mean ± SEM for state specific changes in firing for each sextile of baseline (AM) spontaneous firing rate (sextile colors as in Figures 4 and 7). While firing rates were minimally affected across periods of NREM and wake, in the Vis Stim + Sleep group (A), increases in firing across post-stimulus REM bouts varied as a function of baseline (AM) spontaneous firing rate ($p = 0.0069$, Kruskal-Wallis one-way ANOVA on ranks). ** indicates $p < 0.01$, Dunn's post hoc test. While a similar trend was seen for Blank Screen + Sleep (B), there was no statistically significant effect of baseline firing rate. Changes in firing across REM were not statistically significant during the 6 h of recovery sleep in Vis Stim + ESD mice (C), or over the first 6 h of ad lib sleep in Vis Stim + LSD mice (D).

3.5 Discussion:

We have previously shown that, following a period of patterned visual experience, sleep facilitates visual response changes (OSRP) among mouse V1 neurons.[6,16,17] While visual responses are not altered across waking exposure to an oriented grating, after a 12-h period of subsequent sleep, firing rate responses to gratings of the same orientation are selectively enhanced.[17] This selective enhancement of firing rate responses is disrupted by post-stimulus sleep deprivation.[6,16,17] The underlying mechanisms for OSRP expression appear to involve thalamocortical long-term potentiation (LTP), as OSRP and LTP are mutually occluding *in vivo*[12] and rely on similar intracellular signaling pathways.[19] This suggests that information content regarding prior visual experience (i.e., orientation-specific information) is relayed from thalamus to cortex during post-stimulus sleep (a hypothesis we address more in **Chapter 4**). Here, we aimed to clarify how this information is distributed among neurons in the sensory cortex, and how this relates to what is known about the heterogeneity of neuronal firing rates, population coupling, and sleep-dependent changes in firing.[7,28,41] We find that sleep-dependent OSRP is not uniform across the population of V1 neurons. Rather, it is expressed preferentially among sparsely firing V1 neurons. These neurons are weakly coupled to V1 population activity (i.e., they are “soloists” rather than “choristers”), are more visually responsive than other V1 neurons, and have greater orientation selectivity than neighboring neurons. These neurons also selectively show firing increases across sleep - a process that (like OSRP itself)[6] is disrupted by partial sleep deprivation. Intriguingly, this same population of neurons also becomes more strongly coupled to population activity across a period of sleep.

Our present data suggest that for sensory cortical areas, the heterogeneous firing rate changes previously reported in frontal cortex across sleep (i.e., increases in firing among sparsely firing neurons, and simultaneous reductions in firing among high firing neurons)[41] may have special functional significance. By preferentially augmenting firing in neurons that show the highest responsiveness and selectivity, sleep may function generally to increase the signal-to-noise ratio of sensory responses. This is particularly relevant after an experience that induces response plasticity in the cortex, such as after visual experience that induces OSRP in V1. This idea is reminiscent of predictions of the "synaptic homeostasis hypothesis" (SHY), which proposes that sleep may improve signal-to-noise ratios in the spiking of neural circuits through firing reductions caused by general synaptic downscaling.[11,22,36] While our present findings do not address the synaptic basis of these changes, we find that improvements in sensory signal-to-noise ratios may be caused by simultaneous increases and decreases in the firing of distinct neuronal populations during sleep.

The fact that these firing rate changes are disrupted by sleep deprivation (either ESD or LSD) suggest that the mechanism underlying these heterogeneous changes in neuronal firing rate is distinctly sleep-dependent. This is supported by our analysis of firing rate changes across bouts of REM, NREM, and wake, where we find increases in firing rates, which are greatest in more sparsely firing neurons, occurring preferentially across periods of REM. This is in line with our prior work, showing firing rate increases in V1 neurons across REM bouts in the hours after visual stimulus presentation, but not after presentation of a blank screen.[17] The fact that we also see increases across REM bouts in our blank screen condition in this study is likely due to the fact that we are assessing

firing rate changes across the entire day (not over the first few hours following visual experience, as in the prior study). Because REM preferentially affects the activity of sparsely firing V1 neurons, this brain state may account for the firing increase seen across the day in this population. Intriguingly, this phenomenon seems to be exactly the opposite of changes in firing seen across REM in the hippocampus,[20,25] and frontal cortex,[41] where neuronal firing decreases across the population.

An unanswered question is what mechanism could mediate differential changes in the firing rates of sparsely firing and high firing neuronal populations across a period of sleep. A number of potential physiological mechanisms, regulated by activity patterns present in thalamocortical circuits during sleep, may explain these apparent simultaneous reductions and enhancements of firing in different neuronal populations.[29,32] One prominent hypothesis proposes that neurons activated by waking experience are preferentially re-activated during subsequent sleep, in the context of sleep-associated oscillations.[1,2,8,23] Thus it is possible that lower-firing neurons are preferentially re-activated during sleep, while higher-firing neurons are not. This could lead to differential activity-dependent plasticity (and thus firing changes) in sparsely firing and higher firing populations across a period of sleep. While our present analyses do not specifically test this mechanism, our previous studies of OSRP have shown that V1 neurons that exhibit the most coherent firing during NREM oscillations show the most dramatic changes in responsiveness to the presented stimulus orientation.[6,16] Another possibility is that, because high-firing neurons in this study likely include fast-spiking interneurons, the firing decreases seen after sleep among higher-firing neurons are due to differential effects of sleep on excitatory and inhibitory neuronal populations. This would be not be an

unprecedented finding - in previous recordings of rat cortical neurons, Vyazovskiy et al. reported significant firing rate decreases across sleep only in physiologically-defined fast spiking interneurons.[40] We and others have speculated previously that suppression of activity in the fast-spiking interneuron population may serve as a critical mechanism for some forms of sleep-dependent plasticity.[3,29] One intriguing possibility, worthy of future study, is that firing rate increases seen across a period of sleep in sparsely-firing neurons are the direct result of disinhibition.

Regardless of the mechanisms underlying the heterogeneous changes we observe in V1 neurons' firing rate and population coupling, the nature of these changes is likely to be highly informative for promoting visual response plasticity. We find that after a period of uninterrupted sleep, the most highly visually-responsive and orientation-selective neurons show increased firing, while less responsive and more poorly-tuned neurons show decreased firing. Moreover, we find that following patterned visual experience (which induces response plasticity), these highly responsive and selective neurons preferentially increase the coupling of their firing to population activity. Together, these data suggest that in the context of sleep-dependent sensory plasticity, neurons which carry highly specific visual information have an increased capacity to influence population activity in V1.

Author Contributions: BC, JD and SA designed research and wrote the article. AS and SA performed research. CB contributed new analytic tools. BC, JD, EP and SA analyzed data.

3.6 References

1. Antony, J., Piloto, L., Wang, M., Pacheco, P., Norman, K., and Paller, K. (2018). Sleep Spindle Refractoriness Segregates Periods of Memory Reactivation. Curr Biol S0960-9822, 30448-30442.

2. Aton, S.J. (2013). Set and setting: How behavioral state regulates sensory function and plasticity. Neurobiol Learn Mem 106, 1-10.

3. Aton, S.J., Broussard, C., Dumoulin, M., Seibt, J., Watson, A., Coleman, T., and Frank , M.G. (2013). Visual experience and subsequent sleep induce sequential plastic changes in putative inhibitory and excitatory cortical neurons. Proc Natl Acad Sci U S A 110, 3101-3106.

4. Aton, S.J., Seibt, J., Dumoulin, M., Jha, S.K., Steinmetz, N., Coleman, T., Naidoo, N., and Frank, M.G. (2009a). Mechanisms of sleep-dependent consolidation of cortical plasticity. Neuron 61, 454-466.

5. Aton, S.J., Seibt, J., and Frank , M.G. (2009b). Sleep and memory. In Encyclopedia of Life Science (Chichester, John Wiley and Sons, Ltd.).

6. Aton, S.J., Suresh, A., Broussard, C., and Frank, M.G. (2014). Sleep promotes cortical response potentiation following visual experience. Sleep 37, 1163-1170.

7. Bachatene, L., Bharmauria, V., Cattan, S., Chanauria, N., Rouat, J., and Molotchnikoff, S. (2015). Electrophysiological and firing properties of neurons: Categorizing soloists and choristers in primary visual cortex. Neurosci Lett 604, 103-108.

8. Batterink, L., Creery, J., and Paller, K. (2016). Phase of Spontaneous Slow Oscillations during Sleep Influences Memory-Related Processing of Auditory Cues. J Neurosci 36, 1401-1409.

9. Chauvette, S., Seigneur, J., and Timofeev, I. (2012). Sleep oscillations in the thalamocortical system induce long-term plasticity. Neuron 75, 1105-1113.

10. Cirelli, C., Gutierrez, C.M., and Tononi, G. (2004). Extensive and divergent effects of sleep and wakefulness on brain gene expression. Neuron 41, 35-43.

11. Cirelli, C., and Tononi, G. (2014). Sleep and synaptic homeostasis. Sleep 38, 161-162.

12. Cooke, S.F., and Bear, M.F. (2010). Visual experience induces long-term potentiation in the primary visual cortex. J Neurosci 30, 16304-16313.

13. de Vivo, L., Bellesi, M., Marshall, W., Bushong, E.A., Ellisman, H., Tononi, G., and Cirelli, C. (2017). Ultrastructural evidence for synaptic scaling across the wake/sleep cycle. Science 355, 507-510.

14. Delorme, J., Kodoth, V., and Aton, S.J. (2018). Sleep loss disrupts Arc expression in dentate gyrus neurons. Neurobiol Learn Mem Epub ahead of print.

15. Diekelmann, S., and Born, J. (2010). The memory function of sleep. Nat Rev Neurosci 11, 114-126.

16. Durkin, J., Suresh, A.K., Colbath, J., Broussard, C., Wu, J., Zochowski, M., and Aton, S.J. (2017). Cortically coordinated NREM thalamocortical oscillations play an essential, instructive role in visual system plasticity. Proceedings National Academy of Sciences 114, 10485-10490.

17. Durkin, J.M., and Aton, S.J. (2016). Sleep-dependent potentiation in the visual system is at odds with the Synaptic Homeostasis Hypothesis. Sleep.

18. Frank, M.G., Issa, N.P., and Stryker, M.P. (2001). Sleep enhances plasticity in the developing visual cortex. Neuron 30, 275-287.

19. Frenkel, M.Y., Sawtell, N.B., Diogo, A.C., Yoon, B., Neve, R.L., and Bear, M.F. (2006). Instructive effect of visual experience in mouse visual cortex. Neuron 51, 339-349.

20. Grosmark, A.D., Mizuseki, K., Pastalkova, E., Diba, K., and Buzsaki, G. (2012). REM sleep reorganizes hippocampal excitability. Neuron 75, 1001-1007.

21. Hill, D.N., Mehta, S.B., and Kleinfeld, D. (2011). Quality metrics to accompany spike sorting of extracellular signals. J Neurosci 31, 8699-8705.

22. Hill, S., and Tononi, G. (2005). Modeling sleep and wakefulness in the thalamocortical system. J Neurophysiol 93, 1671-1698.

23. Huber, R., Ghilardi, M.F., Massimini, M., and Tononi, G. (2004). Local sleep and learning. Nature 430, 78-81.

24. Mackiewicz, M., Shockley, K.R., Romer, M.A., Galante, R.J., Zimmerman, J.E., Naidoo, N., Baldwin, D.A., Jensen, S.T., Churchill, G.A., and Pack, A.I. (2007). Macromolecule biosynthesis - a key function of sleep. Physiol Genomics 31, 441-457.

25. Miyawaki, H., and Diba, K. (2016). Regulation of Hippocampal Firing by Network Oscillations during Sleep. Curr Biol 26, 893-902.

26. Ognjanovski, N., Maruyama, D., Lashner, N., Zochowski, M., and Aton, S.J. (2014). CA1 hippocampal network activity changes during sleep-dependent memory consolidation. Front Syst Neurosci 8, 61.

27. Ognjanovski, N., Schaeffer, S., Mofakham, S., Wu, J., Maruyama, D., Zochowski, M., and Aton, S.J. (2017). Parvalbumin-expressing interneurons coordinate hippocampal network dynamics required for memory consolidation. Nature Communications 8, 15039.

28. Okun, M., Steinmetz, N.A., Cossell, L., Iacaruso, M.F., Ko, H., Bartho, P., Moore, T., Hoefer, S.B., Mrsic-Flogel, T.D., Carandini, M., et al. (2015). Diverse coupling of neurons to populations in sensory cortex. Nature 521, 511-515.

29. Puentes-Mestril, C., and Aton, S.J. (2017). Linking network activity to synaptic plasticity during sleep: hypotheses and recent data. Frontiers in Neural Circuits 11, doi: 10.3389/fncir.2017.00061.

30. Ribeiro, S., Goyal, V., Mello, C.V., and Pavlides, C. (1999). Brain gene expression during REM sleep depends on prior waking experience. Learn Mem 6, 500-508.

31. Ribeiro, S., Mello, C.V., Velho, T., Gardner, T.J., Jarvis, E.D., and Pavlides, C. (2002). Induction of hippocampal long-term potentiation during waking leads to increased extrahippocampal zif-268 expression during ensuing rapid-eye-movement sleep. JNeurosci 22, 10914-10923.

32. Roach, J.P., Pidde, A., Katz, E., Wu, J., Ognjanovski, N., Aton, S.J., and Zochowski, M.R. (2018). Resonance with sub-treshold oscillatory drive organizes activity and optimizes learning in neural networks. Proc Natl Acad Sci U S A In Press.

33. Sato, T., Suzuki, T., and Mabuchi, K. (2007). Fast automatic template matching for spike sorting based on Davies-Bouldin validation indices. Conf Proc IEEE Eng Med Biol Soc, 3200-3203.

34. Seibt, J., Dumoulin, M., Aton, S.J., Coleman, T., Watson, A., Naidoo, N., and Frank, M.G. (2012). Protein synthesis during sleep consolidates cortical plasticity in vivo. Curr Biol 22, 676-682.

35. Thompson, C.L., Wisor, J.P., Lee, C.-K., Pathak, S.D., Gerashchenko, D., Smith, K.A., Fischer, S.R., Kuan, C.L., Sunkin, S.M., Ng, L.L., et al. (2010). Molecular and Anatomical Signatures of Sleep Deprivation in the Mouse Brain. Front Neurosci 4.

36. Tononi, G., and Cirelli, C. (2003). Sleep and synaptic homeostasis: a hypothesis. Brain Res Bull 62, 143-150.

37. Tononi, G., and Cirelli, C. (2014). Sleep and the price of plasticity: From synaptic and cellular homeostasis to memory consolidation and integration. Neuron 81, 12-34.

38. Ulloor, J., and Datta, S. (2005). Spatio-temporal activation of cyclic AMP response element-binding protein, activity-regulated cytoskeletal-associated protein and brain-derived nerve growth factor: a mechanism for pontine-wave generator activation-dependent two-way active-avoidance memory processing in the rat. Journal of Neurochemistry 95, 418-428.

39. Vyazovskiy, V.V., Cirelli, C., Pfister-Genskow, M., Faraguna, U., and Tononi, G. (2008). Molecular and electrophysiological evidence for net synaptic potentiation in wake and depression in sleep. advanced online publication.

40. Vyazovskiy, V.V., Olscese, U., Lazimy, Y.M., Faraguna, U., Esser, S.K., Williams, J.C., Cirelli, C., and Tononi, G. (2009). Cortical firing and sleep homeostasis. Neuron 63, 865-878.

41. Watson, B.O., Levenstein, D., Green, J.P., Gelinas, J.N., and Buzsaki, G. (2016). Network homeostasis and state dynamics of neocortical sleep. Neuron 90, 839-852.

42. Yang, G., Lai, C.S., Cichon, J., Ma, L., Li, W., and Gan, W.B. (2014). Sleep promotes branch-specific formation of dendritic spines after learning. Science 344, 1173-1178.

Chapter 4 Cortically-coordinated NREM thalamocortical oscillations play an essential, instructive role in visual system plasticity.

This chapter includes the manuscript: **Durkin, J**., Suresh, A. K., Colbath, J., Broussard, C., Wu, J., Zochowski, M., Aton, S. J. (2017). Cortically-coordinated NREM thalamocortical oscillations play an essential, instructive role in visual system plasticity. *Proceedings of the National Academy of Sciences*, *114*(39), 10485-10490.

4.1 Abstract:

Two long-standing questions in neuroscience are how sleep promotes brain plasticity, and why some forms of plasticity occur preferentially during sleep vs. wake. Establishing causal relationships between specific features of sleep (*e.g.*, network oscillations) and sleep-dependent plasticity has been difficult. Here we demonstrate that presentation of a novel visual stimulus (a single oriented grating) causes immediate, instructive changes in the firing of mouse lateral geniculate nucleus (LGN) neurons - leading to increased firing rate responses to the presented stimulus orientation (relative to other orientations). However, stimulus presentation alone does not affect V1 neurons, which show response changes only after a period of subsequent sleep. During post-stimulus NREM sleep, LGN neurons' overall spike-field coherence (SFC) with V1 delta (0.5-4 Hz) and spindle (7-15 Hz) oscillations increased, with neurons most responsive to the presented stimulus showing greater SFC. To test whether coherent communication between LGN and V1 was essential for cortical plasticity, we first tested the role of layer

6 corticothalamic (CT) V1 neurons in coherent firing within the LGN-V1 network. We found that rhythmic optogenetic activation of CT V1 neurons dramatically induced coherent firing in LGN neurons, and to a lesser extent, in V1 neurons in the other cortical layers. Optogenetic interference with CT feedback to LGN during post-stimulus NREM sleep (but not REM or wake) disrupts coherence between LGN and V1, and also blocks sleep-dependent response changes in V1. We conclude that NREM oscillations relay information regarding prior sensory experience between the thalamus and cortex to promote cortical plasticity.

4.2 Significance Statement:

Previous studies have demonstrated a role of state-specific neural activity in plasticity; however a mechanism for these changes has yet to be elucidated. Here, we demonstrate that sensory response changes occur in thalamic neurons immediately following novel visual experience, but that subsequent NREM oscillations are required for subsequent response changes in primary visual cortex (V1). Consequently, we show that disruption of NREM oscillations specifically blocks sleep-dependent plasticity in V1. We conclude that following a novel sensory experience, neural activity patterns unique to NREM facilitate transfer of information from visual thalamus to V1, leading to adaptive response changes in V1 neurons.

4.3 Introduction:

Converging behavioral,[1] biochemical,[2-4] neuroanatomical,[5] and electrophysiological[2,6-8] evidence supports the idea that following novel sensory

experiences, sleep can promote cortical plasticity. The sleep-dependent mechanisms driving these changes have remained elusive. Sleep-associated changes in network activity,[1,6,7,9,10] neuromodulator tone,[11] transcription,[4] translation,[4] and protein phosphorylation[2,3] have all been correlated with cortical plasticity following novel experiences.[12] In recent years, neuroscientists have speculated that the high-amplitude, low-frequency thalamocortical oscillations that characterize NREM sleep play a critical role in promoting sensory cortical plasticity and learning.[12] While it has been hypothesized that such NREM oscillations promote general synaptic "downscaling",[13] converging data suggest that they could instead promote synaptic strengthening.[5-7,9] While rhythmic stimulation of the cortex at frequencies meant to mimic NREM oscillations (1-2 Hz) is sufficient to promote cortical plasticity and learning,[9,10] it is unclear whether naturally-occurring oscillations are necessary for sleep-dependent processes. Another critical question is whether NREM oscillations play an instructive role in experience-initiated plasticity - i.e., whether these oscillations relay information about prior experience through thalamocortical circuitry.

Orientation-specific response potentiation (OSRP) in mouse V1[14] is initiated by a novel visual stimulus (a flickering grating of a single orientation) presented over a period of several minutes.[7] OSRP is expressed in V1 several hours later, as enhanced neuronal responses to stimuli of the same orientation; critically, sleep deprivation following visual experience prevents OSRP consolidation.[7,8] Recent data suggest that OSRP is mediated by potentiation of LGN synapses in V1.[15] To clarify the role of thalamocortical (and corticothalamic; CT) communication in OSRP consolidation, we first tested how visual experience alone affected neuronal firing and OSRP in both LGN and V1 neurons, and

then determined how coherent firing between the two areas was affected during subsequent sleep. We also tested the effects of optogenetic manipulations of layer 6 CT neurons, aimed at either mimicking or disrupting NREM sleep oscillations, on both neuronal firing patterns and OSRP following visual experience.

4.4 Results:

4.4.1 LGN, but not V1, neurons show immediate orientation-specific response changes following visual stimulation.

Previous studies (by our lab[7,8] and others[14]) have demonstrated that orientation preference in V1 neurons is unchanged immediately after presentation of a single oriented grating stimulus, even for stimulus durations of up to an hour. In order to test whether LGN neurons are similarly unaffected across stimulus presentation, we generated orientation tuning curves for individual V1 and LGN neurons in anesthetized mice, before and after a 30-min grating presentation. Surprisingly, many LGN neurons show dramatic orientation-specific response changes during this treatment (e.g., the ratio of neuronal firing rate for X^o over the neuronal firing rate for the orthogonal, $X+90^o$). These increases in $X^o/X+90^o$ were present across a number of recordings, for different presented stimulus orientations (**Fig. 4.1**; **SI Appendix, Figs. S4.1 & S4.2;** *n* = 147 neurons from 7 experiments), but (consistent with our previous findings[7]) were not seen in V1 neurons recorded from the same mice (*n* = 32 neurons). Among many of the recorded LGN neurons, visually-evoked firing rate responses increased significantly across the 30-min grating presentation, a phenomenon that we had not previously seen

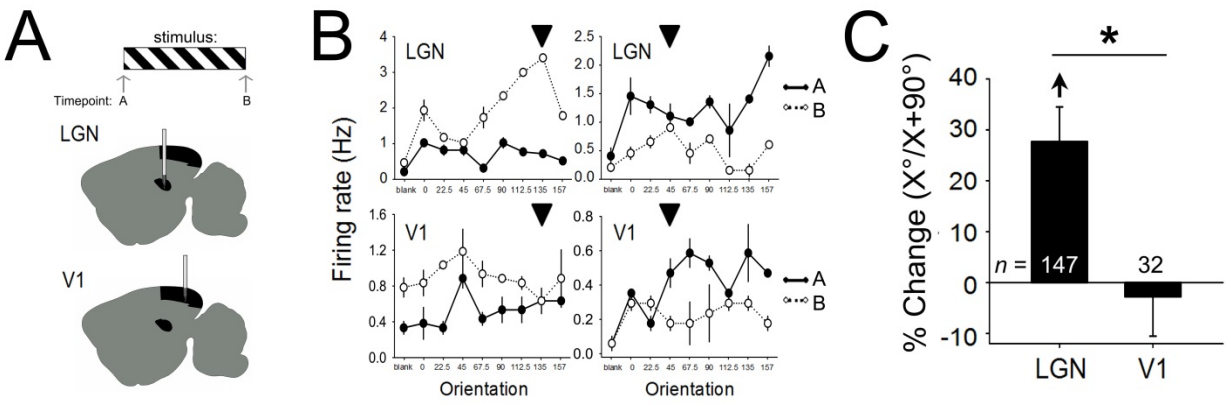

Figure 4.1. Visual experience immediately alters response properties in LGN, but not V1, neurons. (A) Visual responses of LGN and V1 neurons were recorded from mice under isoflurane anesthesia. At timepoint A, mice were presented randomly with a series of oriented full-field grating stimuli (0, 22.5, 45, 67.5, 90, 112.5, 135, and 157.5) and a blank screen (bl) to assess baseline orientation tuning and visual responsiveness. One stimulus was chosen at random and presented for a 30 min period. At timepoint B, visual response properties were reassessed. **(B)** Tuning curves for representative LGN neurons (top) show increased relative responses to the presented orientation (vs. other orientations; presented stimulus indicated with arrowhead) from timepoint A (solid line) to timepoint B (dotted line). Consistent with our prior findings (7), V1 neurons (bottom) do not show an enhanced response to the presented orientation immediately following stimulus presentation. Values indicate mean firing rate response (± SEM) to each stimulus. **(C)** Immediately following visual stimulus presentation, LGN neurons (but not V1 neurons) showed a significant increase in relative responsiveness to the presented stimulus orientation (relative to the orthogonal orientation [X°/X+90°]; arrowhead indicates $p < 0.05$, RM ANOVA on ranks; * indicates $p < 0.05$ for LGN vs. V1 neurons).

in V1 (**Fig. 4.2A**).[8] The amount that individual neurons' firing rates changed across stimulus presentation, while heterogeneous, predicted the amount of change in X^{o}/X+90^{o} after stimulus presentation (**Fig. 4.2B; SI Appendix, Fig. S4.6A**). This rapid response change did not result in an increase in the proportion of LGN neurons selective for the presented stimulus orientation (**SI Appendix, Figs. S4.1 & S4.2**); rather, neuronal firing rate responses to X^{o} selectively increased (e.g., relative to X+90^{o} and X±45^{o}).

To better understand the relationship of these firing rate changes to OSRP seen in V1 across a period of post-stimulus sleep, we simultaneously recorded both LGN and V1 neurons in non-anesthetized animals, during and after presentation of a grating at the beginning of the rest phase (CT0). Here again, we found that firing rate responses increased significantly across stimulus presentation in LGN, but not V1 (**Fig. 4.2C**). Firing increases were not seen in LGN neurons recorded from mice presented with a blank screen (*N.S.*; **Fig. 4.2C**). Firing rate increases among LGN neurons during stimulus presentation predicted increases in X^{o}/X+90^{o} measured across the rest period (**Fig. 4.2D; SI Appendix, Fig. S4.6B**). Critically, as we had previously shown for V1 neurons following OSRP induction,[8] firing rates in LGN neurons remained elevated during post-stimulus NREM sleep (**Fig. 4.2E**). Taken together, these data suggest that oriented grating presentation leads to: 1) rapid changes in X^{o}/X+90^{o} in LGN neurons, and 2) long-lasting changes in firing of LGN neurons during subsequent NREM sleep.

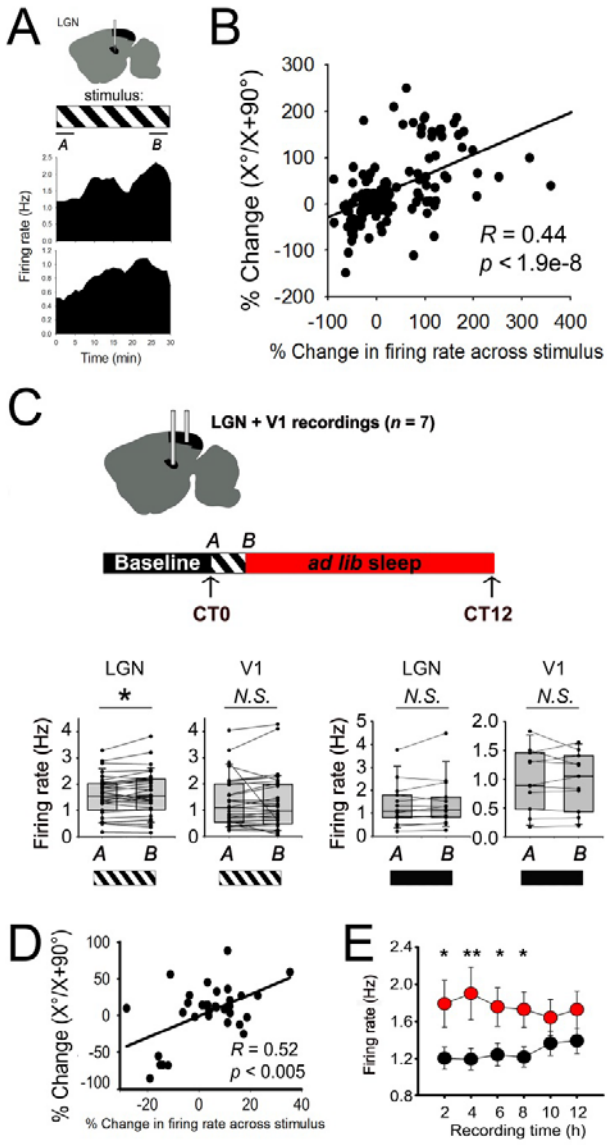

Figure 4.2. Stimulus-induced firing enhancement in LGN neurons predicts response changes and persists during subsequent NREM sleep. (A) Two representative LGN neurons recorded from an anesthetized mouse show firing rate increases across the 30-min stimulus presentation (mean rate plotted in 1 min bins). **(B)** Firing rate increases predicted the change in $X^o/X+90^o$ (i.e., OSRP) across stimulus presentation. Pearson product moment *R* and *p* values are shown for 147 LGN neurons. **(C) Top:** Mice implanted with electrodes targeting both LGN and V1 were recorded over a 24-h baseline period, were presented with an oriented grating at CT0, and were then allowed 12 h of *ad lib* sleep. Visual response properties were assessed at CT0 and CT12. **Bottom, left:** V1 neurons showed no change in firing rate between the first and last 5 min of 30-min grating presentation (timepoint *A* and timepoint *B* respectively, *N.S.,* Wilcoxon signed rank test, *n* = 34 neurons from 6 mice). However, LGN neuronal firing rates increased significantly (*p* =0.018, Wilcoxon signed rank test, *n* = 35 neurons). **Bottom, right:** Neither V1 or LGN neurons showed a significant change in firing rate between the first and last 5 min of a 30-min blank screen presentation (*N.S.,* Wilcoxon signed rank test, *n* = 16 and 11 neurons, respectively, from 3 experiments). **(D)** As was true in anesthetized recordings, firing rate increases in LGN neurons across stimulus presentation predicted OSRP across the day. Pearson product moment *R* and *p* values are shown for 35 stably-recorded LGN neurons. **(E)** Compared to baseline recording (black), LGN neurons' firing rates during the first 8 h of post-stimulus NREM (red) remained significantly elevated (two-way RM ANOVA, treatment x time interaction $p < 0.001$; *$p<0.05$, **$p<0.01$).

4.4.2 LGN neurons show increased SFC with NREM thalamocortical oscillations during OSRP consolidation.

OSRP is expressed in V1 only after several hours of post-stimulus sleep; critically, sleep deprivation following visual experience prevents OSRP consolidation (**SI Appendix, Fig. S4.3**).[7,8] To assess whether communication *between* LGN and V1 changes during post-stimulus sleep, we continuously recorded LGN and V1 neuronal firing and corresponding local field potential (LFP) activity (**SI Appendix, Figs. S4.4** and **S4.5**). Recordings spanned a 24-h period of baseline sleep and wake, 30 min stimulus presentation, and a subsequent 12-h OSRP consolidation window. We then characterized the temporal relationships (in the form of SFC) between LGN neuronal firing and V1 LFP oscillations during OSRP consolidation (**Fig. 4.3**). LGN neurons' SFC with V1 delta and spindle oscillations increased during NREM in the hours following oriented grating presentation (**Fig. 4.3B; SI Appendix, Fig. S4.6C**).

We also tested whether LGN neurons underwent an increase in coherent firing during NREM *per se*, by assessing the periodicity of firing before and after oriented grating exposure. We found that following stimulus presentation, coherent LGN neuronal firing in the delta frequency band predicted the extent of their OSRP across the post-stimulus period (**Fig. 4.3C; SI Appendix, Fig. S4.6D**). These data suggest that as is true for V1 neurons,[7] waking visual experience leads to changes in LGN neurons' coherent firing during subsequent NREM sleep. Because OSRP is present in only in the LGN immediately following experience, we hypothesized that LGN-V1 coherence during NREM oscillations could promote sleep-dependent OSRP consolidation in V1.

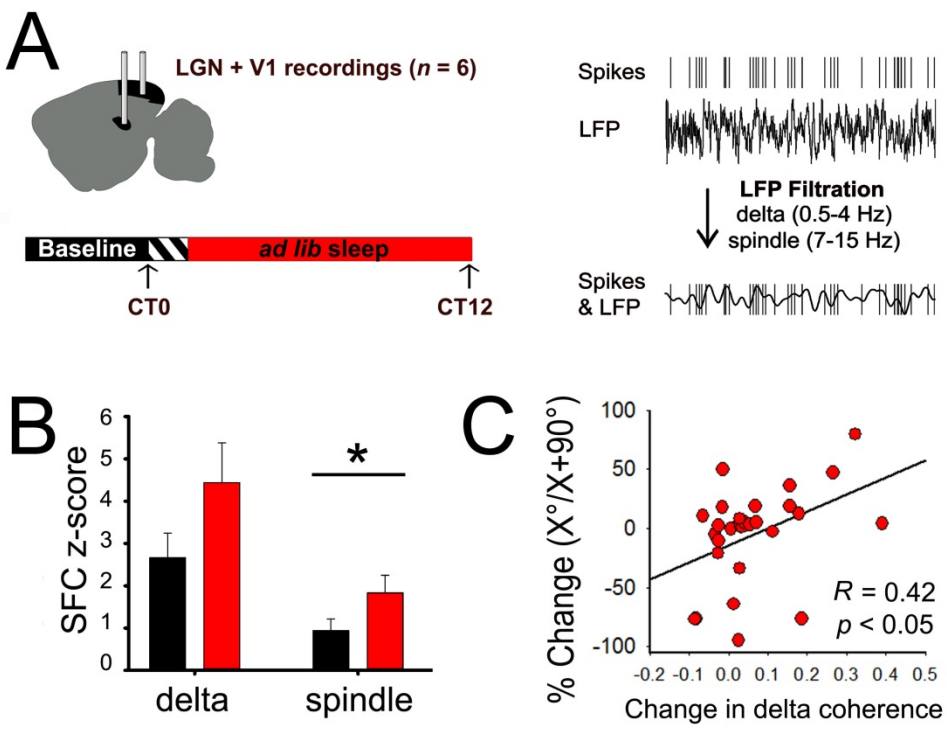

Figure 4.3. LGN neurons show increased SFC with V1 NREM oscillations following stimulus presentation. (A) Mice implanted with electrodes targeted to LGN and V1 were recorded as described in Fig. 2C. LGN SFC with V1 oscillations was calculated during NREM at baseline and after stimulus presentation. **(B)** Following stimulus presentation, LGN neurons showed significantly increased SFC with V1 LFPs filtered at spindle frequency (* indicates $p = 0.01$, Wilcoxon signed rank test). There was a similar trend for increased SFC in delta frequency band ($p = 0.088$, Wilcoxon signed rank test). **(C)** Increases in LGN neurons firing periodicity at delta frequencies during NREM predicted their ORSP across the day. Pearson product moment R and p values are shown for 35 stably-recorded LGN neurons.

4.4.3 Layer 6 CT input is sufficient to drive coherent firing in the LGN-V1 network.

CT input is necessary for coordinating NREM delta and spindle oscillations within thalamic circuits.[16,17] Thus CT-mediated coordination might be critical for promoting the observed changes in LGN-V1 coherence during post-stimulus NREM sleep. To test the sufficiency of V1 layer 6 (L6) CT input to drive coherent firing in LGN and V1, we recorded LGN and V1 firing patterns in transgenic mice expressing channelrhodopsin 2 (ChR2) in L6 CT neurons (*Ntsr1:ChR2*) (**Fig. 4.4A-B, G-H; SI Appendix, Fig. S4.7**). After recording baseline activity in both areas, we measured changes in firing rhythmicity in response to rhythmic optogenetic activation of V1 L6 CT neurons across a range of frequencies: 0.5, 1, 2, 3, and 4 Hz. In both V1 and LGN recordings, we observed phase-locking of both neurons' firing and LFP activity to optogenetically-induced rhythms of CT activity (**Fig. 4.4B, H**). Only a subset of stimulation frequencies (1, 2, and 3 Hz) increased V1 neurons' firing coherence significantly from baseline (**Fig. 4.4C**). In contrast, stimulation at all frequencies increased LGN neurons' firing coherence, and led to more pronounced (i.e., higher-amplitude) firing rhythms compared with those induced in V1 (**Fig. 4.4I**). The proportion of LGN neurons significantly affected by optogenetic stimulation of V1 CT neurons (**Fig. 4.4L**) was also much greater than the proportion of neurons affected in V1 (**Fig. 4.4F**).

Optogenetic stimulation of L6 CT neurons similarly affected the rhythmicity of LFP activity in both V1 (**Fig. 4.4D-E**) and LGN (**Fig. 4.4J-K**). Optogenetic activation of V1 CT neurons also induced higher-frequency (11-15 Hz) spindle-like LFP events in V1 (**SI Appendix, Fig. S4.8A**). These events were time-locked to rhythmic optogenetic

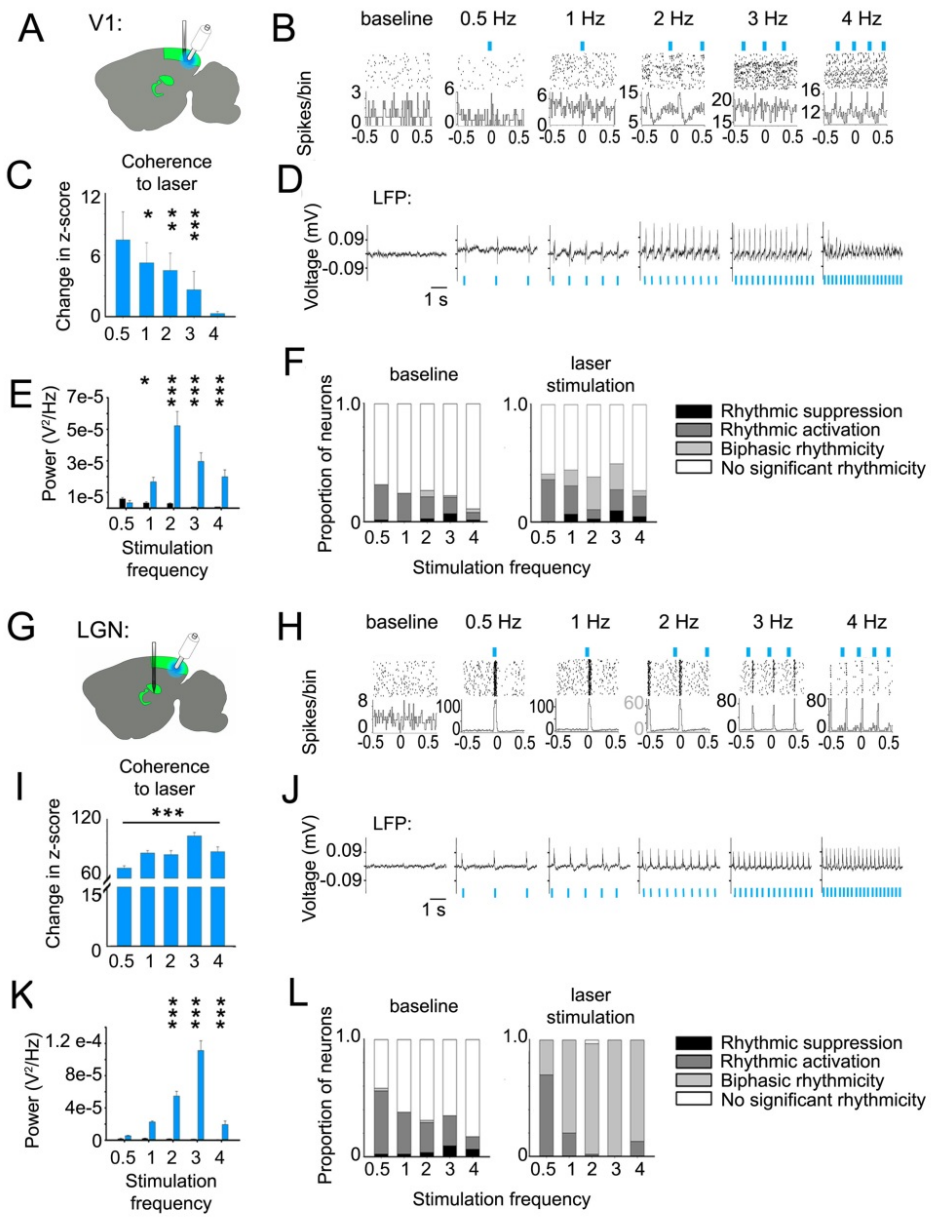

Figure 4.4. Stimulation of ChR2-expressing CT neurons induced coherent firing in V1 and LGN. (A) For V1 recordings from anesthetized *Ntsr1::ChR2* mice, a 32-channel silicone probe was lowered into V1 until stable recordings were obtained, and an optical fiber was targeted to V1 L6. Neuronal responses were aggregated across all layers of visual cortex. **(B)** Peri-event spike rasters and histograms are shown for a representative neuron at baseline, and during optogenetic stimulation of V1 L6. **(C)** V1 neurons showed increased coherent firing at the frequency of optogenetic stimulation compared to baseline. *, **, and *** indicate $p < 0.05$, 0.01, and 0.001, Wilcoxon signed rank test. **(D)** LFP activity is shown at baseline and during optogenetic stimulation. **(E)** LFP power at the frequency of stimulation (blue bars) was significantly increased from baseline (black bars) values during stimulation. * and *** indicate $p < 0.05$ and 0.001, Holm-Sidak *post hoc* test vs. baseline. **(F)** The proportion of V1 neurons which showed statistically significant ($p < 0.01$) periodic suppression, activation, both are shown for each frequency during baseline (top) and during optogenetic stimulation (bottom). **(G)** For LGN neuronal recordings in anesthetized *Ntsr1::ChR2* mice, a 32-channel silicone probe was lowered into LGN until stable recordings were obtained, and an optical fiber was targeted to V1 L6. **(H-L)** Data for LGN spiking and LFP activity are shown as in panels B-F. For L, all LGN neurons showed significant rhythmicity during optogenetic stimulation of L6 CT neurons.

stimulation, and varied in density and duration based on stimulation frequency (**SI Appendix, Fig. S8B-C**).

4.4.4 Optogenetic inhibition of L6 CT neurons disrupts V1-LGN coherence during NREM sleep.

We next tested whether optogenetic inhibition of L6 CT neurons could disrupt coherent NREM oscillations following induction of OSRP. To do this, we virally transduced L6 CT neurons in V1 with archaerhodopsin3 (Arch)[18] in L6 CT neurons in V1 (**SI Appendix, Fig. S9**). Light delivery to V1 of transduced mice reliably and reversibly suppressed firing in the majority of V1 L6 neurons (and target neurons in the LGN) over the timescale of seconds to minutes (**Fig. 5A; SI Appendix, Fig. S10**). NREM-targeted light delivery in the hours following visual stimulus presentation significantly reduced delta and spindle-frequency LFP power in V1, relative to baseline NREM sleep (**Fig. 5B; SI Appendix, Fig. S11**). Spindle-frequency coherence between LGN LFPs and V1 LFPs was significantly reduced during NREM-targeted inhibition of V1 CT neurons (**Fig. 5C**; see also **SI Appendix, Fig. S8**). This was associated with a disruption in the temporal relationship between V1 and LGN fields, leading to longer delays (relative to lag times seen at baseline) between V1 and LGN spindle-frequency activity (an effect not seen in the absence of CT inhibition; **Fig. 5D;** *N.S.* for delta frequency activity, **SI Appendix, Fig. S12**). LGN neurons' SFC with V1 delta and spindle oscillations was also significantly reduced during V1 CT inhibition (**Fig. 5E**). Taken together, these changes demonstrate that inhibition of L6 CT neurons desynchronizes NREM oscillations and thalamocortical communication during OSRP consolidation.

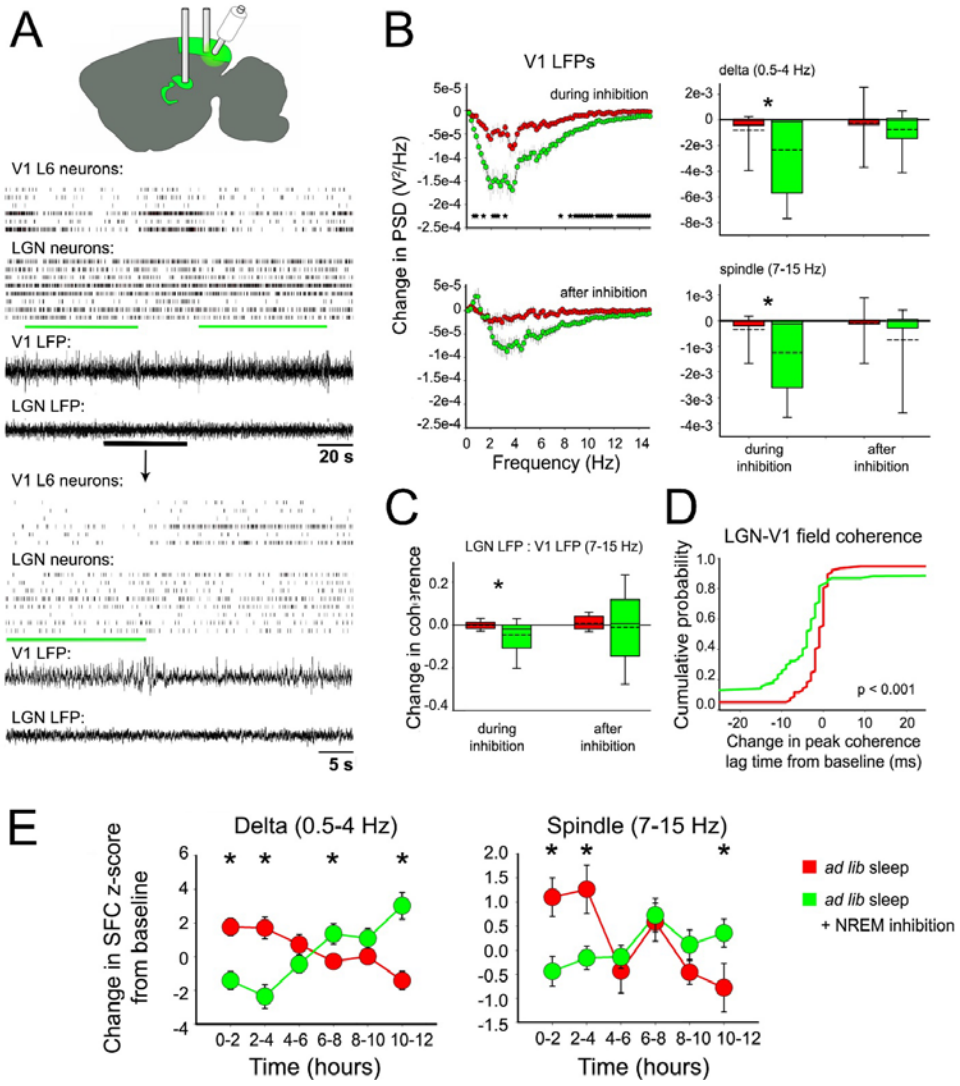

Figure 4.5. NREM-targeted optogenetic inhibition of V1 L6 CT neurons disrupts coherent thalamocortical oscillations. (A) LGN and V1 activity was simultaneously recorded in *Ntsr1-cre* transgenic mice transduced with Arch-GFP. L6 V1 CT neurons were optogenetically inhibited across bouts of NREM sleep in the first 6 h of the post-stimulus *ad lib* sleep period. Light delivery reliably inhibited L6 neuronal firing, and slightly reduced firing in LGN neurons. **(B) Left:** V1 power spectral density during NREM-targeted L6 inhibition (expressed as a change from baseline; n = 64 LFPs from 11 mice, green) was significantly reduced relative to that of no laser (non-inhibited) control mice (n = 76 LFPs from 14 mice, red; * indicates $p < 0.05$ for no laser vs. inhibited conditions, Bonferroni-corrected Student's t-test for each frequency value). **Right:** Total integrated spectral power changes (from baseline) across delta (0.5-4 Hz) and spindle (7-15 Hz) frequency bands was significantly decreased during inhibition (green; $p < 0.01$, and $p < 0.001$, respectively) when compared with no laser control mice (red). Power recovered to normal levels after the 6-h inhibition period (*N.S.*, Mann-Whitney rank sum test). **(C)** Spindle-frequency coherence was decreased between V1 and LGN LFPs during NREM inhibition (n = 77 LFP pairs recorded across both inhibition and control conditions in 4 mice; $p < 0.001$ and $p = 0.786$, respectively for during and after 6-h NREM-targeted inhibition; Mann-Whitney rank sum test). **(D)** NREM-targeted inhibition caused an increase in the time lag between V1 and LGN LFPs at their maximum spindle-frequency coherence, relative to baseline ($p < 0.001$, Kolmogorov-Smirnov test for inhibition vs. no laser conditions). **(E)** NREM-targeted inhibition of L6 CT neurons decreased inter-areal SFC between LGN and V1. LGN spike to V1 LFP SFC at delta frequency: condition x time interaction $p < 0.001$, and at spindle frequency: main effect of time $p = 0.01$ and condition x time interaction $p < 0.001$; 2-way RM ANOVA; n = 54 neurons from 7 mice and 40 neurons from 5 mice for no laser control and inhibition conditions, respectively. V1 spike and LGN LFP SFC at delta frequency: main effect of time $p < 0.05$ and condition x time interaction $p < 0.001$, and at spindle frequency: *N.S.*; n = 29 neurons from 6 mice and 17 neurons from 4 mice for no laser control and inhibition conditions, respectively. * indicates $p < 0.05$, Holm-Sidak *post hoc* test.

4.4.5 Optogenetic inhibition of CT neurons during NREM, but not REM or wake, disrupts V1 plasticity.

We next tested the necessity of state-specific CT activity for consolidation of OSRP in V1. Following presentation of a visual stimulus to induce OSRP, Arch-expressing mice underwent a 6-h period of state-targeted V1 CT neuron inhibition, during bouts of either NREM, REM, or wake (**Fig. 4.6A**; **SI Appendix, Fig. S4.15**). This intervention had no significant effect on sleep architecture across either the 6-h period of optogenetic inhibition, or 6 h of subsequent recovery sleep (*N.S.,* Two Way ANOVA; **SI Appendix, Figs. S4.16** and **S4.17**). There were no significant differences in V1 OSRP between control mice without CT neuron inhibition, mice with REM- or wake-targeted inhibition of CT neurons, and mice expressing a control (YFP) transgene following NREM-targeted light delivery to V1 (*N.S.,* Holm-Sidak test). However, inhibition of CT neurons during NREM blocked OSRP in a manner similar to sleep deprivation ($p < 0.001$, ANOVA; **Fig. 4.6B**; **SI Appendix, Figs. S4.19** and **S4.20**). Similarly, the distribution of orientation preference changed across a period of sleep (leading to a greater proportion of neurons preferring X°) in control mice without CT neuron inhibition, mice with REM- or wake-targeted inhibition of CT neurons, and mice expressing a control (YFP) transgene, but not mice with NREM-targeted inhibition (**SI Appendix, Fig. S4.20**). NREM-targeted CT inhibition appeared to specifically disrupt sleep-associated OSRP consolidation, as there were no immediate effects of L6 CT neuron inhibition on orientation tuning in any layer of V1 (**SI Appendix, Fig. S4.14**). Thus these data suggest that CT coordination of NREM oscillations in the LGN-V1 network plays a critical role in promoting sleep-dependent V1 OSRP.

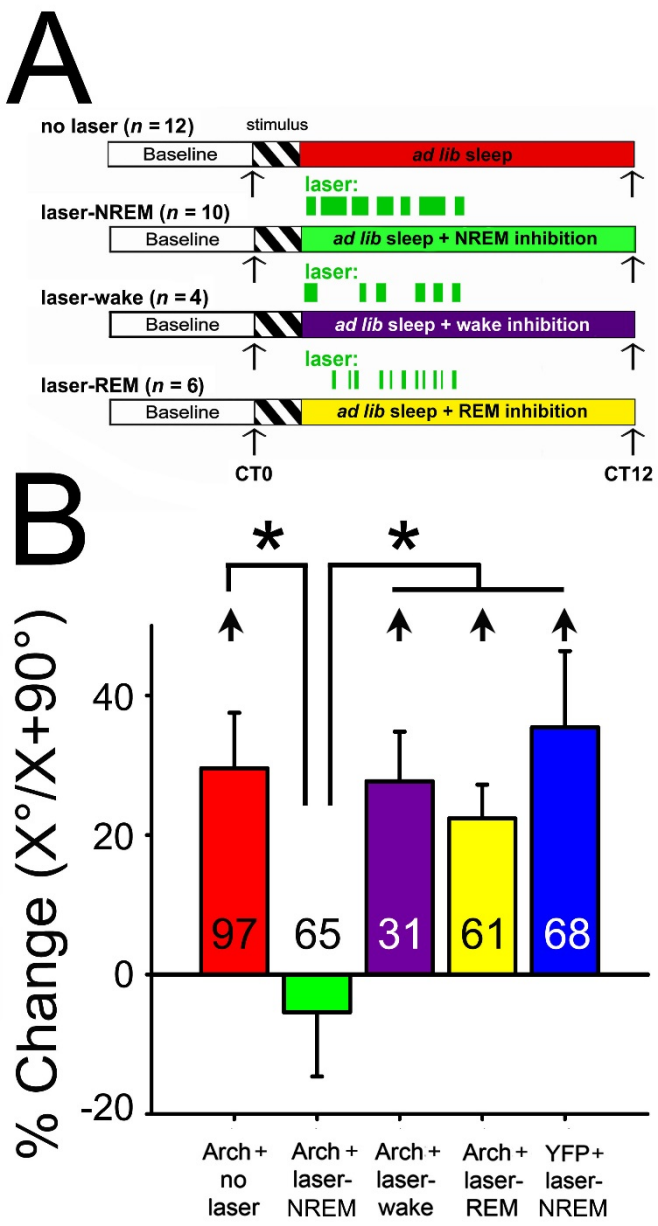

Figure 4.6. NREM-targeted inhibition of CT neurons disrupts consolidation of V1 response plasticity after visual experience. (A) Experimental paradigm for evaluating the effects of post-stimulus state-targeted optogenetic inhibition of V1 CT neurons on OSRP consolidation. **(B)** NREM-targeted inhibition of V1 CT neurons (laser-NREM) reduced OSRP in V1, while inhibition in other states did not affect OSRP. * indicates $p < 0.001$, Dunn's *post hoc* test versus no laser controls, laser-wake, laser-REM, and YFP-expressing control mice with light delivery targeted to V1 during NREM ($p < 0.001$; Kruskal Wallis ANOVA on ranks). With the exception of neurons recorded from mice with NREM-targeted inhibition, neurons recorded from all groups showed a significant increase in relative responsiveness to the presented stimulus orientation (relative to the orthogonal orientation [X°/X+90°]; arrowhead indicates $p < 0.05$, RM ANOVA on ranks).

4.5 Discussion:

Our present data show that novel visual experience rapidly alters response properties in LGN neurons, to enhance their responsiveness in favor of the presented stimulus orientation. This change is selective, occurring prior to expression of V1 OSRP, which relies on subsequent sleep (**SI Appendix, Fig. S4.3**).[7] This experience also alters the temporal relationship between LGN neurons' firing and V1 activity during subsequent NREM oscillations.

Previous studies have found that a subset of mouse LGN neurons show orientation-selective responses.[19-21] However, until now, it was unknown whether orientation-selective responses in the LGN (like that in V1) can change in response to visual experience. Our data suggest that sensory response plasticity does occur in LGN neurons. Prior work in the somatosensory system[22,23] suggested that thalamic neurons can change their response properties rapidly following disruption of peripheral sensory input. To our knowledge, these are the first data demonstrating that, following novel sensory experience, thalamic neurons in the visual pathway also show rapid response plasticity, and that these changes precede response plasticity in V1.

Why does subsequent OSRP in V1 require post-stimulus sleep? One possibility is that information is relayed between LGN and V1 during post-stimulus NREM, which in turn drives plasticity in the cortex. This interpretation is consistent with what is known about the circuit-level mechanisms of OSRP consolidation. LGN-to-V1 long-term potentiation (LTP) and OSRP are mutually occluding *in vivo*,[15] suggesting that potentiation of thalamocortical synapses underlies OSRP consolidation in V1. We have previously shown that OSRP consolidation is dependent on post-stimulus sleep.[7,8] Here

we show that in freely-sleeping mice, disruption of V1 CT neurons' activity during NREM oscillations is sufficient to block OSRP consolidation. While CT neurons also influence the firing of neurons in the other layers of V1,[24] we find that their effects on firing among LGN neurons are much more widespread and dramatic (**Fig. 4.4**). We also find that optogenetic inhibition of CT neurons disrupts communication between LGN and V1 during NREM delta and spindle oscillations (**Fig. 4.5**). Because we have previously shown that coherent firing of V1 neurons during NREM oscillations predicts the extent of OSRP consolidation,[7] a parsimonious interpretation is that thalamocortical coherence during NREM is essential for promoting OSRP in V1. Based on our current data, we conclude that information regarding stimulus characteristics of prior experience is relayed between the thalamus and cortex during subsequent NREM oscillations.

We find that V1-to-LGN CT communication, which coordinates thalamocortical oscillations associated with NREM sleep, plays an essential role for consolidating sensory response plasticity in V1.

Materials and Methods:

For anesthetized recording of visual response properties, or effects of L6 stimulation, 2-3 month old mice were anesthetized with isoflurane and a 32-site silicon probe was inserted into either V1 or LGN for neuronal recording. For chronic recording from behaving mice, 2 month old mice were implanted with drivable headstages composed of two bundles with seven stereotrodes each, using previously-described methods.[7] Signals from each electrode were split and differentially filtered to obtain spike data and LFP data at each recording site. Individual neurons were tracked throughout the

experiment as described previously.[7,25] Complete materials and methods are in ***SI Materials and Methods***.

Acknowledgements:

Support for this research was provided by a Young Investigator Award from the Brain and Behavioral Research Foundation, an Alfred P. Sloan Foundation Fellowship, and a research grant (EY021503) from the National Institutes of Health to S.J.A., and a National Science Foundation Graduate Research Fellowship to J.D. The authors are grateful to Sha Jiang and Amanda Morrison for expert technical assistance with these studies.

4.6 References:

1. Huber R, Ghilardi MF, Massimini M, & Tononi G (2004) Local sleep and learning. *Nature* 430(6995):78-81.

2. Aton SJ*, et al.* (2009) Mechanisms of sleep-dependent consolidation of cortical plasticity. *Neuron* 61(3):454-466.

3. Dumoulin MC*, et al.* (2015) Extracellular Signal-Regulated Kinase (ERK) Activity During Sleep Consolidates Cortical Plasticity In Vivo. *Cereb. Cortex* 25(2):507-515.

4. Seibt J*, et al.* (2012) Protein synthesis during sleep consolidates cortical plasticity in vivo. *Curr Biol* 22(8):676-682.

5. Yang G*, et al.* (2014) Sleep promotes branch-specific formation of dendritic spines after learning. *Science* 344(6188):1173-1178.

6. Aton SJ*, et al.* (2013) Visual experience and subsequent sleep induce sequential plastic changes in putative inhibitory and excitatory cortical neurons. *Proc Natl Acad Sci U S A* 110(8):3101-3106.

7. Aton SJ, Suresh A, Broussard C, & Frank MG (2014) Sleep promotes cortical response potentiation following visual experience. *Sleep* 37(7):1163-1170.

8. Durkin J & Aton SJ (2016) Sleep-Dependent Potentiation in the Visual System Is at Odds with the Synaptic Homeostasis Hypothesis. *Sleep* 39(1):155-159.

9. Chauvette S, Seigneur J, & Timofeev I (2012) Sleep oscillations in the thalamocortical system induce long-term neuronal plasticity. *Neuron* 75(6):1105-1113.

10. Miyamoto D*, et al.* (2016) Top-down cortical input during NREM sleep consolidates perceptual memory. *Science* 352(6291):1315-1318.

11. Gais S & Born J (2004) Low acetylcholine during slow-wave sleep is critical for declarative memory consolidation. *PNAS* 101(7):2140-2144.

12. Aton SJ (2013) Set and setting: How behavioral state regulates sensory function and plasticity. *Neurobiol Learn Mem* 106:1-10.

13. Tononi G & Cirelli C (2003) Sleep and synaptic homeostasis: a hypothesis. *Brain Res Bull* 62(2):143-150.

14. Frenkel MY*, et al.* (2006) Instructive effect of visual experience in mouse visual cortex. *Neuron* 51(3):339-349.

15. Cooke SF & Bear MF (2010) Visual experience induces long-term potentiation in the primary visual cortex. *J Neurosci* 30(48):16304-16313.

16. Contreras D, Destexhe A, Sejnowski TJ, & Steriade M (1996) Control of spatiotemporal coherence of a thalamic oscillation by corticothalamic feedback. *Science* 274(5288):771-774.

17. Timofeev I & Steriade M (1996) Low-frequency rhythms in the thalamus of intact-cortex and decorticated cats. *J Neurophysiol* 76(6):4152-4168.

18. Chow BY*, et al.* (2010) High-performance genetically targetable optical neural silencing by light-driven proton pumps. *Nature* 463(7277):98-102.

19. Piscopo DM, El-Danaf RN, Huberman AD, & Niell CM (2013) Diverse visual features encoded in mouse lateral geniculate nucleus. *J Neurosci* 33(11):4642-4656.

20. Zhao X, Chen H, Liu X, & Cang J (2013) Orientation-selective responses in the mouse lateral geniculate nucleus. *J Neurosci* 33(31):12751-12763.

21. Tang J, Ardila Jimenez SC, Chakraborty S, & Schultz SR (2016) Visual receptive field properties of neurons in the mouse lateral geniculate nucleus. *PLoS ONE* 11(1).

22. Nicolelis MA, Lin RC, Woodward DJ, & Chapin JK (1993) Induction of immediate spatiotemporal changes in thalamic networks by peripheral block of ascending cutaneous information. *Nature* 361(6412):533-536.

23. Krupa DJ, Ghazanfar AA, & Nicolelis MA (1999) Immediate thalamic sensory plasticity depends on corticothalamic feedback. *Proc Natl Acad Sci U S A* 96(14):8200-8205.

24. Bortone DS, Olsen SR, & Scanziani M (2014) Translaminar inhibitory cells recruited by layer 6 corticothalamic neurons suppress visual cortex. *Neuron* 82(2):474-485.

25. Ognjanovski N*, et al.* (2017) Parvalbumin-expressing interneurons coordinate hippocampal network dynamics required for memory consolidation. *Nature Communications* In press.

4.7 Chapter 4 SI Materials and Methods

4.7.1 Mouse husbandry.

All animal husbandry and surgical/experimental procedures were approved by the University of Michigan IACUC. Following surgical procedures, mice were individually housed in standard caging with beneficial environmental enrichment (nesting material, toys, and novel foods) throughout all subsequent experiments. With the exception of OSRP experimental days, during which lights were kept off, lights were maintained on a 12 h:12 h light: dark cycle (lights on at 8 AM), and food and water were provided *ad lib*.

4.7.2 Anesthetized recordings of visual response properties.

For anesthetized recording of visual responses from LGN and V1 **(Figs. 4.1 & 4.2A-B)**, C57BL/6J mice were anesthetized with isoflurane (0.5-0.8%) and 1 mg/kg chlorprothixene (Sigma). A 2-shank, linear silicon probe (250 µm spacing between shanks) with 25 µm spacing between recording sites (16 sites/shank; Cambridge Neurotech) was slowly advanced into LGN or V1 until stable recordings (with consistent spike waveforms continuously present for at least 30 minutes prior to baseline recording) were obtained. At each recording site, following a baseline recording, anesthetized mice were presented with phase-reversing grating stimuli (spatial frequency 0.05 cycles/degree, 100% contrast, reversal frequency 1.0 Hz) of 8 orientations (0, 22.5, 45, 67.5, 90, 112.5, 135, or 157.5 degrees from horizontal) and a blank screen (to assess spontaneous firing) in the visual field contralateral to the recorded hemisphere. Stimuli were presented in an interleaved manner, to assess baseline visual properties. Mice were then presented with one orientation, chosen at random, for a prolonged period of 30 min.

Immediately following stimulus presentation, mice were again presented with full-field grating stimuli of the 8 orientations listed above and a blank screen to reassess visual response properties. OSRP, and changes in other neuronal visual response properties were quantified as described below. Following all recordings, mice were euthanized and perfused for verification of microelectrode placement.

4.7.3 Optogenetic stimulation of L6 CT neurons.

For experiments described in **Figs. 4.4 & S4.8,** *Ntsr1-Cre* mice were crossed with B6;129S-*Gt(ROSA)26Sor*$^{tm32(CAG-COP4*H134R/EYFP)Hze}$/J mice (Jackson laboratories) to yield mice expressing Channelrhodopsin-2 (ChR2) specifically in L6 CT neurons (*Ntsr1::Chr2*). To assess the effects of CT stimulation on LGN and V1 neurons, *Ntsr1::Chr2* mice were anesthetized with isoflurane and chlorprothixene as described above. A 32-site silicon probe with 250 µm spacing (Cambridge Neurotech) was slowly advanced into right hemisphere LGN or V1 until stable recordings were obtained. And optical fiber was placed 0.5 mm ventral into cortex for delivery of laser light to V1 Layer 6 neurons. A 15-minute baseline was recorded, followed by 5 minute periods of rhythmic optogenetic stimulation with 473 nm laser light (approximately 3 mW/mm^2; CrystaLaser) at the following frequencies: 0.5, 1, 2, 3, and 4 Hz. Stimulation periods were separated by 10-minute intervals to allow neuronal firing to return to baseline levels. Following all optogenetic experiments, mice were perfused and brains were processed for histological assessment. Optic fiber and electrode position were validated prior to data analysis.

4.7.4 Surgical procedures.

For chronic recordings in **Figs. 4.2 & 4.3,** 2 month old male and female C57BL/6J mice were implanted with custom-built drivable headstages (EIB-36 Neuralynx) under isoflurane anesthesia, using previously described techniques.[1] Each headstage was composed of two bundles (each approximately 200 µm in diameter) of seven stereotrodes each (25 µm nichrome wire, California Fine Wire; Grover Beach, CA). For combined V1/LGN recording (**Figs. 4.2 & 4.3**), one bundle was placed in right hemisphere LGN (2.25 mm posterior and 2.25 mm lateral from bregma, 2.25 mm ventral to cortical surface) and the other in ipsilateral V1 (3.0 mm posterior and 2.5 mm lateral from bregma, 0.2-0.5 mm ventral to cortical surface). Reference and ground electrodes were placed over left hemisphere V1 and cerebellum, respectively, and three electromyography (EMG) electrodes were placed deep in the nuchal muscle.

For optogenetic inhibition of layer 6 V1 neurons (**Fig. 4.5 & 4.6**), 6 week-old, male and female *Ntsr1-cre* transgenic mice (which express Cre recombinase selectively in layer 6 corticothalamic neurons;[2] B6.FVB(Cg)-Tg(Ntsr1-cre)GN220Gsat/Mmucd; Jackson) underwent bilateral V1 transduction with AAV9.CBA.Flex.Arch-GFP.WPRE.SV40 (“Arch-GFP”; Addgene 22222; PENN Vector core). A volume of 1 µl was injected via a 33 gauge beveled syringe needle at a rate of 0.2 µl/min (3.0 mm posterior and 2.5 mm lateral from bregma, 0.5-0.7 mm ventral to cortical surface). A second group of *Ntsr1-cre* mice were transduced with a YFP (control) expression vector AAV9.EF1a.DIO.eYFP.WPRE.hGH (Addgene 27056; PENN Vector core). Viral titers were between 1.61e13 and 4.65e13 GC/ml. Mice were allowed to recover for 2-3 weeks before implantation with drivable headstages. For combined V1/LGN recording (**Fig. 4.5**),

one bundle was placed in right hemisphere LGN (2.25 mm posterior and 2.25 mm lateral from bregma, 2.25 mm ventral to cortical surface) and the other in ipsilateral V1 (3.0 mm posterior and 2.5 mm lateral from bregma, 0.2-0.5 mm ventral to cortical surface). An optical fiber was placed adjacent to V1 electrodes. For V1-only recordings (**Fig. 4.6**), the two bundles were placed into right hemisphere V1, 1.0 mm apart, with the optical fiber tip equidistant between them. Reference, ground, and EMG electrodes were placed as described above.

4.7.5 Chronic stereotrode recording.

After mice recovered from surgical procedures (1-2 weeks), chronic stereotrode recording was carried out using previously-described procedures.[1,3] Mice (in their home cage) were placed inside a sound-attenuated recording chamber (Med Associates) and were tethered using a lightweight cable for neural recording. Mice were habituated to daily handling, restraint, and head fixation over a period of 5 days. During this period, electrode bundles were lowered into V1 and/or LGN in 10-20 µm steps until stable neuronal recordings were obtained. Recording stability was defined by the continuous presence of spike waveforms on individual electrodes for at least 24 h prior to the onset of baseline recording. Signals from each electrode were split and differentially filtered to obtain spike data (200 Hz-8 kHz) and LFP/EMG activity (0.5-200 Hz). Data were amplified at 20x, digitized, further digitally amplified at 20-100x, and recorded using Plexon Omniplex software and hardware (Plexon Inc.; Dallas, TX). For all chronic recordings, single-unit data was referenced locally (e.g., intra-LGN for LGN recordings; intra-V1 for V1

recordings) to a recording channel without single-unit activity, to eliminate low-frequency noise.

4.7.6 OSRP induction and measurement.

A continuous 24-h baseline recording was carried out for each mouse, starting at CT0. The following day at CT0, mice were head-fixed. Phase-reversing gratings (spatial frequency 0.05 cycles/degree, 100% contrast, reversal frequency 1.0 Hz) of 4 orientations (0, 45, 90, and 135 degrees from horizontal) and a blank screen (for assessment of spontaneous activity) were presented to the left visual field (i.e., contralateral to the hemisphere in which visual responses were recorded . Each of these stimuli was presented 8 times (10 s/presentation) in a random, interleaved fashion. Neuronal firing rate responses were quantified and averaged for each stimulus orientation (and blank screen). Immediately following this baseline test, a single grating stimulus (of a randomly-selected orientation) was continuously presented over a 30-min period to induce OSRP. Firing rate changes in LGN and V1 neurons across stimulus presentation were calculated by measuring each neuron's average firing rates over the first and last 5 min of stimulus presentation.

Mice were then returned to their home cage and recordings continued until CT12 in complete darkness (to prevent additional visual experience). Between 30-min grating presentation and testing, mice were either allowed to sleep *ad libitum*, or were kept awake over the first 6 h, using gentle handling.[1] For state-specific optogenetic inhibition (**Figs. 4.5 & 4.6**), freely-sleeping mice had green laser light (532 nm; 1-10 mW/mm^2) delivered to V1 during bouts of either NREM (laser-NREM; n = 10 experiments with Arch-GFP-

expressing mice, *n* = 8 experiments with YFP-expressing mice), REM (laser-REM; *n* = 5), or wake (laser-wake; *n* = 5) (with behavioral state assessed in real-time, based on LFP activity, EMG activity, and infrared video recording of animal behavior). *Post hoc* analysis of laser targeting efficiency was calculated as the percent of light delivery that was properly targeted to the state, and the percent of the state that received light coverage (**Fig. S4.16**).

At CT12 following stimulus presentation to induce OSRP, mice were again head-fixed and presented with a series of gratings to re-assess orientation preference. Orientation preference for stably-recorded neurons (i.e., those with consistent spike waveforms on the two stereotrode channels across 24-h baseline recording, and across the 12-h OSRP experiment) was quantified as the ratio of mean firing rate responses for the presented orientation (X°) to that of the orthogonal to presented stimulus (X+90°) as described previously. Changes in this measure were quantified by subtracting baseline (X°/X+90°) ratio from evening (X°/X+90°) ratio; this difference was then expressed as a percent change from baseline (**Fig. 4.1C**, **Fig. 4.6B**, **Fig. S4.1B, and Fig. S4.3B**). As an additional measure, changes in the ratio of responsiveness to the presented orientation and to oblique (±45°) orientations (X°/X±45°) were calculated (**Fig. S4.1**, **& Fig S4.18B**). An orientation selectivity index (OSI90; used to indicate the strength or orientation tuning, regardless or orientation preference; **Fig. S4.1E & Fig. S4.18C**) was also calculated for each neuron, as 1 - [(average firing rate at 90 degrees from preferred orientation)/(average firing rate at the preferred stimulus orientation)]**.**[4] Neuronal visual responsiveness (to any visual stimulus) was assessed statistically using previously-described ANOVA-based methods;[5] only visually responsive neurons were included in

analysis of OSRP. Using this metric, the proportion of V1 neurons classified as visually responsive vs. non-responsive (**Fig. S4.20B**) was similar to that reported elsewhere.[6] With the exception of data presented in **Figs. S4.2B & S4.20B**, only visually responsive neurons were included in analyses of visual response properties and OSRP. There were no significant differences between male and female mice with regards to OSRP expression within control (no laser) conditions (p = 0.70, Mann Whitney rank sum test).

4.7.7 Histology and immunohistochemistry.

At the conclusion of each recording, mice were deeply anesthetized with barbiturate injection, and an electrolytic lesion was made at each electrode site (2 mA, 3s per electrode). Mice were then perfused with formalin and euthanized. Brains were post-fixed, cryosectioned at 50 µm, and stained with DAPI (DAPI Fluoromount-G Mounting Media; SouthernBiotech[7]) for assessment of electrode placement (**Fig. S4.13**).

To characterize the extent of V1 viral transduction with Arch-GFP, four *Ntsr1-cre* mice were transduced as described above. After a 3-week recovery period to allow for sufficient expression of the virus, mice were perfused with 4% paraformaldehyde in ice cold 0.1M phosphate buffered saline. Brains were post-fixed and cryosectioned at 50 µm. Coronal sections through V1 were stained with mouse anti-NeuN (MAB377; 1:500; Millipore[8]) and secondary goat anti-mouse IgG1 594 (A-21125; 1:1000; Thermo Fisher Scientific[9]). Images were collected for all brain slices containing virally-transduced visual cortical regions. A region of interest was drawn around V1 L6 on each coronal slice using ImageJ software. Within this region, both the total number of NeuN+ layer 6 cells, and the number of NeuN+/GFP+ neurons was counted. Quantification of the proportion of V1 L6

neurons expressing GFP was independently verified by two scorers (**Fig. S4.9**). For characterization of ChR2-GFP expression, four *Ntsr1::ChR2* mice were perfused with 4% paraformaldehyde, and brains were post-fixed, sectioned, and stained for NeuN as described above. Quantification of the proportion of layer 6 V1 cells expressing GFP was carried out as described above (**Fig. S4.7A-B**).

4.7.8 Single unit discrimination.

Single-neuron data were discriminated offline using standard principle component-based procedures as described previously (**Fig. S4.4**).[1,10,11] Briefly, spikes from individual neurons were discriminated on the basis of spike waveform shape and width, relative spike amplitude on the two stereotrode recording wires, and relative positioning of spike waveform clusters in three-dimensional principal component space. Single-neuron isolation was verified using standard techniques.[12] Clusters with interspike interval (ISI)-based absolute refractory period violations were eliminated from analysis. Waveform cluster separation (for channels with more than one discriminated single unit) was first validated using MANOVA on the first 3 principal components ($p < 0.05$ for all sorted clusters; mean p value = 0.02 ± 0.01), and further characterized using the Davies-Bouldin (DB) validity index (a metric with inter-cluster distance as the denominator, thus lower values indicate better cluster separation).[13] The mean (± SEM) DB value for all sorted waveform clusters (across all groups) was 0.32 ± 0.03, which compares favorably with DB values from single-unit data used in other studies.[14,15] Only those neurons that 1) met the criteria described above and 2) were reliably discriminated and continuously recorded throughout each experiment (*i.e.*, those stably recorded across both 24-h baseline and

12-h experimental condition) were included in firing rate analyses from behaving mice. For multielectrode recording from anesthetized mice, only those neurons reliably discriminated and stably recorded across baseline and optogenetic inhibition conditions were included in subsequent analyses.

4.7.9 Data analysis.

Intracortical LFP and nuchal EMG signals were used to categorize recorded data into REM, NREM, and wake states **(Fig. S4.5A)** over 10-s intervals of recording using custom software. For analyses of changes in LGN and V1 firing rate or spike-field coherence (SFC), only visually responsive neurons (assessed using criteria described above) were included. Firing rate and power spectral density were calculated separately within REM, NREM, and wake using NeuroExplorer software (Plexon). SFC was calculated by bandpass filtering LFPs corresponding to stably-recorded neurons, for either delta (0.5-4 Hz) or spindle (7-15 Hz) frequencies. Spike and LFP data were aligned and a spike triggered average was calculated for each neuron's spike trains.[10] For normalization purposes (*i.e.*, for comparing SFC changes between experimental groups), these data were z-scored by randomizing spike times 100 times relative to LFPs, over a time window of up to 20 s (for delta) and 1.43 s (for spindle) (**Fig. 4.3B**). SFC raw values and z-scores were then measured as changes from baseline in control conditions and laser-NREM conditions and compared via two-way RM ANOVA (**Fig. 4.5E**). Coherence between LGN and V1 LFPs was quantified in MATLAB. Briefly, LFPs from LGN were aligned to a reference LFP in V1, the LGN LFP was moved in time relative to the V1 LFP (± 200 ms and ± 100 ms lag time, respectively, for delta and spindle frequencies), and

correlations between the fields were calculated at each lag time. Changes in peak correlation amplitude from baseline were compared between rest and laser-NREM conditions using Mann Whitney rank sum test (**Fig. 4.5C; Fig. S4.12A**). Changes in lag times between V1 and LGN fields were plotted as a cumulative probability distribution and assessed by Komlogorov-Smirnov test (**Fig. 4.5D; Fig. S4.12B**). For analysis of spindle occurrence during optogenetic stimulation experiments (**Fig. S4.8**), V1 LFPs were band-pass filtered at 11-15 Hz. Spindle-like events were defined as ≥ 6 peaks or troughs of filtered signal that surpassed mean signal amplitude by 1.5 standard deviations.

Wilcoxon signed rank tests were used to assess firing rate changes over stimulus presentation, (**Fig. 4.2C**). Correlations between firing rate changes, spike field coherence, and visual response properties were assessed by Pearson product moment, and fit with a linear regression (**Figs. 4.2B,D & 4.3C**). All measures of change induced by optogenetic manipulation in **Fig. 4.5** were expressed as a change from baseline values (i.e., experimental – baseline). For analysis of power spectral density, Student's t-tests were conducted at each frequency bin from 0-15 Hz (n = 76 bins) and a Bonferroni correction for multiple comparisons was applied to the results (**Fig. 4.5B**). Area under the curve was calculated for delta (0.5-4 Hz) and spindle (7-15 Hz) frequency bins to assess changes in power at these frequencies (**Fig. 4.5B**).

To ensure state-specific optogenetic manipulation had no effect on sleep architecture, a 2-way ANOVA was used to quantify proportions of time spent in each state (factor A: experimental condition, factor B: time of day; **Fig. S4.17**). Effects of state-specific optogenetic inhibition of CT neurons were assessed by 1-way RM ANOVA (**Fig. 4.6B**).

To address potential confounds from nested data, within-mouse averages were generated for data in **Figs. 4.1C, 4.2B, 4.2D, 4.3B, 4.3C, and 4.6B.** These values are now plotted in **Figs. S4.1B, S4.6A, S4.6B, S4.6C, S4.6D, & S4.20B**, respectively.

4.8 Chapter 4 SI Figures

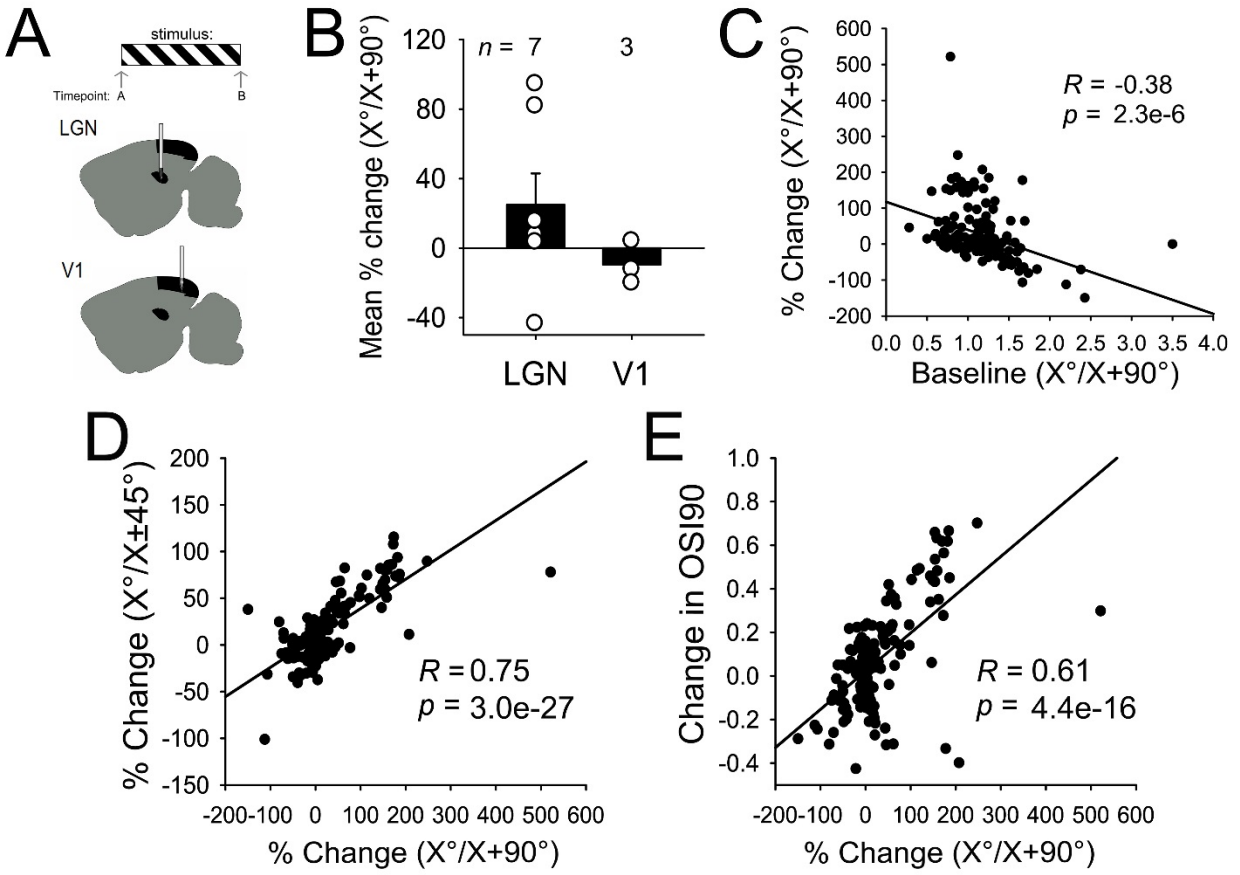

Figure S4.1. Features of OSRP expressed by LGN neurons after visual stimulus presentation. (A) Experimental design for anesthetized recordings, as described in Fig. 1A. **(B)** Changes in the responsiveness to the presented oriented grating stimulus (vs. orthogonal orientation) averaged across LGN or V1 for each mouse. These average changes were highly variable in LGN, but generally followed the same trend as shown in Fig. 1C. **(C)** Among LGN neurons, the degree of OSRP (change in [X°/X+90°]) after stimulus presentation was inversely related to baseline (X°/X+90°) ratio. The extent of OSRP in individual LGN neurons was positively correlated with **(D)** relative increases in responsiveness to the presented orientation vs. oblique orientations and **(E)** orientation selectivity (OSI90) increases. Pearson product moment *R* and *p* values are shown for 147 LGN neurons.

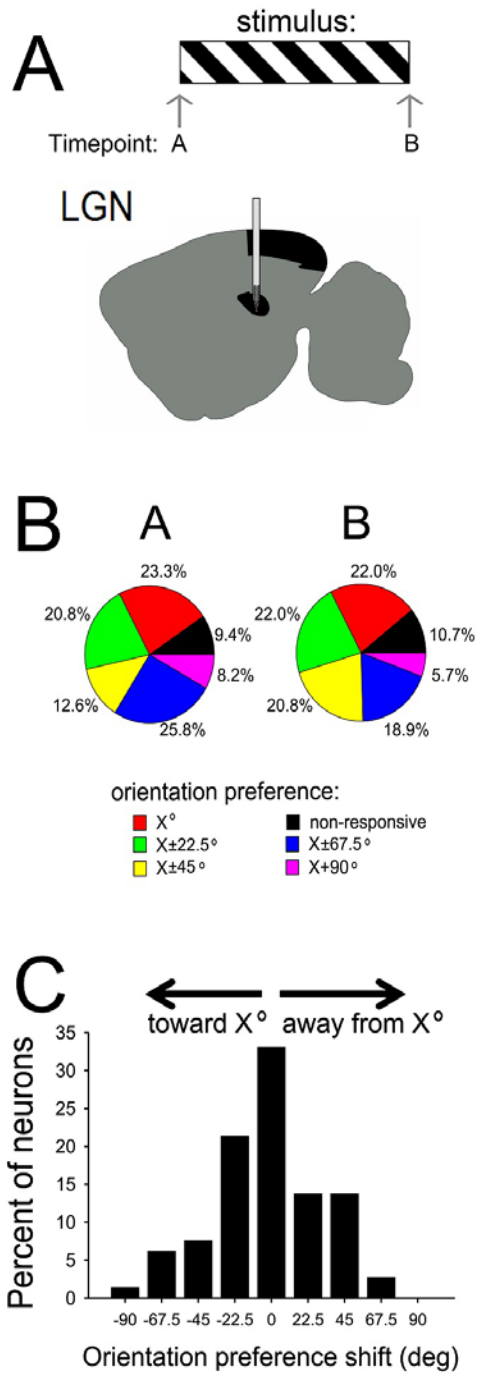

Figure S4.2. Distribution of orientation-specific responses in LGN neurons, and changes in orientation preference across stimulus presentation. (A) Schematic of LGN neuronal recordings from anesthetized mice as described in Fig. 1A. **(B)** Distributions of orientation preference among visually responsive LGN neurons (and proportions of non-responsive neurons) before (timepoint A) and after (timepoint B) stimulus presentation. OSRP measured across stimulus presentation in LGN was not associated with an increase in the proportion of LGN neurons preferring the stimulus (X°) orientation, although the proportions of neurons preferring the orthogonal (X+90°) and X±67.5°orientations were reduced slightly. **(C)** Distribution of the changes in preferred orientation for individual LGN neurons across stimulus presentation. Data are presented for all visually responsive neurons. 0 indicates no change, while negative and positive shifts, respectively, indicate shifts in response preference toward and away from the presented stimulus orientation.

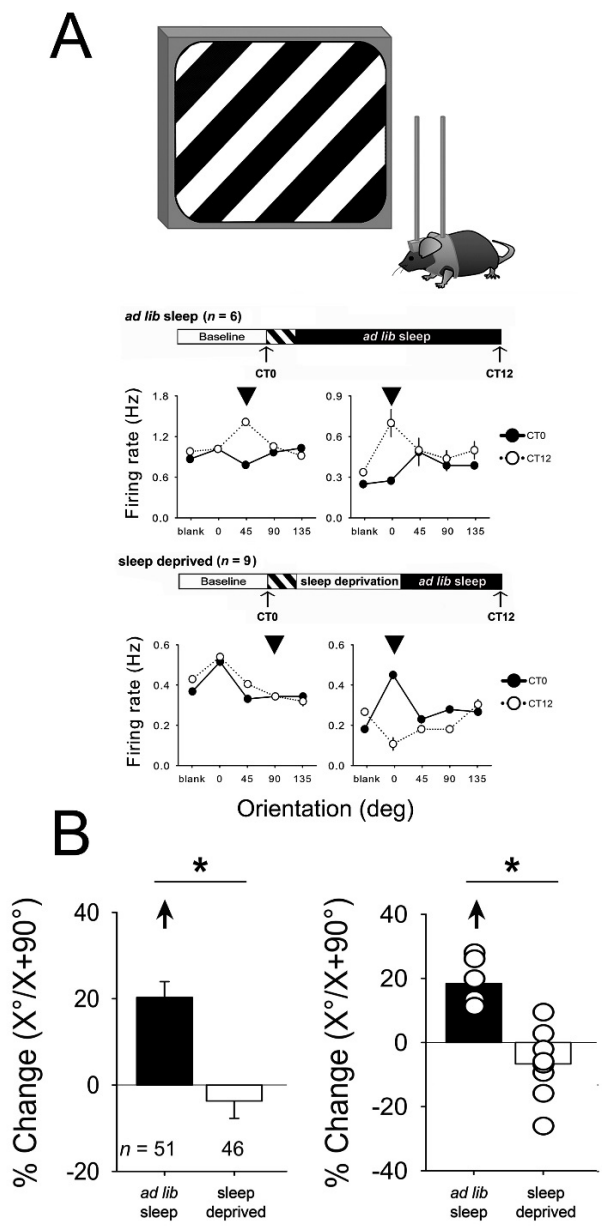

Figure S4.3. Orientation-specific response potentiation (OSRP) in V1 is sleep-dependent. (A) Schematic of OSRP experiment. Mice were implanted with V1 stereotrodes for continuous recording of neurons and local field potentials. At CT0, following a 24-h baseline recording period, mice were temporarily head-fixed and shown a series of oriented gratings (0, 45, 90, and 135 degrees) to measure V1 neurons' baseline visual response properties (first black arrow). One grating of a single orientation was then selected for 30-min presentation, to induce ORSP. Following stimulus presentation, mice were either allowed *ad lib* sleep, or were sleep deprived for the first 6 h by gentle handling. At CT12, visual response properties were reassessed (second black arrow). Tuning curves at CT0 and CT12 (black and white respectively) for 2 representative neurons recorded from a C57BL/6J mouse allowed *ad lib* sleep, and for 2 representative neurons recorded from a sleep deprived mouse. Values indicate mean firing rate response for each stimulus, ± SEM. *n* indicates the total number of mice recorded in each condition. Arrowheads indicate the orientation of the grating presented over 30 min to induce OSRP. **(B)** OSRP is calculated as % change in the ratio of firing rate responses to stimuli of the presented and orthogonal orientation between CT0 and CT12. Analysis is shown for individual neurons **(left)** and averaged values for each mouse **(right)**. Following *ad lib* sleep, V1 neurons show a significant increase in preference for the presented stimulus orientation (arrowhead indicates $p < 0.05$, RM ANOVA on ranks), which is not seen in sleep deprived mice (* indicates $p < 0.05$ for *ad lib* sleep vs. sleep deprived). *n* indicates the total number of neurons recorded in each condition.

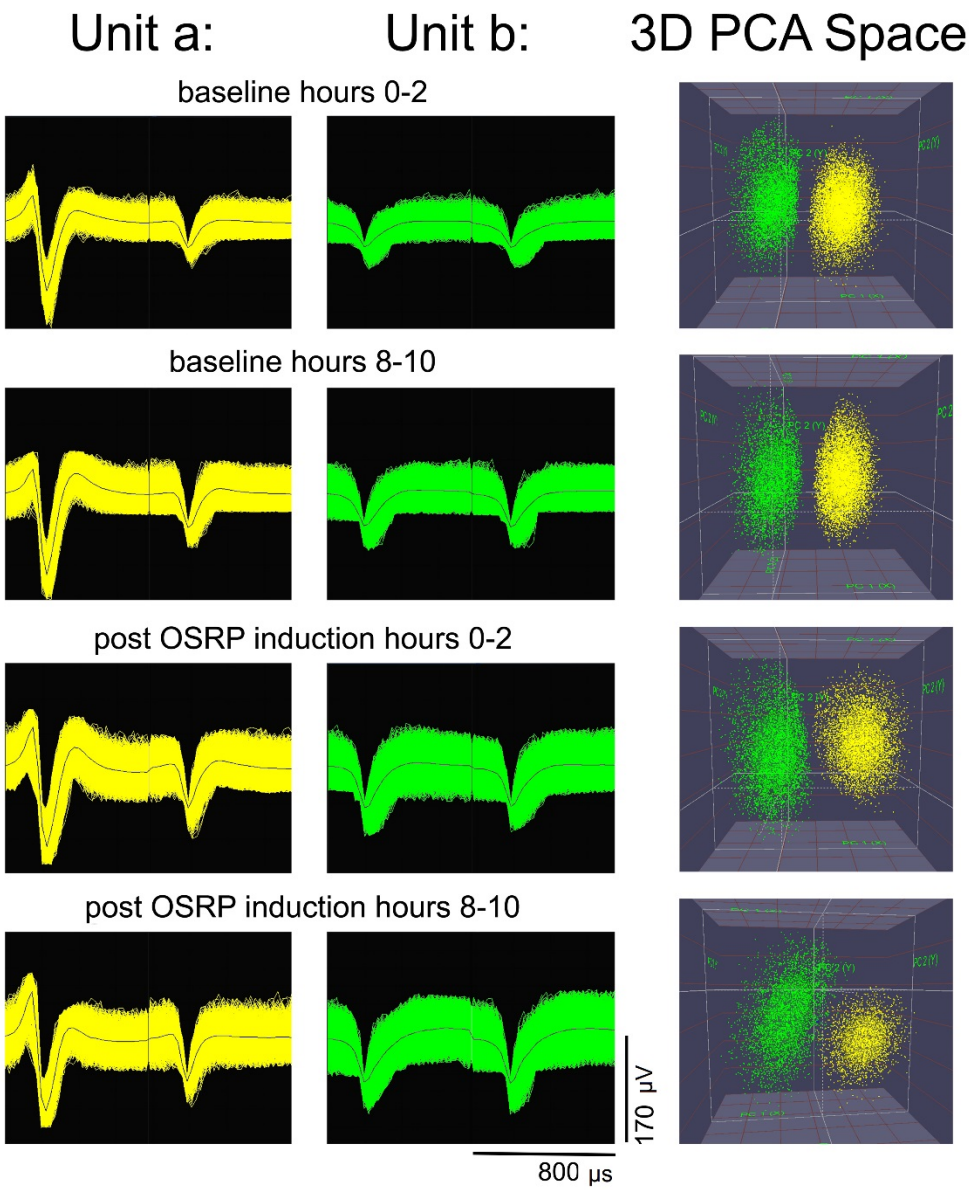

Figure S4.4. Spike sorting and spike cluster stability over time. Left: Spike waveforms for 2 representative neurons recorded on the same stereotrode across 2-h windows at baseline, and following stimulus presentation on the second day of recording. **Right:** Clusters of spike waveforms in 3-dimensional principal component space. For all recordings, cluster separation was validated using MANOVA ($p < 0.05$ for all sorted clusters; mean p value = 0.02 ± 0.01), and further characterized using the Davies-Bouldin (DB) validity index (mean DB index = 0.32 ± 0.03).

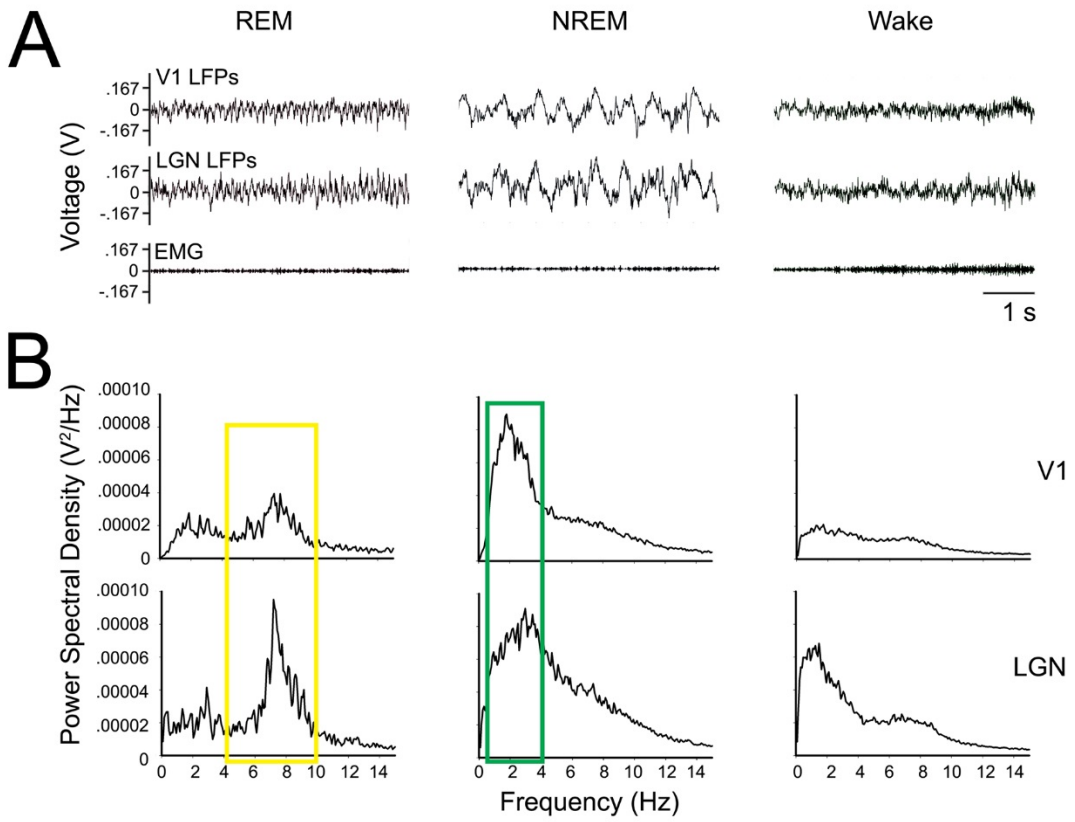

Figure S4.5. Representative LFP and EMG data used for sleep scoring. (A) Representative V1 (top) and LGN (middle) LFPs and EMG (bottom) traces during REM sleep **(left)**, NREM sleep **(middle)**, and wake **(right)**. (**B)** Power spectral density (PSD) graphs for V1 **(top)** and LGN **(bottom)**. REM sleep is characterized by high theta frequency (4-10 Hz) activity (highlighted in yellow) in the LFP and low EMG activity. NREM sleep is characterized by high amplitude delta frequency (0.5-4 Hz) activity (highlighted in green) in the LFP and low EMG activity. Wake is characterized by low amplitude LFP activity and higher, more variable EMG activity.

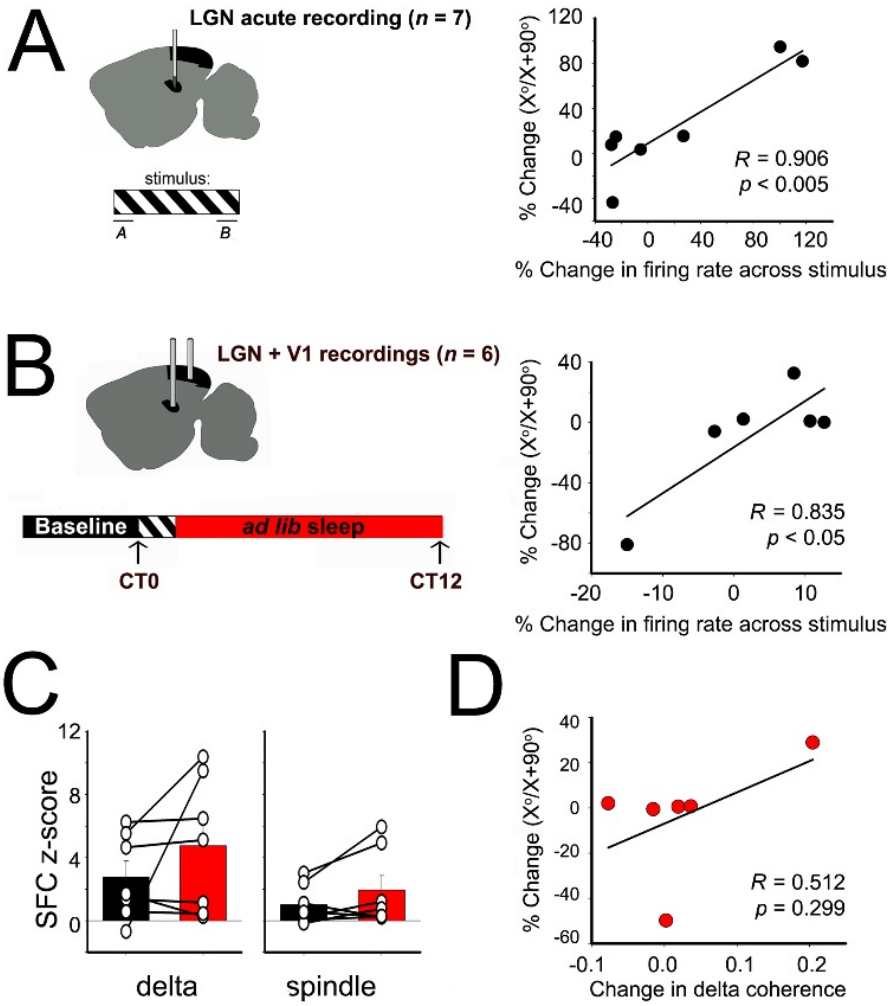

Figure S4.6. Changes in neuronal firing properties induced by stimulus presentation predict OSRP. (A) Left: Schematic of anesthetized LGN recording. **Right:** The mean values from each mouse with data presented in Fig. 2B are shown. Per animal mean LGN neuron firing rate changes over stimulus presentation predict mean per animal OSRP measures (*R* and *p* values are shown for Pearson product moment). **(B) Left:** Schematic of chronic recording in mice implanted with LGN and V1 stereotrodes. **Right:** Per animal means of firing rate data from Fig. 2D. There is a similar, significant relationship between mean LGN neuron firing rate changes and mean OSRP per animal (*R* and *p* values are shown for Pearson product moment). **(C)** Per animal means of SCF data from Fig. 3B. When averaged within each animal the changes in delta and spindle SFC are not significant (*N.S.,* Wilcoxon signed rank test). **(D)** Per animal means of data in Fig. 3C. There is no significant relationship between the change in delta coherence and the % change in OSRP measurement when data is aggregated into averages per animal, although the trend is similar to that shown for Fig. 3C (*N.S.,* Pearson product moment).

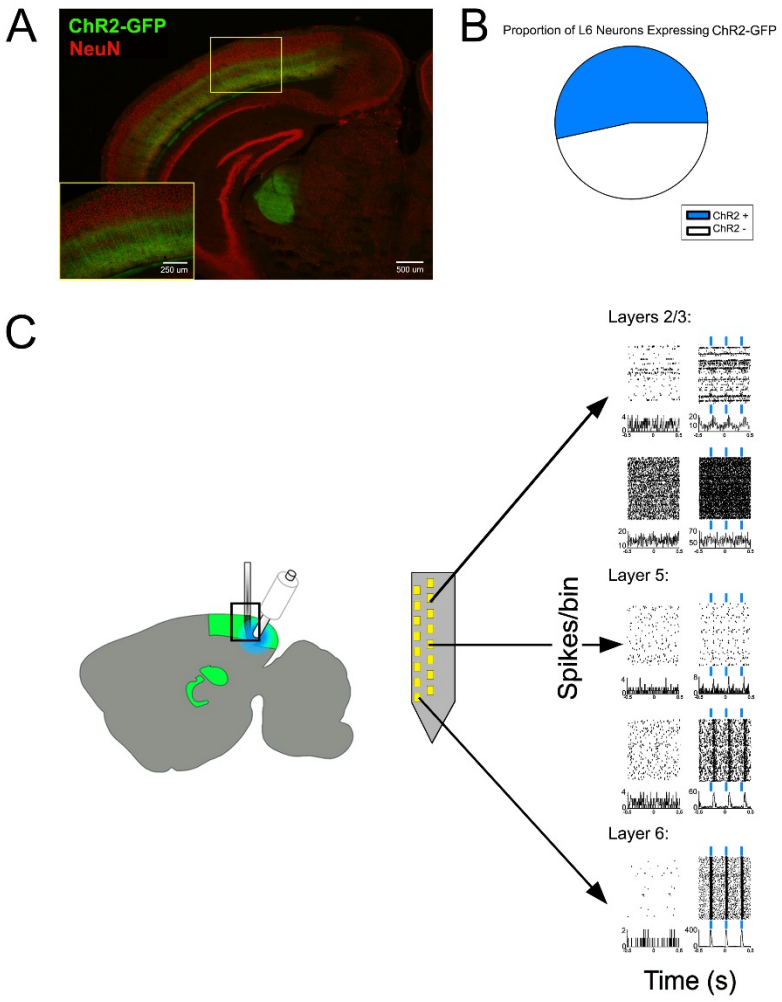

Figure S4.7. ChR2-GFP expression in V1 L6 neurons and recording during optogenetic stimulation. (A) GFP expression in V1 L6 neurons of *Ntsr1::ChR2* crossed transgenic mice. Wide field images show axon termini in thalamic nuclei, inset shows cell bodies in V1. **(B)** Histological assessment of n = 4 transgenic mice showed ChR2-GFP expression in 53.4 ± 1.5% of all NeuN+ V1 L6 neuronal cell bodies (a similar proportion to the number of L6 neurons which project to thalamus [16]). **(C)** Schematic of recording of neuronal activity during optogenetic stimulation in *Ntsr1::ChR2* mice. Linear probes with 25 um spacing between sites allowed for recording of multiple cortical layers across V1 simultaneously. Representative data are shown for neurons simultaneously recorded across V1 layers during optogenetic stimulation. Only within L6 (where neurons were directly activated by light delivery) was neuronal spiking precisely timed to light pulses.

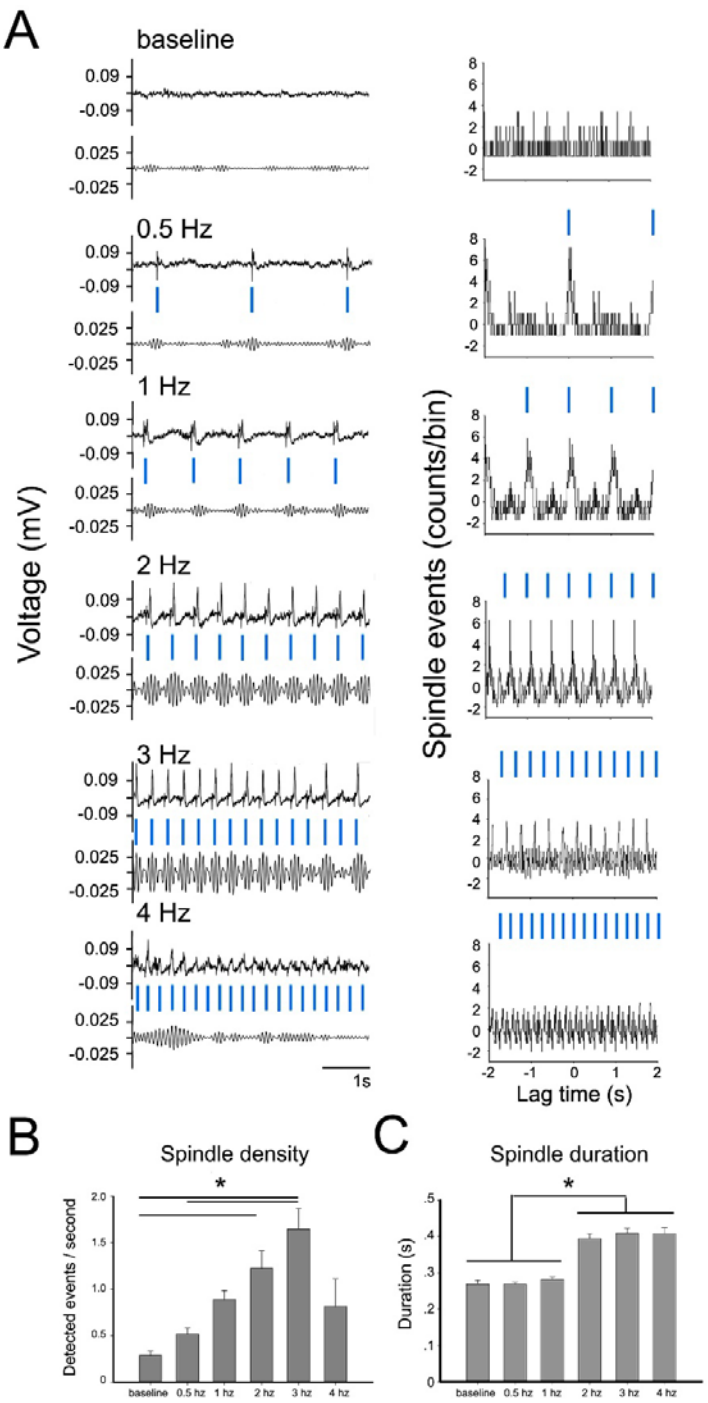

Figure S4.8. Stimulation of V1 L6 neurons induces sleep spindle-like oscillation in V1. (A) Left: Representative raw and filtered (11-15 Hz) LFPs recorded from V1 at baseline (in the absence of light delivery to V1), and during optogenetic stimulation of L6 neurons at a range of frequencies. **Right:** An automated spindle detection algorithm (see SI Materials and Methods) was used to detect the occurrence of spindles. The timing of spindle occurrence is shown relative to timing of light delivery to V1. **(B)** Frequency of occurrence for spindle-like events (mean ± SEM) at baseline and during optogenetic stimulation. The density of spindle-like events was significantly increased during optogenetic stimulation at 2 Hz and 3 Hz (one-way ANOVA; * indicates $p < 0.05$, $p < 0.005$, and $p = 0.01$ for 2 Hz vs. baseline, 3 Hz vs. baseline, and 3 Hz vs. 0.5 Hz, Holm-Sidak *post hoc* test). **(C)** Durations of spindle-like events (mean ± SEM) elicited by optogenetic stimulation of L6 neurons at various frequencies, and under baseline conditions without stimulation (one-way ANOVA on ranks; * indicates $p < 0.001$, Dunn's Method *post hoc*).

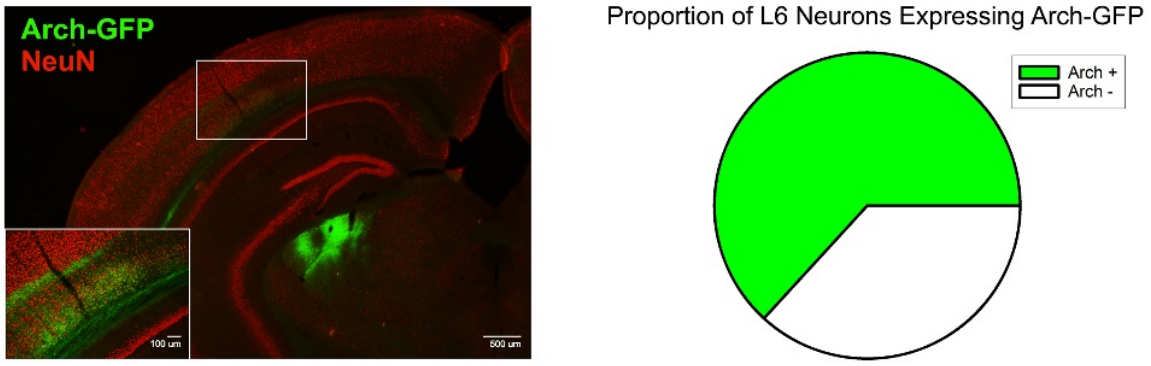

Figure S4.9. Arch-GFP expression in V1 L6 neurons. Left: GFP expression in V1 L6 neurons of virally-transduced *Ntsr1-cre* transgenic mice. Wide field image shows axon termini in LGN, inset shows cell bodies in L6. **Right:** Histological assessment of n = 4 transduced mice showed Arch-GFP expression in 63.2 ± 1.6% of all NeuN+ V1 L6 neuronal cell bodies (a similar proportion to the number of L6 neurons which project to thalamus [16]).

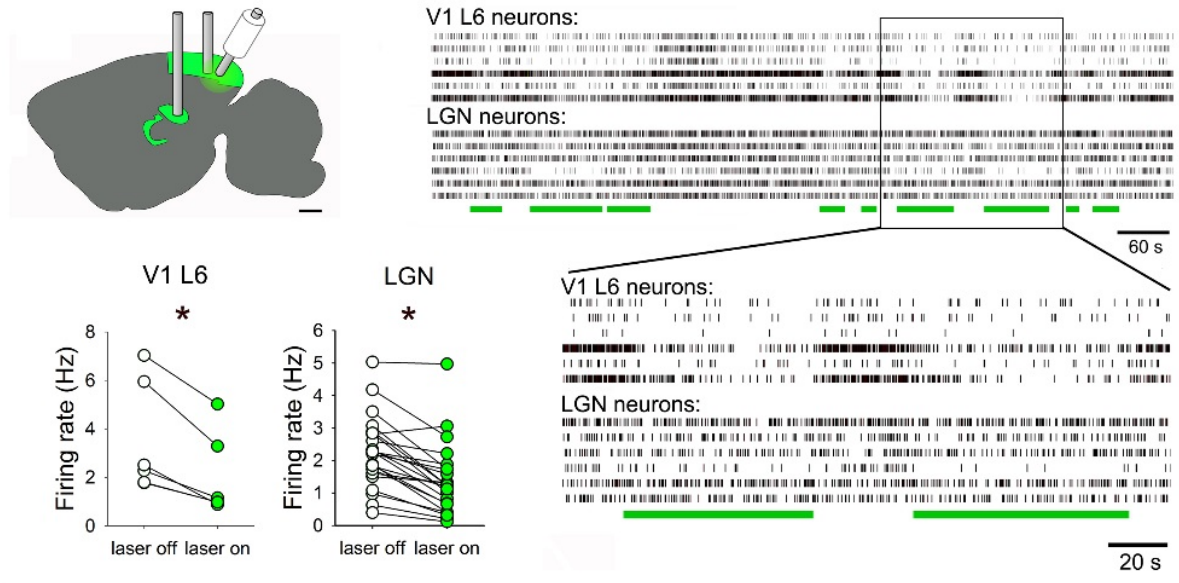

Figure S4.10. Optogenetic inhibition of L6 CT neurons in freely-behaving mice. Top, left: Experimental schematic, showing placement of stereotrode bundles for continuous, simultaneous recording of LGN and V1 neuronal activity in Arch-GFP-transduced *Ntsr1-cre* transgenic mice. **Top, right:** Spike rasters for simultaneously-recorded L6 and LGN neurons during optogenetic inhibition (laser light delivery times indicated by green bars). **Bottom, left:** Light delivery led to a significant reduction in both V1 L6 neurons' (n = 6) and LGN neurons' (n = 23) firing rates. * indicates $p < 0.005$, Wilcoxon signed rank test. **Bottom, right:** Inset from longer spike raster above.

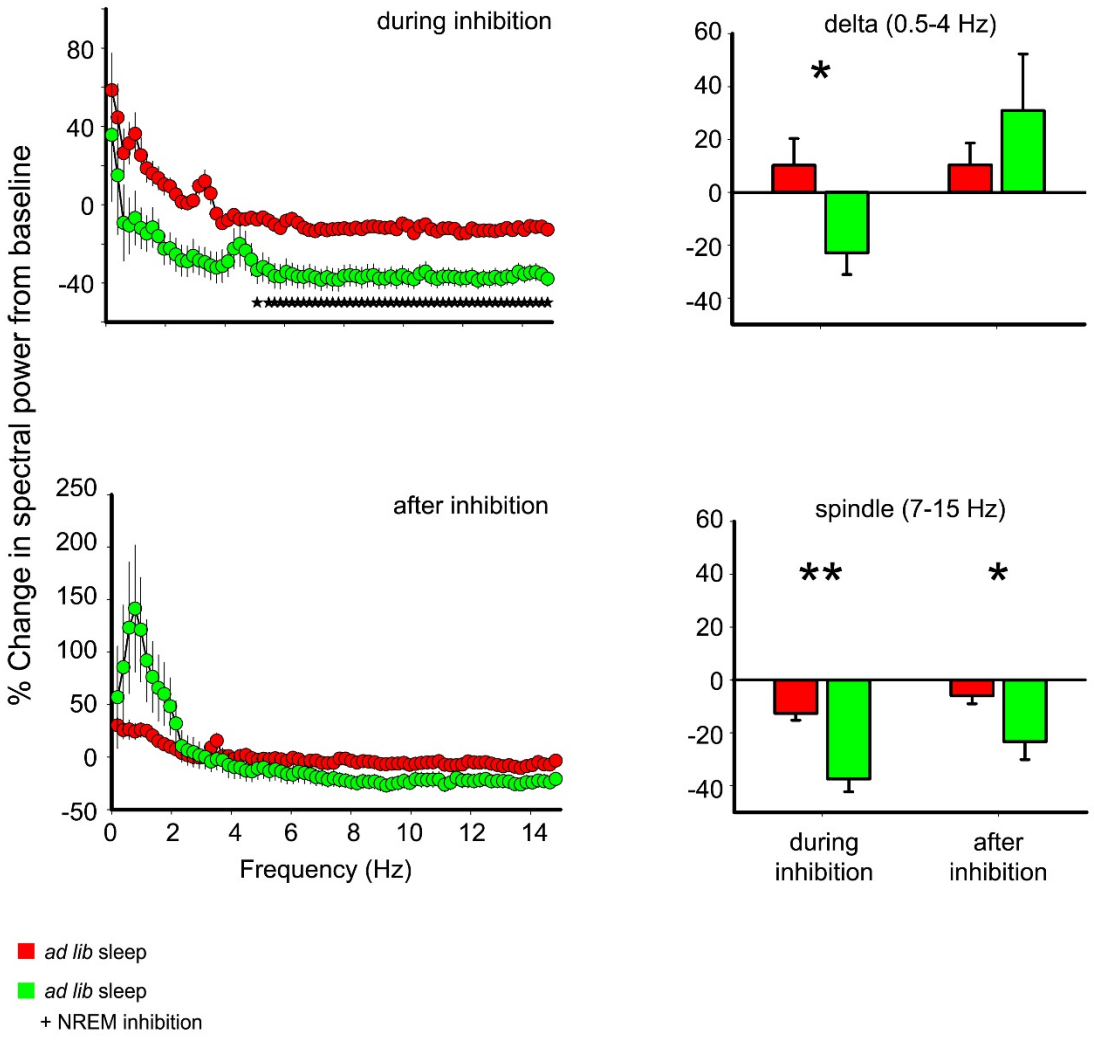

Figure S4.11. Power spectral changes during NREM-inhibition of CT neurons as a percent change from baseline. Left: During the 6 hours following OSRP induction, percent change in spectral power from baseline was significantly different between *ad lib* sleep mice and NREM-specific inhibition mice (*$p < 0.05$, t-test after Bonferroni correction). No significant differences were detected following the inhibition period. **Right:** Percent changes from baseline in summed spectral power at delta **(top)** and spindle **(bottom)** frequencies were calculated for *ad lib* sleep and NREM inhibition conditions. Percent change in summed delta power was significantly more negative for NREM inhibition LFPs versus control LFPs during inhibition, but not after ($p = 0.015$ and $p = 0.337$, respectively; t-test). Percent change in summed spindle power was significantly more negative for NREM inhibition LFPs versus control LFPs during and after inhibition ($p = 0.0000054$ and $p = 0.0135$, respectively; t-test). *$p < 0.05$ and **$p < 0.0001$.

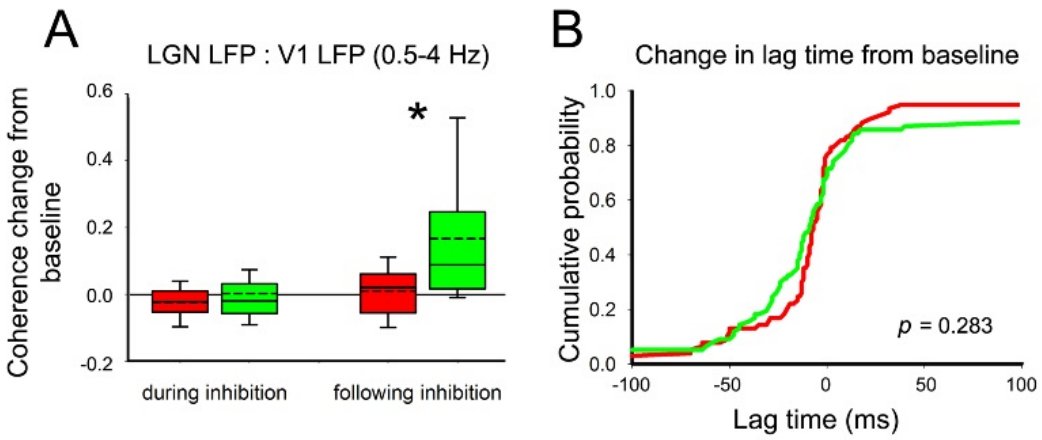

Figure S4.12. NREM delta-frequency coherence between V1 and LGN LFPs under control and optogenetic inhibition conditions. (A) Delta-frequency coherence between V1 and LGN LFPs was not significantly affected during NREM-specific inhibition of L6 CT neurons, but was increased relative to no laser control conditions after the inhibition period ($p = 0.418$ and $p < 0.001$, respectively; Mann-Whitney rank sum test). **(B)** For delta-frequency activity, there was no shift in the time lag between LGN and V1 LFPs (relative to baseline) with NREM-targeted inhibition of CT neurons ($p = 0.283$, Kolmogorov-Smirnov test vs. no laser condition).

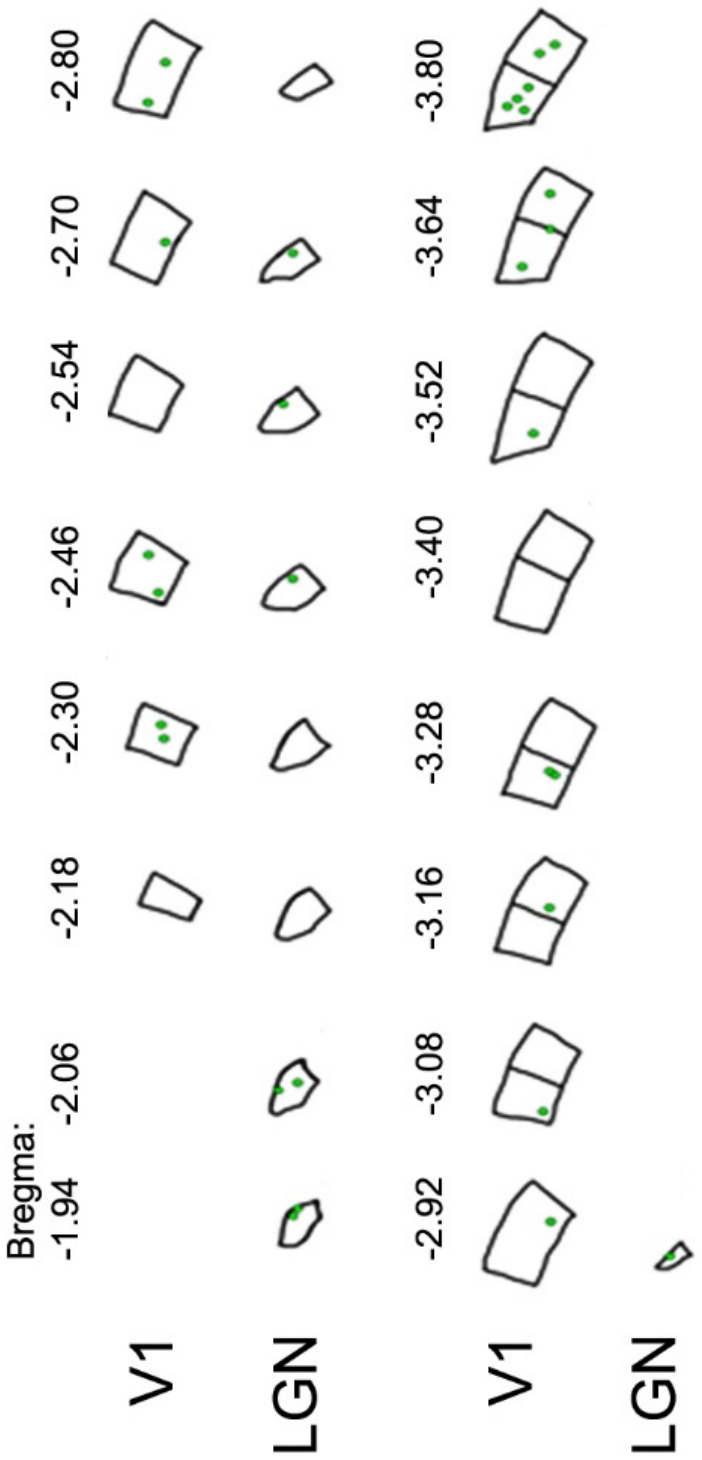

Figure S4.13. LGN and V1 recording sites. Locations of stereotrode recordings in all experiments from freely-behaving mice. Anterior-posterior position in coronal sections relative to bregma (in mm) shown in LGN, monocular and binocular right-hemisphere V1.

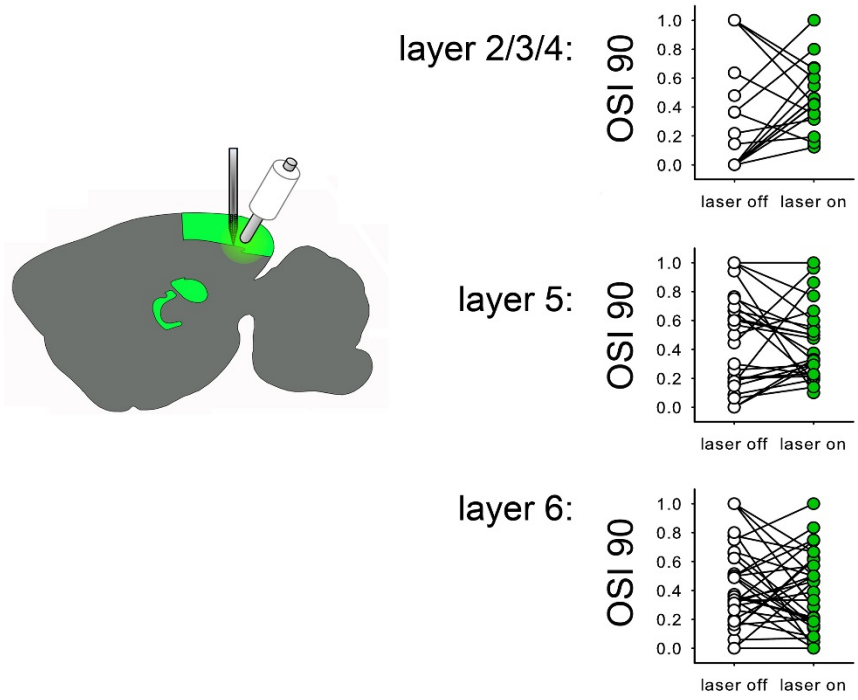

Figure S4.14. Direct effects of optogenetic inhibition of L6 CT neurons on V1 orientation tuning. V1 response properties recorded in anesthetized Arch-GFP-transduced mice before and during optogenetic inhibition of CT neurons (*n* = 24 neurons from layer 2/3/4, *n* = 32 neurons from layer 5, and *n* = 38 neurons from layer 6, recorded from *n* = 5 mice). Neuronal orientation tuning was not significantly or consistently altered in any layer by optogenetic inhibition (*N.S.* for all layers, Wilcoxon signed rank test).

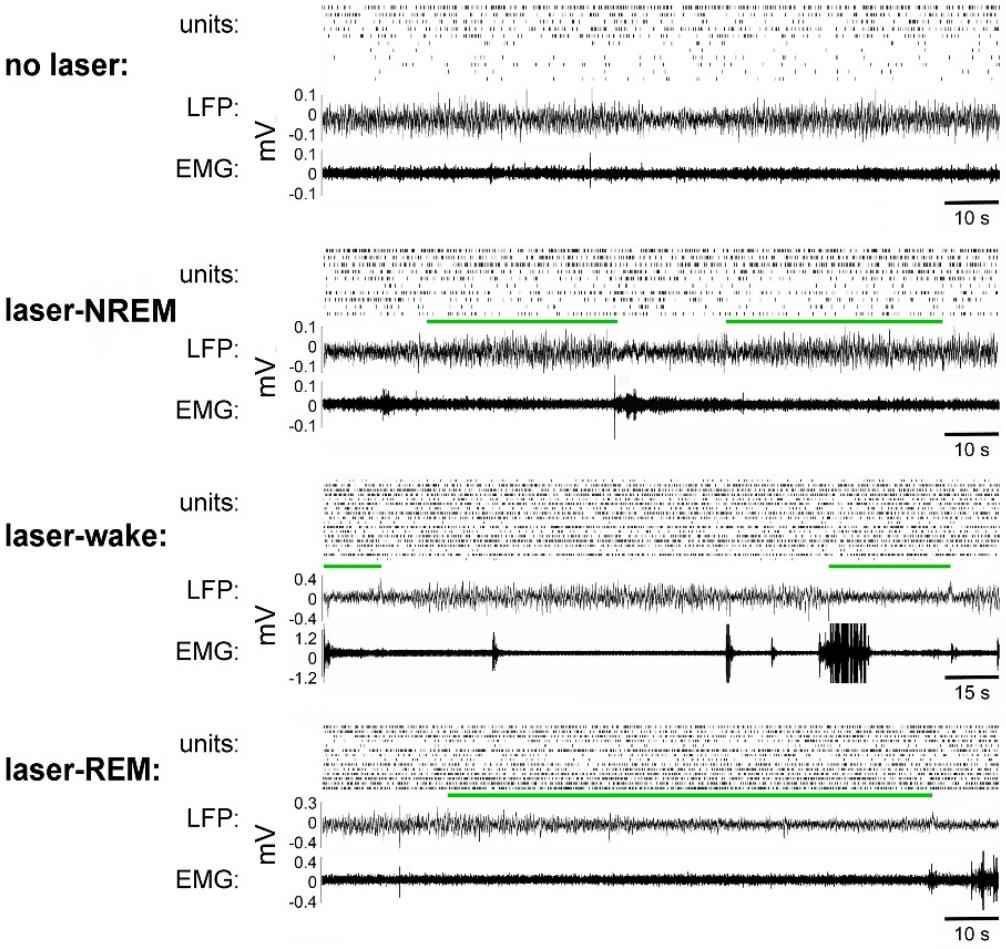

Figure S4.15. Electrophysiological activity recorded during state-specific inhibition of L6 CT neurons. Representative examples V1 spike rasters, V1 LFPs, and EMG activity during state-targeted inhibition of L6 neurons. Laser on times are indicated with green bars below rasters.

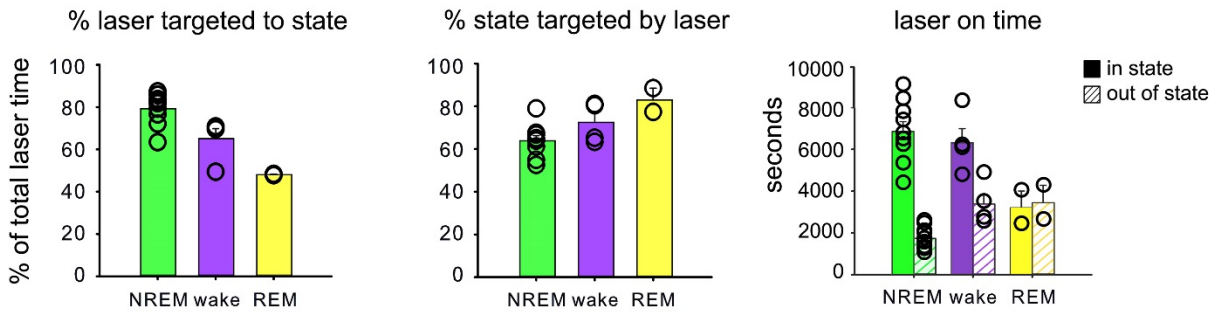

Figure S4.16. State targeting of inhibition of L6 CT neurons. Left: Percent of laser on time accurately targeted to state in laser-NREM (green) laser-wake (violet) and laser-REM (yellow) conditions. **Middle:** Percent of time in target state with laser on in the 3 conditions. **Right:** Laser on time (in s) for each condition, corresponding to time in and out of the targeted state, in the 3 conditions.

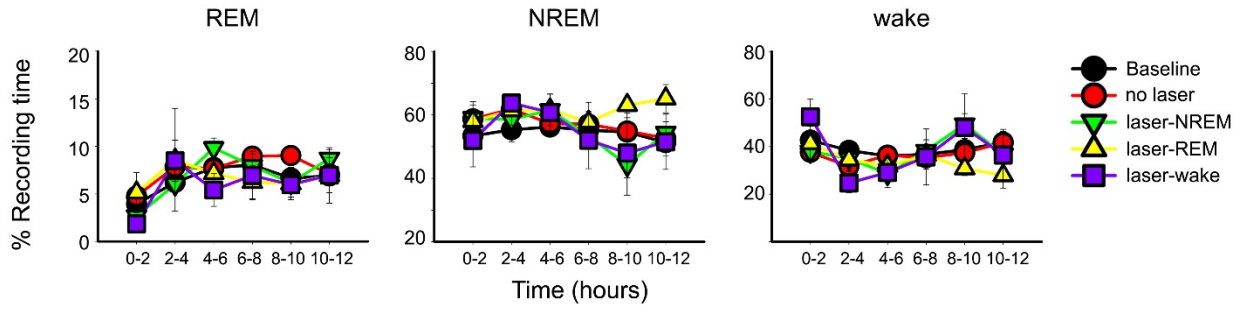

Figure S4.17. Sleep architecture is unaffected by state-specific inhibition of L6 CT neurons. % time spent in (from left to right) REM, NREM, and wake, for mice in the various state-targeted optogenetic inhibition conditions. Values are presented in 2-h windows across the rest phase (CT0-12), corresponding to the *ad lib* sleep period between stimulus presentation and OSRP assessment. State-targeted inhibition had no significant effect on sleep architecture ($p = 0.161$, $p = 0.186$, and $p = 0.350$ for REM, NREM, and wake, respectively; 2-way RM ANOVA).

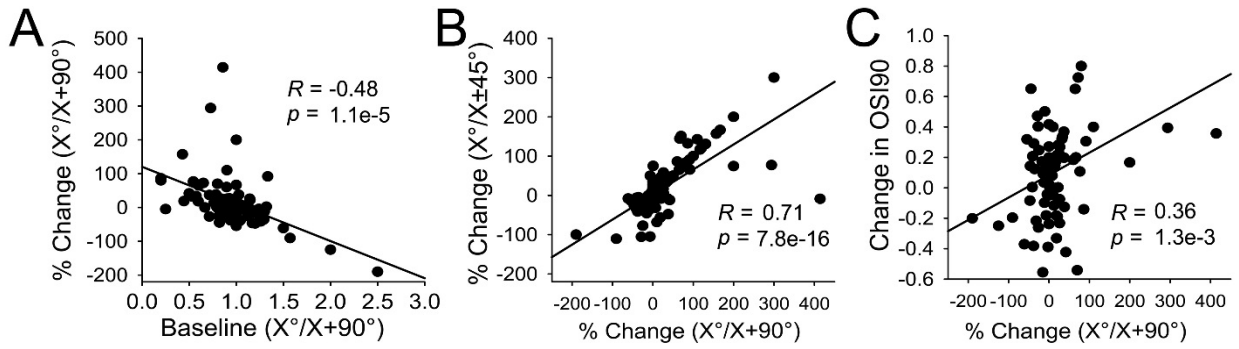

Figure S4.18. Features of OSRP expressed by V1 neurons after a period of sleep. (A) Among V1 neurons recorded from mice in the control (no laser) group, the degree of OSRP (change in [X°/X+90°]) after a period of sleep was inversely related to pre-stimulus baseline (X°/X+90°) ratio. The extent of OSRP in individual V1 neurons was positively correlated with **(B)** relative increases in responsiveness to the presented orientation vs. oblique orientations and **(C)** orientation selectivity (OSI90) increases (Pearson product moment). Pearson product moment *R* and *p* values are shown for 97 neurons.

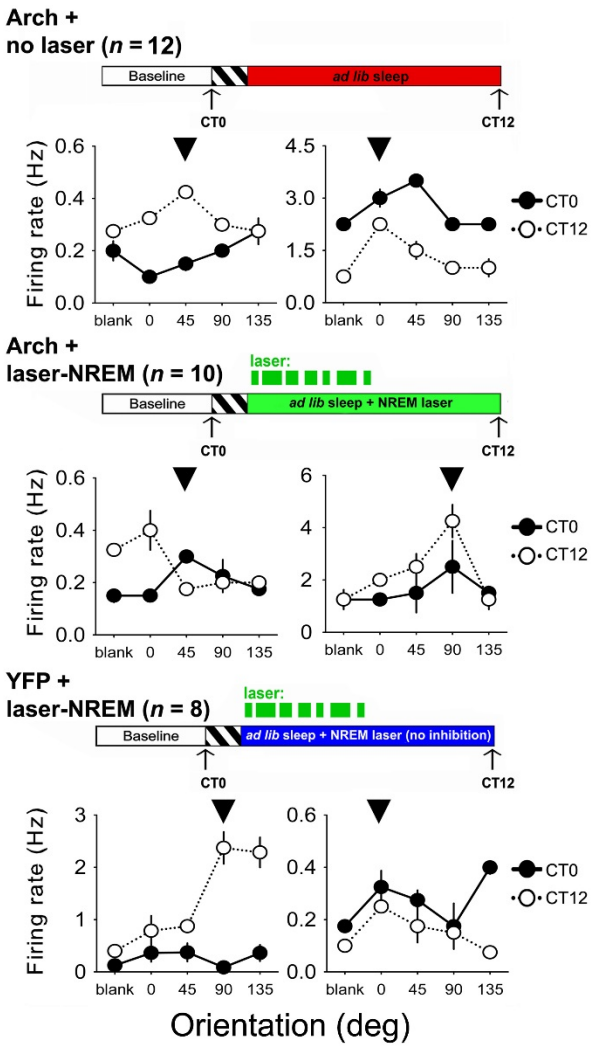

Figure S4.19. Response property changes in representative V1 neurons. Representative tuning curves for V1 neurons recorded at baseline (CT0; black) and following post-stimulus sleep (CT12; white) for mice in no laser **(top)**, laser-NREM **(middle)**, and laser-NREM YFP control **(bottom)** conditions. Values indicate mean firing rate response for each stimulus, ± SEM. *n* indicates the total number of mice recorded in each condition. Arrowheads indicate the orientation of the grating presented over 30 min to induce OSRP.

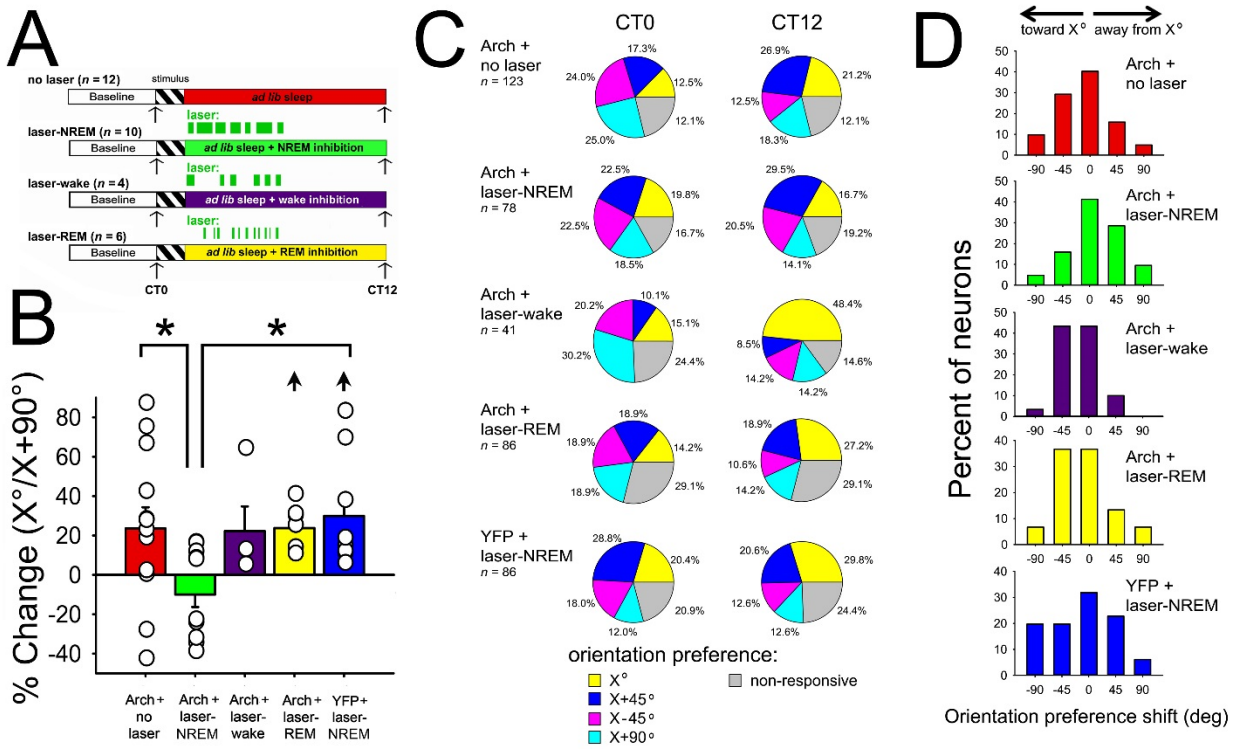

Figure S4.20. Per animal averages of OSRP reflect changes at the individual neuron level. (A) Experimental paradigm for evaluating the effects of post-stimulus state-targeted optogenetic inhibition of V1 CT neurons on OSRP consolidation. **(B)** Mean OSRP measured within individual animals is shown for each of the treatment groups. NREM-targeted inhibition of V1 CT neurons (laser-NREM) reduced OSRP in V1, while inhibition in other states did not affect OSRP. * indicates $p < 0.05$, Dunn's *post hoc* test versus no laser controls and YFP-expressing control mice with light delivery targeted to V1 during NREM ($p < 0.001$; Kruskal Wallis ANOVA on ranks). Arrowhead indicates $p < 0.05$, RM ANOVA on ranks. **(C)** Distributions of orientation preference among visually responsive V1 neurons (and proportions of non-responsive neurons) at baseline, and after a period of post-stimulus sleep. OSRP after a period of post-stimulus sleep was generally associated with an increase in the proportion of V1 neurons preferring the stimulus (X°) orientation, and a general reduction in the proportion of neurons preferring other orientations. Such changes were present in all groups of mice, except those receiving NREM-targeted optogenetic inhibition of L6 neurons (where response distributions were virtually unchanged across the experiment). **(D)** Distribution of the changes in preferred orientation for individual V1 neurons across stimulus presentation. Data are presented for all visually responsive neurons. 0 indicates no change, while negative and positive shifts, respectively, indicate shifts in response preference toward and away from the presented stimulus orientation. With the exception of mice receiving NREM-targeted optogenetic inhibition of L6 neurons, these distributions were skewed in favor of shifts toward the presented stimulus (X°).

4.9 Chapter 4 SI References:

1. Aton, S.J., Suresh, A., Broussard, C., and Frank, M.G. (2014). Sleep promotes cortical response potentiation following visual experience. Sleep *37*, 1163-1170.

2. Olsen, S.R., Bortone, D.S., Adesnik, H., and Scanziani, M. (2012). Gain control by layer six in cortical circuits of vision. Nature *483*, 47-52.

3. Durkin, J., and Aton, S.J. (2016). Sleep-Dependent Potentiation in the Visual System Is at Odds with the Synaptic Homeostasis Hypothesis. Sleep *39*, 155-159.

4. Aton, S.J., Seibt, J., Dumoulin, M., Jha, S.K., Steinmetz, N., Coleman, T., Naidoo, N., and Frank, M.G. (2009). Mechanisms of sleep-dependent consolidation of cortical plasticity. Neuron *61*, 454-466.

5. Frenkel, M.Y., Sawtell, N.B., Diogo, A.C., Yoon, B., Neve, R.L., and Bear, M.F. (2006). Instructive effect of visual experience in mouse visual cortex. Neuron *51*, 339-349.

6. Niell, C.M., and Stryker, M.P. (2008). Highly selective receptive fields in mouse visual cortex. J Neurosci *28*, 7520-7536.

7. Monteiro, M., Almeida, C.F., Caridade, M., Ribot, J.C., Duarte, J., Agua-Doce, A., and Graca, L. (2010). Identification of regulatory Foxp3+ invariant NKT cells induced by TGF-β. J Immunol *185*, 2157-2163.

8. Garcia, A.D.R., Doan, N.B., Imura, T., Bush, T.G., and Sofroniew, M.V. (2004). GFAP-expressing progenitors are the principal source of constitutive neurogenesis in adult mouse forebrain. . Nature Neuroscience *7*, 1233-1241.

9. Chen, S., Lee, B., Lee, A.Y.F., Modzelewski, A.J., and He, L. (2016). Highly Efficient Mouse Genome Editing by CRISPR Ribonucleoprotein Electroporation of Zygotes. . J Biol Chem *jbc-M116*.

10. Aton, S.J., Broussard, C., Dumoulin, M., Seibt, J., Watson, A., Coleman, T., and Frank , M.G. (2013). Visual experience and subsequent sleep induce sequential plastic changes in putative inhibitory and excitatory cortical neurons. Proc Natl Acad Sci U S A *110*, 3101-3106.

11. Ognjanovski, N., Maruyama, D., Lashner, N., Zochowski, M., and Aton, S.J. (2014). CA1 hippocampal network activity changes during sleep-dependent memory consolidation. Front Syst Neurosci *8*, 61.

12. Hill, D.N., Mehta, S.B., and Kleinfeld, D. (2011). Quality metrics to accompany spike sorting of extracellular signals. J Neurosci *31*, 8699-8705.

13. 13. Sato, T., Suzuki, T., and Mabuchi, K. (2007). Fast automatic template matching for spike sorting based on Davies-Bouldin validation indices. Conf Proc IEEE Eng Med Biol Soc, 3200-3203.

14. Nicolelis, M.A., Dimitrov, D., Carmena, J.M., Crist, R., Lehew, G., Kralik, J.D., and Wise, S.P. (2003). Chronic, multisite, multielectrode recordings in macaque monkeys. PNAS *100*, 11041-11046.

15. Herry, C., Ciocchi, S., Senn, V., Demmou, L., Muller, C., and Luthi, A. (2008). Switching on and off fear by distinct neuronal circuits. Nature *454*, 600-606.

16. Bortone, D.S., Olsen, S.R., and Scanziani, M. (2014). Translaminar inhibitory cells recruited by layer 6 corticothalamic neurons suppress visual cortex. Neuron *82*, 474-485.

Chapter 5 Discussion

5.1 Summary and Conclusions

Humanity has been fascinated with sleep for millennia. Sleep has been a repeating motif in art, literature, and philosophy because it is a mystery and it is essential. One of the earliest portrayals of sleep was as the Greek god Hypnos, the twin brother of Thanatos, the god of death. This close association between sleep and death encapsulates early theories about sleep, which Aristotle called, “a border-land between living and not-living.” These beliefs proved highly influential, as the association between sleep and death prevailed and continued to inspire artists and writers for centuries. Consequently, philosophers (and even scientists) [1] believed that sleep was a time when the brain and the body were simply “off.” René Descartes famously proposed that during sleep, the animal spirits stopped flowing from the pineal gland, and the brain effectively deflated.[2] Thus, when Nathaniel Kleitman’s electroencephalogram recordings of the sleeping brain demonstrated for the first time that the brain was *not* silent during sleep, he was met with resistance and disbelief.[3] However, work by Kleitman, William C. Dement and others showed that sleep states are characterized by their own unique physiology.[3] While sleep is believed to play a role in many essential life processes,[4-9] sleep-specific brain activity is thought to play a fundamental role in reorganization of neural circuits and storage of information.[10-15]

State-specific neural activity has been correlated with improvements in learning and memory retention. However, the mechanisms governing sleep's effects on cognition have not been well described. As discussed in **Chapter 1**, many theories have been proposed, arguably the most influential among them the Synaptic Homeostasis Hypothesis (SHY). SHY states that during wake, synapses are potentiated for encoding of new experiences, while sleep acts to globally "downscale" synapses.[16] This global downscaling would allow for an increase in signal-to-noise ratios for "learned" synapses. However, recent research from our lab and many others conflicts with the notion of global synaptic downscaling. In particular, our work on Orientation Specific Response Potentiation (OSRP), an LTP-like modification of visual cortical responses to grating stimuli, has shown that sleep can promote plasticity that is *not* a product of synaptic downscaling.[17] We expanded upon these findings to show that increases in visual cortical firing rates, which accompany OSRP, occur specifically across sleep bouts, as discussed in **Chapter 2**.[18]

As another challenge to widely accepted dogma, we set out to test whether sleep uniformly (globally) affects neuronal activity. In **Chapter 3**,[19] we demonstrated that across sleep, low-firing neurons are more likely to increase firing rates, while high-firing neurons are more likely to decrease firing rates. Thus, sleep allows for the renormalization of firing rates, a process that is independent of prior waking experience and is blocked by sleep deprivation. Furthermore, we showed that low-firing V1 neurons tended to fire more independently of the rest of the population, and were more selective in their visual responses, consistent with encoding more visual information. These neurons were also more likely to show changes consistent with OSRP. Thus, in the context of OSRP, weakly-

coupled, sparsely-firing neurons were more likely to have orientation-specific visual responses enhanced across sleep. Interestingly, this suggests a role for sleep in *differentially* modulating the activity of visual cortical neurons in response to novel visual experience.[19]

Early work describing OSRP from the Bear lab showed that is strongly resembles thalamocortical LTP.[20] As discussed in **Chapter 1**, OSRP relies on similar signaling pathways as LTP, and also occludes with thalamocortical LTP, induced by theta-burst stimulation of TC neurons projecting from LGN to V1. Combining this knowledge with the sleep-dependent nature of OSRP, we decided to investigate if the LGN showed immediate, stimulus-specific changes in activity following novel visual experience. Because V1 did not show any immediate changes in spontaneous firing rates or evoked firing rates,[17,18] we hypothesized that information about the presented stimulus may be stored earlier in the visual circuit, in the LGN, for transfer to V1 during subsequent sleep. Indeed, in **Chapter 4** we demonstrated that LGN shows immediate increases in firing rates across stimulus presentation, followed by *specific* enhancements in responses to the presented stimulus during the post-stimulus visual test (**Fig 4.1 A-C; Fig 4.2 A-B**).[21]

In addition to showing immediate changes in visual responsiveness, LGN neurons that underwent plasticity were more likely to fire coherently with NREM-specific oscillations in visual cortex. These oscillations are thought to be involved in consolidation of many learning paradigms, as their power and prevalence tend to increase following learning, often in a regionally specific manner. Thus, we hypothesized that coherent NREM oscillations would be crucial for consolidation of plasticity in V1. We demonstrated for the first time that reversible disruption of corticothalamic feedback (via optogenetic

manipulation) reduces the coherence of NREM oscillations (**Figure 4.5**). Furthermore, inhibition of CT neurons during NREM, but not REM or wake, blocked consolidation of OSRP in V1 (**Figure 4.6**). Thus, we concluded that coherent NREM oscillations are crucial for consolidation of OSRP, possibly playing a role in the transfer of visual information from LGN to V1 (**Chapter 4**).[21]

Ultimately, we hypothesize that NREM oscillations are regulating the transfer of sensory information from the LGN to V1. Though this hypothesis is rather vague, we believe it is an interesting first step in addressing key questions about the function of state-specific thalamocortical activity. From our data, it is clear that the fundamental question that still needs to be resolved is how does sleep modulate neural activity in a "bidirectional" manner, where some neurons are selected for potentiation (as is OSRP) and some are not?[20,21]

One of the more attractive proposed mechanisms for this neuron-specific (or synapse-specific) regulation relies on calcium activity.[13,22] When calcium levels are high, it activates the CAMKII pathway, favoring trafficking of AMPA receptors and LTP mechanisms. In contrast, under low levels of calcium, protein phosphatases like the enzyme calcineurin are preferentially activated, favoring LTD mechanisms.[13] As NREM oscillations, especially sleep spindles, are accompanied by large calcium transients, this could be one possible explanation for the differential effects of these oscillations on plasticity. For example, neurons whose spike times are better locked to NREM oscillations may show higher levels of calcium, favoring potentiation, while others may have lower, but more sustained, calcium levels leading to LTD.[13,23] In addition to the experiments

described in the next section, future work could benefit from analysis focused on calcium activity, such as calcium imaging in the context of OSRP consolidation.

5.2 Future Directions

Our data can be interpreted in a number of ways, and there are interesting follow-up studies to be done to address these possible interpretations. Firstly, we have shown that sleep and sleep-specific activity is necessary for OSRP expression in V1, but that LGN shows immediate changes in response properties following stimulus presentation. One interesting questions would of course be is sleep-dependent neural activity sufficient for OSRP expression. There are a number of ways to approach this. Performing optogenetic enhancement of oscillations during sleep-deprivation would be an interesting experiment, however there are a number of technical difficulties when exciting neurons. First and foremost is that simply applying laser pulses at a particular frequency is not a guarantee that this will elicit coordinated activity at that frequency.

One potential alternative to the technical issues with optogenetics would be taking advantage of the circadian regulation of mouse sleep behavior. We have previously shown that OSRP cannot be consolidated overnight (i.e., CT12 to CT0) and interpreted this as being due to the relative lack of sleep in mice during this timepoint. It would be interesting to induce OSRP at CT12, and immediately introduce some sort of hypnotic, such as zolpidem, which is known to boost sleep spindle density. Though this would be a very “artificial” type of sleep, it would allow us to begin to address what physiology and network conditions are sufficient for OSRP consolidation. Furthermore, it would be interesting to see if, in placebo conditions, there is still an immediate change in LGN

response properties as we would see if stimulus presentation occurred at CT0. Other future directions would include resolving the contributions of LGN and TRN activity to OSRP consolidation.

One caveat to our experiments manipulating layer 6 neurons is that some layer 6 neurons project intracortically. Although our stimulation experiments (see **Fig. 4.4**) indicate that the layer 6 neurons expressing Cre in NTSR1-Cre mice have greater influence over LGN neurons than other V1 neurons, we cannot exclude a possible effects of intracortical activity on OSRP in these experiments. Thus, experiments targeting the thalamocortical connections between LGN and V1 are necessary to demonstrate the role of this pathway in consolidation OSRP.

Previous experiments utilizing the GPR26-Cre mouse line to target LGN neurons proved insufficient to probe the function of these neurons, as expression of Cre in this line is not limited to TC neurons, but also may be affecting local interneurons or connections with the TRN. Thus an alternative, more specific approach, should be employed. To precisely target the thalamocortical LGN neurons of interest, a combination of retrograde Cre virus injected in V1 and Cre-dependent opsin (or DREADD) injected in LGN could be performed. State-specific inhibition of the LGN following induction of plasticity could clarify the role of TC activity in consolidation of OSRP. Next, we would want to know the relative contributions of NREM oscillations to this form of plasticity. Isolating the delta oscillation is not necessarily possible, but targeting of the sleep spindle is more achievable, though this strategy comes with its own drawbacks.

Previous attempts to manipulate TRN function in sleep-dependent plasticity have proved difficult. Work by Halassa et al.,[24] as well as work done by Robert McCarley

(personal correspondence) has shown that optogenetic manipulation of the TRN can increase or decrease spindle number, but has a large effect on sleep architecture overall. Because spindles are hypothesized to maintain sleep, decreasing spindles throughout the brain leads to increased awakening and shorter sleep bouts and total sleep duration. However, an attempt to manipulate one portion of the TRN to affect *local* (i.e., nucleus-specific) spindle production has not been reported in the literature. One could attempt to express opsins or DREADDs in the visually projecting TRN, by retrograde transfection via the LGN into a PV-cre mouse line. Though it is unclear what effect this manipulation would have on total sleep architecture, the existence of locally enriched spindle activity indicates that spindles may be targeted in a more localized fashion. Other potential manipulations include the use of hypnotics which can have differential effects on spindle production. Zolpidem, for example, boosts spindle density, while olanzapine reduces spindle density. These drugs appear to have similar effects on slow wave activity and REM sleep, potentially providing a way to examine the role of spindles specifically in a bidirectional manner.

5.3 References

1. Pavlov, P. I. (2010). Conditioned reflexes: an investigation of the physiological activity of the cerebral cortex. *Annals of neurosciences*, *17*(3), 136.

2. Descartes, R., & Hall, T. S. (1972). *Treatise of man*. Harvard University Press.

3. Dement, W. C. (2005). History of sleep medicine. *Neurologic clinics*, *23*(4), 945-965.

4. Berger, R. J., & Phillips, N. H. (1995). Energy conservation and sleep. *Behavioural brain research*, *69*(1-2), 65-73.

5. Xie, L., Kang, H., Xu, Q., Chen, M. J., Liao, Y., Thiyagarajan, M., ... & Takano, T. (2013). Sleep drives metabolite clearance from the adult brain. *Science*, *342*(6156), 373-377.

6. Hanlon, E. C., & Van Cauter, E. (2011). Quantification of sleep behavior and of its impact on the cross-talk between the brain and peripheral metabolism. *Proceedings of the National Academy of Sciences*, *108*(Supplement 3), 15609-15616.

7. Graven, S. N., & Browne, J. V. (2008). Sleep and brain development: the critical role of sleep in fetal and early neonatal brain development. *Newborn and Infant Nursing Reviews*, *8*(4), 173-179.

8. Parmeggiani, P. L., Calasso, M., & Cianci, T. (1981). Respiratory effects of preoptic-anterior hypothalamic electrical stimulation during sleep in cats. *Sleep*, *4*(1), 71-82.

9. De Manaceine, M. (1897). *Sleep: Its physiology, pathology, hygiene, and psychology*. W. Scott.

10. Jenkins, J. G., & Dallenbach, K. M. (1924). Obliviscence during sleep and waking. *The American Journal of Psychology*, *35*(4), 605-612.

11. Steriade, M., & Timofeev, I. (2003). Neuronal plasticity in thalamocortical networks during sleep and waking oscillations. *Neuron*, *37*(4), 563-576.

12. Diekelmann, S., & Born, J. (2010). The memory function of sleep. *Nature Reviews Neuroscience*, *11*(2), 114.

13. Benington, J. H., & Frank, M. G. (2003). Cellular and molecular connections between sleep and synaptic plasticity. *Progress in neurobiology*, *69*(2), 71-101.

14. Clawson, B. C., Durkin, J., & Aton, S. J. (2016). Form and function of sleep spindles across the lifespan. *Neural plasticity*, *2016*.

15. Puentes-Mestril, C., & Aton, S. J. (2017). Linking network activity to synaptic plasticity during sleep: Hypotheses and recent data. *Frontiers in neural circuits*, *11*, 61.

16. Tononi, G., & Cirelli, C. (2006). Sleep function and synaptic homeostasis. *Sleep medicine reviews*, *10*(1), 49-62.

17. Aton, S. J., Suresh, A., Broussard, C., & Frank, M. G. (2014). Sleep promotes cortical response potentiation following visual experience. *Sleep*, *37*(7), 1163-1170.

18. Durkin, J., & Aton, S. J. (2016). Sleep-dependent potentiation in the visual system is at odds with the synaptic homeostasis hypothesis. *Sleep*, *39*(1), 155-159.

19. Clawson, B. C., Durkin, J., Suresh, A. K., Pickup, E. J., Broussard, C. G., & Aton, S. J. (2018). Sleep Promotes, and Sleep Loss Inhibits, Selective Changes in Firing Rate, Response Properties and Functional Connectivity of Primary Visual Cortex Neurons. *Frontiers in systems neuroscience*, *12*.

20. Cooke, S. F., & Bear, M. F. (2010). Visual experience induces long-term potentiation in the primary visual cortex. *Journal of Neuroscience*, *30*(48), 16304-16313.

21. Durkin, J., Suresh, A. K., Colbath, J., Broussard, C., Wu, J., Zochowski, M., & Aton, S. J. (2017). Cortically coordinated NREM thalamocortical oscillations play an essential, instructive role in visual system plasticity. *Proceedings of the National Academy of Sciences*, *114*(39), 10485-10490.

22. Sejnowski, T. J., & Destexhe, A. (2000). Why do we sleep? 1. *Brain research*, *886*(1-2), 208-223.

23. Seibt, J., Richard, C. J., Sigl-Glöckner, J., Takahashi, N., Kaplan, D. I., Doron, G., ... & Larkum, M. E. (2017). Cortical dendritic activity correlates with spindle-rich oscillations during sleep in rodents. *Nature communications*, *8*(1), 684.

24. Halassa, M. M., Siegle, J. H., Ritt, J. T., Ting, J. T., Feng, G., & Moore, C. I. (2011). Selective optical drive of thalamic reticular nucleus generates thalamic bursts and cortical spindles. *Nature neuroscience*, *14*(9), 1118.